ABSTRACT

THERMAL TREATMENT OF ORGANIC CONTAMINATED SOLIDS AND WASTE: EXPERIMENT, MODEL AND MASS BALANCE

by
Hsien-Tsung Chern

A number of processes can be used to remediate contaminated soils. The thermal technologies for remediation of contaminated soils are summarized in this study. Each of these treatment process along with their system components are identified and described. Waste applicability is included for each treatment technology. A detailed list of feasible treatment processes is presented with descriptions of site demonstration results to aid in selection of a given process. Technology status is summarized to provide current information on the processes.

Energy components are discussed for cost requirement and safety considerations in thermal treatment applications. It is determined that the heat loss from kiln shell to environment demands the major fraction (56 percent) of the energy requirements in the bench scale thermal desorber. However, only 6 percent of total energy requirement is due to this heat loss to environment in a full scale desorber. The major heat required in a full scale desorber is used for treatment of water which consumes approximately 48 percent of the energy.

Data on concentrations of PCDD/F in the feed, and in the effluent from modern Municipal Solid Waste Incinerators (MSWI) are surveyed and evaluated to determine if more PCDD/F are destroyed than formed in the Municipal Solid Waste (MSW) incineration process. The results show that a range of 0.8 to 87 pg(I-TE)/g or 0.16 – 17.4

grams(I-TE) PCDD/F in 2×10^8 kg waste is present in the feed to a MSW incinerator. For 7.2 g(I-TE) PCDD/F in the feed to a MSW incinerator per year; the output in the combined gas and solid streams ranges from 0.11 to 12 g(I-TE) per year. This data indicates that input and output levels of PCDD/F in modern, efficient municipal solid waste incineration are of similar magnitude.

A bench scale rotary kiln thermal desorber was constructed and tested. Operation parameters such as kiln temperature, solid residence time, kiln tilt, kiln rotary speed, soil feed rate, and purge gas flowrate are varied to quantify their effects and determine optimum conditions. Results show that the thermal desorber system is highly effective in removing semivolatile organics from field contaminated soils. Temperature and solid residence time are two primary parameters affecting the desorption results. Higher temperatures and longer residence times result in higher removal efficiency. The result of mass balances for carbon illustrated that most of carbon recovery ranged from 45 to 115 percent in 20 experimental runs.

A detailed heat and mass transfer model for thermal desorption of contaminants in/on soils has been developed for application in a rotary kiln thermal desorber. The heat balance and the heat flow between soil, gas and kiln wall are incorporated. Temperature profiles of gas and soil are calculated using the fourth order Runge-Kutta method. Evaporation rates of moisture and organic contaminants derived by Wendt et al. is applied for the mass balance calculation. A comparison of modeling results with experimental data for gas and soil temperature profiles as well as the mass flow rates of moisture and organic contaminants with experimental data is in reasonable agreement. Improvements in the model development are recommended.

THERMAL TREATMENT OF ORGANIC CONTAMINATED SOLIDS AND WASTE: EXPERIMENT, MODEL AND MASS BALANCE

by

Hsien-Tsung Chern

A Dissertation
Submitted to the Faculty of
New Jersey Institute of Technology
in Partial Fulfillment of the Requirements for the Degree of
Doctor of Philosophy in Environmental Science

Department of Chemistry and Environmental Science

August 2002

APPROVAL PAGE

THERMAL TREATMENT OF ORGANIC CONTAMINATED SOLIDS AND WASTE: EXPERIMENT, MODEL AND MASS BALANCE

Hsien-Tsung Chern

Dr. Joseph W. Bozzelli, Dissertation Advisor — **Date**
Distinguished Professor of Chemistry and Environmental Science, NJIT

Dr. Jeffrey M. Grenda, Committee Member — **Date**
Senior Research Engineer, ExxonMobil Research and Engineering Company, Annandale, NJ

Dr. Lev Krasnoperov, Committee Member — **Date**
Professor of Chemistry and Environmental Science, NJIT

Dr. Namunu J. Meegoda, Committee Member — **Date**
Professor of Civil Engineering, NJIT

Dr. Victor Ososkov, Committee Member — **Date**
Adjunct Professor of Chemistry and Environmental Science, NJIT

Dr. Richard Trattner, Committee Member — **Date**
Emeritus Professor of Chemistry and Environmental Science, NJIT

BIOGRAPHICAL SKETCH

Author: Hsien-Tsung Chern

Degree: Doctor of Philosophy

Date: August 2002

Undergraduate and Graduate Education :

- Doctor of Philosophy in Environmental Science,
  New Jersey Institute of Technology, Newark, NJ, 2002
- Master of Science in Environmental Science,
  New Jersey Institute of Technology, Newark, NJ, 1991
- Bachelor of Science in Civil Engineering,
  Chung-Yuan Christian University, Chung-Li, Taiwan, 1984

Major : Environmental Science

Presentations and Publications:

Chern, H. and Bozzelli J.W., "Comment on Formation of Dioxins during the Combustion of Newspapers in the Presence of Sodium Chloride and Poly(vinyl chloride)", *Environ. Sci. Technol.*, 36, 9, 2107 (2002).

Chern, H. and Bozzelli, J. W., "Do Modern MSW Incinerators Actually Destroy More PCDD/F Than They Produce?" *The 33th Mid-Atlantic Industrial and Hazardous Waste Conference*, Manhattan College, Riverdale, NY, June 18-20, 2001.

Chern, H. and Bozzelli J.W., "Modeling of Heat and Mass Transfer in a Rotary Kiln Thermal Desorber for Removal of Organic Contaminants from Soils", *The Seventh International Congress on Combustion By-Products: Origins, Fate and Health Effects*. Research Triangle Park, NC, June 4-6, 2001.

Chern, H. and Bozzelli J.W., "Analysis of Heat Requirements and Potential for Thermal Runaway in Application of Thermal Desorption to Soil Decontamination". *The 11th Annual Conference of the Academy of Certified Hazardous Materials Managers program*, Atlantic City, NJ, October 5-8, 1997.

Chern, H. and Bozzelli J.W., "Modeling of Heat Transfer in a Rotary Kiln Thermal Desorber for Removal of Petroleum from Soils". *The Division of Environmental Chemistry, Conference of American Chemical Society*, New Orleans, LA March 24-29, 1996.

Chern, H., LaRosa, A. and Bozzelli, J. W., "Thermal Desorption of Organic Contaminants from Sand using a Continuous Feed Rotary Kiln", *Hazardous Waste Management Handbook: Technology, Perception, and Reality*. Prentice-Hall, Inc., Englewood Cliffs, NJ, pp. 157-169, 1994.

This dissertation is dedicated to my parents

ACKNOWLEDGEMENT

I wish to express my sincere gratitude to my advisor, Dr. Joseph W. Bozzelli, for his guidance, advice and support through this research. Special thanks to Dr. Lev N. Krasnoperov for his help with detail of kiln model. I would also like to thank Dr. Richard Trattner, Dr. Namunu Meegoda, Dr. Victor Ososkov, and Dr. Jeffrey Grenda for serving as members of my dissertation committee as well as their valuable comments and advice.

I am grateful to all of my colleagues and friends in Dr. Bozzelli's research group: Dr. Chiung-Chu Chen, Ms. Zhu Li, Mr. Jongwoo Lee, and Ms. Hongyan Sun. They together have created a highly motivated environment which is very important to my research work.

Finally I would like to thanks my parents and sisters. Their encouragement, comfort and love helped me to stay focused till completion of my study through all these years.

TABLE OF CONTENTS

TABLE OF CONTENTS
(Continued)

TABLE OF CONTENTS
(Continued)

TABLE OF CONTENTS
(Continued)

Chapter **Page**

LIST OF TABLES

LIST OF TABLES
(Continued)

LIST OF TABLES
(Continued)

LIST OF FIGURES

LIST OF FIGURES
(Continued)

LIST OF FIGURES
(Continued)

LIST OF FIGURES
(Continued)

LIST OF FIGURES
(Continued)

CHAPTER 1

INTRODUCTION

A number of processes can be used for remediation of contaminated soils, and one of the more popular and versatile of these techniques is thermal treatment. Thermal treatment technologies are either destruction or removal types of treatment. Available thermal treatment technologies for remediation of contaminated soils include separation technologies such as thermal desorption, as well as destruction technologies of incineration and pyrolysis.

The objective of this study is to collect information and data on thermal treatment of organic contaminated soils. The available thermal technologies for remediation of contaminated soils are summarized. Each treatment processes, as well as the associated treatment system components, are identified and described. The energy considerations during thermal treatment process are described. The possibility of thermal runaway in the thermal desorption processing of solids and soils contaminated with organic compounds is also examined. Organic concentration conditions are delineated, example calculations are performed and calculational procedures are illustrated. Calculations include heat capacity and heat losses of and from the rotary kiln desorber unit, input heat and heat balance from possible combustion processes. Specific heat acceptor components include heat capacity of the kiln, heat transfer to the atmosphere via conduction, radiation and convection, de-sorption energies, vaporization energies of both the organics and water, heating of the contaminated soil, and heating of purge gas. Heat input includes chemical reaction (combustion), and energy to the kiln for the normal desorption process.

A bench scale rotary kiln thermal desorber is constructed and tested in this study. This rotary kiln is 20 inches in length of rotary section and 4.0 inches in inside diameter. Operation parameters such as kiln temperature, solid residence time, kiln tilt, kiln rotary speed, soil feed rate, and purge gas flowrate are varied to quantitate their effects and determine optimum conditions. The carbon mass in the input soil and in effluent streams is evaluated to determine the mass balance for carbon in the chosen runs. Sampling and instrumental analysis methods included ultrasonic and soxhlet extraction, Gas Chromatography Mass Spectrometer, Fourier Transfer Infrared Spectroscopy, Infrared and Gas Chromatographic Flame Ionization Detector, to identify and quantitatively analyze mass balance on carbon and organic contaminant removal of the target soil. The experimental results are used to validate a mathematical model which incorporates heat and mass transfer between gas, soil, moisture and organic contaminants in the thermal desorber.

A computer model is developed for heat and mass transfer in a rotary kiln thermal desorber, where soil or solids are inlet and then heat is applied to volatilize water (moisture) and contaminants or other volatile species in soil with a purge for exhaust. The rotary kiln reactor is considered as a computation domain which is divided into cylindrical volume segments (also called computation cells) or radial slices. These computational cells serve as increments in the model treatment. Conservation of energy and mass is formulated in each radial volume segment, where convection, conduction and radiation energy transfer is coupled with energy balance that includes volatilization of both moisture and organic contaminants. The governing equations for each computation cell (segment) are solved numerically using an iterative method and a fourth order

Runge-Kutta method. The results from the mathematical model are compared with the experimental data.

Data on concentrations of PCDD/F in the feed, and in the effluent from modern municipal solid waste incinerators (MSWI) are surveyed and evaluated to determine if more PCDD/F are destroyed than formed in the Municipal Solid Waste (MSW) incineration process. PCDD/F concentrations in the feed of MSW incinerators are assigned into four different waste categories with associated PCDD/F levels. Estimation of PCDD/F concentrations in the output of MSW incinerators considers the production rate of gaseous PCDD/F emissions plus levels in the solid effluent streams (bottom ash, boiler ash and air pollution control residues).

CHAPTER 2

THERMAL TECHNOLOGIES FOR REMEDIATION OF CONTAMINATED SOILS

2.1 Introduction

A number of processes can be used for remediation of contaminated soils, and one of the more popular and versatile of these techniques is thermal treatment. Thermal treatment technology has a number of variable features. It is immediate, it requires a relatively small land area for set-up and operation, and it is a proven means of removal for many types of organic wastes. It is, however, a more costly treatment process when compared to biodegradation alternatives or vegetation (plant) extraction.

Thermal treatment technologies are either destruction or removal types of treatment. Most of the technologies are ex situ, which refers to the treatment process that occur with the soil moved from its original place; the treatment can take place either on-site or off-site. Of the 113 demonstrations being conducted under the United States Environmental Protection Agency (US EPA) Superfund Innovative Technology Evaluation (SITE) Program in 1999, 16.8% of the technologies being evaluated are thermal desorption (removal and collection), and 8.8% are thermal destruction [1].

Available thermal treatment technologies for remediation of contaminated soils include separation technologies such as thermal desorption; as well as destruction technologies of incineration and pyrolysis [2,3]. Separation technologies will have an off-gas stream that may require further treatment. Destruction technologies typically have a solid residue (ash) and possibly a liquid residue from the air pollution control equipment that will require treatment or disposal.

Incineration is the most common form of thermal destruction, which is intended to permanently destroy organic contaminants; it converts them to CO_2, H_2O, HCl, or other minerals. It utilizes high temperatures, typically 870 to 1,200°C, plus an oxidizing atmosphere and often turbulent combustion conditions to destroy wastes [4]. Incineration involves a complex system of interacting pieces of equipment. It represents an integrated system of components for waste preparation, feed, mixing, combustion, time and subsequent emission controls. An incineration system concept flow diagram is shown in Figure 2.1. Rotary kiln, fluidized bed, and infrared radiation heating are three common types of incineration systems for treating contaminated soils. Different designs and methods affect the engineering factors and operation parameters such as heating source

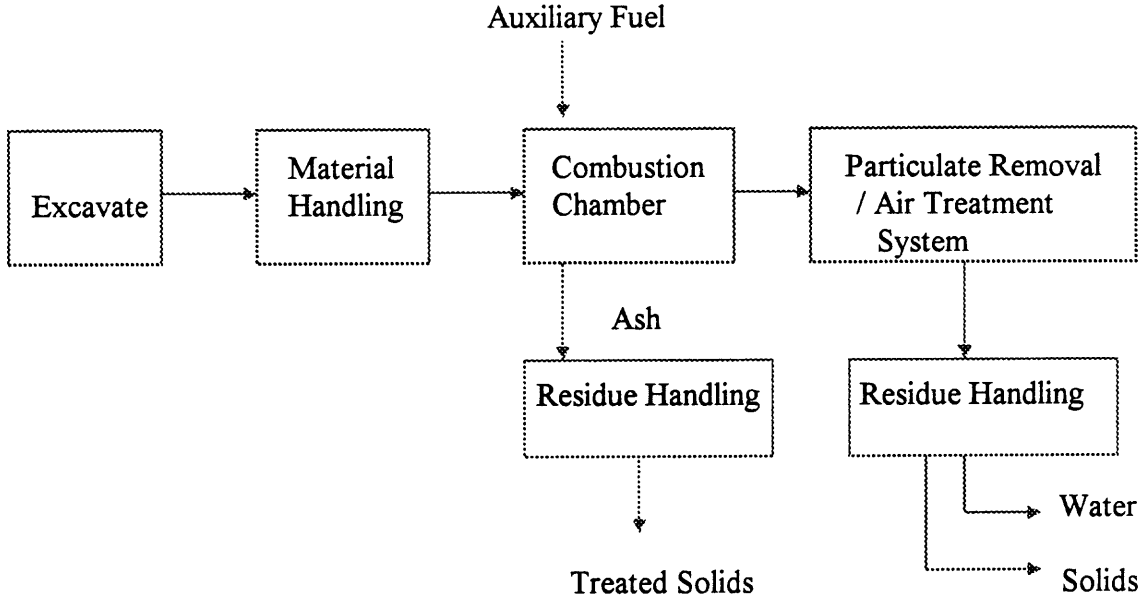

Figure 2.1 Schematic diagram of incineration.

arrangement, operation temperature required for the furnace, and solids residence time during which the contaminated soil is subject to the target temperature.

Thermal desorption technology is based on a physical separation system. The process physically separates (desorbs) organics from the soil without decomposition or with limited decomposition. Volatile and semi-volatile organics are removed from contaminated soil in thermal desorbers, usually operated at a temperature lower than 550°C. The bed temperatures and residence times of the desorbers are designed to quantitatively volatilize selected contaminants. Certain less volatile compounds may not be volatilized at low temperatures.

The thermal desorption process often uses an inert carrier gas to transport the volatilized organics and water to a gas treatment or collection system. The organic compounds in the exhaust gas may be treated in an afterburner or collected by physical/chemical treatment system. Collection typically uses a condenser followed by a cyclone, baghouse, wet scrubber or some combination of these devices. Thermal desorption systems are classified into three types: direct-fired rotary desorber, indirect-fired rotary desorber, and direct or indirect-fired conveyor systems. A schematic diagram of thermal desorption system is provided in Figure 2.2.

Pyrolysis, a third technology, means a chemical decomposition or change due to heating in the absence of oxygen. The objective of pyrolysis is usually a volatilization, but it is also accompanied by varied amounts of char formation. Volatilization includes evaporation of volatile species; it also includes bond cleavage reactions in higher

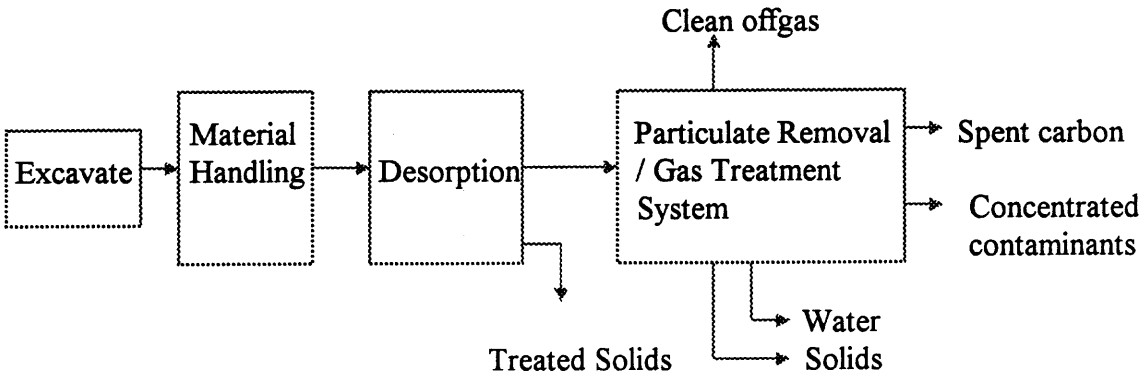

Figure 2.2 Schematic diagram of thermal desorption.

molecular weight species (often polymers) into smaller fragment molecules (often radicals), which enter the gas phase. The fragment radicals or species can further react, to smaller species by chain branching beta scission reactions, or can undergo combinations to intermediate size molecules.

It is usually not plausible to achieve a completely oxygen-free atmosphere and in practice, a nominal amount of oxidation (ca. 1 percent) will occur because some oxygen will be present in any pyrolysis system. The oxidation products in this fuel rich application are usually carbon monoxide. Thermal desorption will also occur under pyrolysis conditions if volatile or semi-volatile materials are present in the contaminated soil.

Application of pyrolysis to remediation technology involves a two-step process. The waste are heated, separating the volatile components (i.e., combustible gases and water vapors) from the nonvolatile char and ash. The volatile components from the first

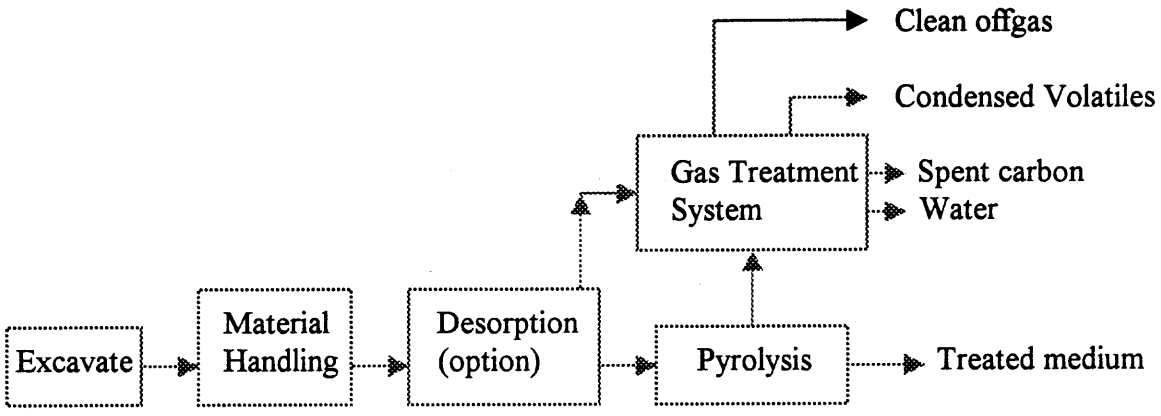

Figure 2.3 Schematic diagram of pyrolysis.

step are often burned under conditions needed to assure incineration of all hazardous components. This two-step process occurs in the pyrolysis chamber at temperatures of 800 to 2,100°F [5]. A general schematic of a pyrolysis technology is displayed in Figure 2.3.

The objective of this paper is to provide guidance for scientists and engineers who need to accomplish a thermal remediation technology, and must choose an appropriate

treatment process based on the current state-of-the-art technology, economics, and include allowance for public opinion(s). It is also intended to aid the engineers in applying their judgment to decide how to apply the technology addressed under the particular circumstances confronted.

The author have tried to summarize the available thermal technologies for remediation of contaminated soils. Each treatment processes, as well as the associated

treatment system components, were identified and described. Waste applicability was also included for each treatment technology. A detail list of feasible treatment processes was addressed with descriptions of site demonstration results to aid in evaluation of a selected process. In addition, energy components were discussed for energy cost requirement and safety considerations. Technology status was summarized to provide the current information on the technologies.

2.2 Thermal Treatment Systems

Thermal treatment systems, which are used in remediation of contaminated soils, may be divided into three major components: contaminated soil pretreatment and handling, the reactors, and post-treatment. Post-treatment includes treatment of gas, solid and liquids effluent from the primary reactor. Each of these will be discussed briefly here.

2.2.1 Contaminated Soil Pretreatment and Handling

Pretreatment of contaminated soils depends upon the nature of the contamination and of the soils being processed. Key soil characteristics that influence the application of thermal treatment include solid size distribution, moisture content, and contaminant characterization such as volatility, corrosiveness, and toxicity. Shredding and screening are usual pretreatment requirements. Blending is often used to effect uniformity of contaminant and moisture levels and to control the levels of contaminant in the process and effluent. Excessively wet media can be dewatered by filter presses and adsorbent addition. Highly acidic media may need neutralization such as treatment with lime to

mitigate corrosion of handling materials and treatment systems. Mechanical devices, such as rams and augers, are used to feed contaminated soils into the reactor.

2.2.1.1 Solid Particle Size Distribution. The maximum range of particle size that can be treated in most rotary kiln desorbers and incinerators is 5 to 7.6 cm due to materials handling limitations. The maximum size of particles for heated screw and belt-type conveyors processes however can be up to 10 cm based upon the screw diameter [6]. Screening, crushing, and shredding are pretreatment steps to reduce particle size of treated materials.

2.2.1.2 Contaminant Characterization. The lower explosive limit of combustible material in the desorber must be a primary consideration. The concentrations of organics in the exhaust gas of some types of thermal desorbers are limited to less than 25 percent of the lower explosive limit [7]. This safety precaution is normally implemented by sampling and analysis of feed materials where levels can then be moderated via blending .

2.2.1.3 Moisture Content. Moisture affects the amount of energy required to heat the medium as well as the handling characteristics of fine-grained soils. Typically less than 40 percent moisture is desired, 20 percent is considered ideal, and 5 percent is too low due to needs of moisture in controlling dust and further losses which occur in prehandling. Low moisture leads to dusting problems [6]. Pretreatment methods include use of filter presses, air drying, blending with drier material, and mixing with treated fines.

2.2.2 Reactors

There are several types of reactors in thermal treatment processes for remediation of contaminated soils. These include rotary kiln, fluidized bed, and conveyer belt flow

reactors with infrared heating for incineration. Rotary and conveyor units are used for thermal desorption. Pyrolysis is a third type of treatment, which can be very similar to thermal desorption if temperatures are similar. These are discussed more detail in Chapter 3.

2.2.3 Gas Post-Treatment

The purpose of an effluent gas post-treatment system is to remove pollutants from the effluent purge gas stream before it is discharged to the atmosphere. These pollutants consist of the original contaminates, plus the combustion or pyrolysis gas products, products of incomplete combustion, and particulate matter. Special measures and resistent materials may be needed to handle heavy metals, sulfur dioxide (SO_2), oxides of nitrogen (NO_x) hydrochloric acid (HCl), and other acids. Equipment used in the gas post-treatment process includes cyclone separators, secondary oxidizers (typically an afterburner or catalytic oxidizer), baghouses (filtration system), scrubbers, evaporative coolers, carbon adsorption filters, and condensers.

The cyclone separators are designed to remove the largest of the entrained particles from the gas stream. Cyclone separators are most efficient in removing larger particles (>15 μm) [6]. There are wet and dry cyclone separators, but only the dry ones are presently in thermal desorption system. The dry cyclone separator is a true inertial separator. Particles entrained in the gas stream enter the cyclone, are directed into a vortex flow pattern, flow to and collect on the wall of the separator because of inertial effects, and eventually drop to the receiver part of the unit. Wet cyclone separators operate on the same principle, but use water to assist in gas cleanup and particle entrainment.

The baghouse contains filters that collect finer entrained particles. Baghouses contain a series of permeable bags that allow the passage of gas but not particulate matter. Baghouses are used to remove particles as small as 0.01 um in diameter, and removal efficiency is relatively high for particles down to 0.5 um in diameter [6].

Destruction or recovery are two general control approaches for the post-treatment of organics. An oxidizer such as afterburner or catalytic oxidizer is used for thermal destruction of organics in the gas stream. The recovery system, which is normally used with indirect-fired units, uses condensation and refrigeration units followed by activated carbon treatment for collection of organics.

Afterburners typically operate between 760 to 980°C, with a 0.5 to 2.0 second gas-phase residence time [6]. Afterburners can be used before or after particulate control. Catalytic oxidizers have been also used for secondary oxidation to a lesser extent. The catalysts normally used are noble metal compounds, such as platinum or rhodium; they are used in small quantities and are deposited on a support material, such as alumina. The catalytic oxidizer must be located downstream from the particulate control and acid gas removal systems due to several reasons: a high-moisture content will adversely affect the operation of a catalytic bed and chlorine or sulfur compounds may poison the bed.

The recovery system uses an eductor scrubber, primary and secondary condensers, and a mist eliminator to recover the organics and water from the effluent gas stream, which is usually nitrogen. A high-energy scrubber is included in systems, which use the approach of direct contacting with water to cool the gas to its saturation temperature. Particulates and approximately 30 percent of the organics and considerable water can be removed from the effluent purge gas stream by this device. The primary condenser is air

cooled and reduces the effluent stream temperature to about 5°C over ambient temperature. Refrigeration in the second condenser reduces the effluent stream temperature to about 4.5°C [6].

Carbon adsorption is used to remove low concentrations of organic compounds from the gas phase. Carbon collection efficiency varies with the specific chemicals which are in the gases and selection of carbon adsorption unit type. Two important design parameters for carbon adsorption units are the empty bed contact time and superficial gas velocity. The empty bed contact time is the ratio of empty bed volume to the volumetric gas-flow rate through the bed. The superficial velocity is the ratio of the volumetric gas-flow rate to the cross-sectional area of the bed. These parameters are used in estimating the operating period before breakthrough.

Venturi scrubbers have been used to remove sulfur dioxide and hydrogen chloride. The venturi scrubbers also have the capability to remove particles larger than 5μm in the gas stream [6]. The heart of the venturi scrubbers is a venturi throat where gases pass through a reduced area reaching velocities in the range of 60 to 180 m/sec and thus enhances mixing. As the high-velocity gas stream removes gases, particles, and droplets from stack exhaust gases, a large number of fine water droplets are formed and entrained. The resultant water stream must be handled.

A significant difference in exhaust gas volume exists, between direct-fired and indirect-fired thermal desorbers. A larger capacity gas post-treatment system is usually required for a direct-fired thermal desorber than is required for an indirect-fired thermal desorber. This results from the increased gas volume incorporating the products of combustion from the fuel source. Indirect-fired systems and electrically heated conveyor

systems are sometimes preferred therefore, due to a smaller quantity of offgas required to be treated.

2.2.4 Solid and Liquid Post-Treatment

Solid post-treatment includes the treatment of ash and treated soils. Post-treatment of solids typically employs water quenching to cool the solid and to control the dust. Stabilization may be necessary if heavy metals are present.

Scrubber purge water from the reactors must be filtered or treated before release for those systems utilizing scrubbers. Total suspended solids can be reduced using granular filters and organics can be removed using carbon absorption treatment.

A considerable quantity of liquids can be recovered from the systems which use a condensing or other recovery treatment approach. The condensed liquid which contains organics and water, needs to be separated and treated. The treatment process involves passing the liquid through a liquid phase granular activated carbon adsorption system. The clean water effluent is recycled to the discharge pugmill for cooling and remoisturizing discharge material. The organics are shipped off for incineration or to recycling facilities.

2.3 Technology Identification and Description

There is a wide variety of equipment available for thermal treatment and remediation of contaminated soils. These range from high temperature devices used for thermal destruction process such as pyrolysis and incineration to more moderate temperature equipment used in thermal desorption processes such as rotary desorbers and heated-conveyors. Technical identification and description of the equipment is provided in the

following sections. Design factors such as heat source and waste feed mechanics, plus operation parameters such as temperature, solid residence time and carrier gas flow, along with advantages/disadvantages of each remediation technologies are discussed. Descriptions of some commercial treatment systems related to the technologies are also presented.

2.3.1 Incineration

Incineration is a process of combustion, resulting from the rapid and exothermic oxidation of substances (fuels, which are usually hydrocarbons). The process is very fast because of the high number of chain branching and the chain propagation reactions which occur at the incinerator temperature, relative to lower temperature processes. The relatively large amount of energy which is given off resulting in the high temperature operation. There are three major types of incinerator used in processes for contaminated soil remediation: rotary kiln, fluidized bed, and infrared radiant heating. A brief discussion of each of these technologies is presented below.

2.3.1.1 Rotary Kiln Incinerator. Rotary kiln incinerators are those in which the primary combustion chamber is a rotating cylinder usually lined with refractory materials. The cylindrical refractory-lined shell is mounted horizontally at a slight incline (usually less than 5 degrees)[8]. Turbulence and agitation are provided by the rotation of the kiln, which may rotate 5 to 25 times per hour. This mixes the waste with the combustion air, enhancing destruction and/or volatilization of the waste species and H_2O. A secondary high temperature combustion chamber may be attached in certain instances for complete

destruction of vapor and particles. Combustion temperatures range from 1,470°F to 2,370°F, with excess air ranging from 140 to 210 percent [8].

Low environmental impact can be anticipated due to the usual high destruction efficiencies in these rotary kilns with afterburner or other secondary combustion. Stack gas emissions are highly dependent on specific waste composition, its physical form, and non uniformity of feed. Emissions may consist of hydrochloric acid, chlorine, some ash and trace metals, which may require scrubbing and subsequent physical/chemical treatment. Scrubbers are also used to neutralize acid emissions.

Rotary kilns are more resistant to damage by high temperatures since they are usually completely refractory-lined. Residence times vary from 0.5 seconds for gases and fine particles to hours for bulky solids. Rotary kilns can be designed for batch feeding, or be equipped with liquid injection chambers. This gives rotary kilns great flexibility in the types of wastes that can be destroyed. A wide variety of wastes such as liquid, semi-solid (sludge), and solid wastes can be treated with rotary kiln incinerators and may be burned simultaneously. Other advantages of rotary kiln incinerators include a flexible feed system design which can be adapted to feed large containers, ease in adjustment of residence time by varying rotation speed of kiln, and resource recovery potential as demonstrated with cement kilns.

Disadvantages of rotary kiln incinerators include a required careful control of temperature in the kiln, which is necessary to prevent refractory damage, leakage at seals on the kiln ends and the feed chute. Gas tight seals are required at both ends of the kiln to prevent leakage, which may result in fugitive emissions that can cause air pollution problems and hazardous to personal working on the unit. Rotary kilns are therefore

usually operated under negative pressure to minimize the leakage problem. Uniformity in the reaction mixture may also be a disadvantage for rotary kilns. A rapid burning or volatilization of the waste or non uniformities in feed rate may cause the sudden excursions fuel equivalence ratios which can result in changes the combustion process or pressure surges which may result in leakage.

A number of companies are involved in the commercial development, operation and promotion of rotary kiln incinerators. For example, ENSCO/Pyrotech (Little Rock, AK) have a commercially available, transportable rotary kiln system. Their MWP2000 unit can accept liquid and solid wastes including soils. It consists of six trailer modules and requires four to six weeks for site set-up and shakedown. ENSCO has three of these systems, with one of these have been in use since 1984 to destroy chlorinated organics in wastewater, sludges and soils at a contaminated waste lagoon site in Florida.

IT Corporation (Knoxville, TN) is promoting their Hybrid Thermal Treatment System (HTTS); it is a commercially available, transportable, large rotary kiln [9]. The HTTS has an indicated capacity of handling more than 20 tons per hour of site soil, geared for effective operation at medium to large size sites.

2.3.1.2 Fluidized-Bed Incinerator. A fluidized bed incinerator uses a cylindrical bed of inert granular material to improve the transfer of heat to the liquids and sludges to be incinerated. Air is injected into the bottom of the vessel through a distributor plate at a rate sufficiently high to cause the particles in the bed to be strongly agitated so they behave, theoretically, as a fluid. Bed temperatures are restricted to the softening point of the bed material; a limitation of about 2,000°F for a sand bed. Chemicals such as salts or eutectic alkali metals are often added to the bed to increase the minimum melting points.

Mixing in the bed and the bed's large surface area provide virtually complete combustion at low excess air levels with minimal temperature variation throughout the bed.

Circulating fluidized-bed combustion is a modified form of fluidized-bed incinerator that has been adapted to use with mobile units on-site. This system circulates wastes and sorbent solids (limestone) through a combustion chamber that has a loop configuration. The second stage of the loop is a cyclone in which solids settle to the bottom for recirculation to the first stage and flue gases are exhausted from the top. Combustion occurs at a relatively low 900°C (which minimizes NO_x formation and ash slagging) with high degree of (nearly complete) mixing due to high turbulence [8]. Efficient combustion is achieved by injection of secondary combustion air at three different places in the combustion chamber. Major components of this system are the combustion chamber; the waste, fuel, and sorbent feeding systems; the ash removal system; the flue gas cooler; the baghouse filter; and the stack.

Advantages of fluidized-bed incinerators are a minimal requirement for excess air, potential to retain waste gases in the bed material, high degree of mixing, which results in a minimization of char and molecular weight growth products. Efficient combustion can be achieved due to the large surface of fluid bed. Wastes with a high moisture content are easily combusted in the fluidized-bed incinerator, due to high level of mixing and this good heat transfer. Maintenance costs are low since the large heat reservoir of the fluid bed minimizes thermal shock to the system. Capital costs are typically only one-half to three-quarters that of rotary kiln systems of comparable capacity.

High operating costs are one of the disadvantages of fluidized-bed incinerator. In addition, maximum combustion temperature is limited by the bed material and throughput

can be lower than in other incinerator designs. Residues are hard to remove from the bed of fluidized-bed incinerator.

The low-temperature fluidized bed developed by Waste-Tech Services Inc. operates at temperatures 1,400 to 1,700°F. The bed material is a mixture of a granular combustion catalyst and limestone. The system accepts liquid waste, sludge or granular solids which are injected into the bottom of the bed by a pneumatic injection tube. Uniformity of injection and possibility of puff formation need to be evaluated. Air is forced through the bed with sufficient velocity for fluidization to occur. Limestone is continuously added to the bed, and bed material is periodically drained from the vessel. Particulate removal is by a multicylone system with a baghouse or other collection system used for final flue gas cleanup. High temperature fluidized beds (1,700 to 2,200°F) are used where the use of catalytic beds is uneconomical or inefficient.

The system can handle dirt and rock associated with hazardous spills or contaminated soil. It has an air distribution header system which allows for bed letdown over the area of the bed. The system provides a residence time of two seconds for gases. Residence time for a particle (or liquid) is its residence in the fluidized bed plus two seconds as a gas.

In the circulating bed incinerator developed by GA Technologies, waste is introduced into a non-mechanical seal along with recirculating bed material from the hot cyclone, both of which are fed into the combustion chamber. An air velocity of 16 to 20 feet per second entrains the bed and waste, which rise through the reaction zone to the top of the combustion chamber and pass into the hot cyclone. Hot gas is separated from the solids in the cyclone and the solids are re-injected to the combustion chamber. The system

operates at 680 to 1,660°F depending on the waste type, with a residence time of two to three seconds for the gas phase and ten seconds to ten hours for solids or liquids. The hot flue gas passes through a convective gas cooler and then through baghouse filters.

2.3.1.3 Infrared Incinerator. The infrared reactor is designed to treat contaminated soils. It is composed of a rectangular carbon steel chamber lined with layers of ceramic fiber blanket. Energy is provided in the form of infrared radiation from silicon carbide resistance heating elements, or indirect fuel-fired radiant U-tubes. Wastes is fed into the combustion chamber by a conveyor belt and exposed to the radiant heat. Exhaust gases pass through a secondary combustion chamber with a higher temperature. Both external particulate control and acid gas scrubbing systems are required for post-treatment. This infrared incineration system has shown promise for the remediation of contaminated soil [2, 9].

The Shirco Infrared System is reported to be suitable for solids, sludges, and contaminated soils [10]. Waste is fed into the primary chamber at temperatures up to 1,800°F to volatilize and partially destroy organic volatiles in the soils matrix. The resultant gas is transported to a secondary combustion zone where it is burned under high temperature conditions of ca. 2,300°F. Secondary air is supplied to ensure excess oxygen for complete combustion. Exhaust gas from the secondary combustion chamber then is quenched and scrubbed by a water-fed venturi scrubber emissions-control-system to remove particulate matter and acid gases. An induced draft fan transfers the gas to the exhaust stack for discharge to the atmosphere. There is no fuel used in the reactor for heating and thus no particulate from this source, in the reactor emissions since energy is introduced by radiation.

2.3.2 Thermal Desorption

Thermal desorption is an ex situ means for physically separating organics from soils, sludges and other solid media. Little or no decomposition of organic contaminants is involved in the process. Air, combustion gas, or inert gas is used as the transfer medium for the vaporized components. Thermal desorption systems are not designed to provide high levels of organic destruction, although the higher temperatures of some systems may sometimes result in localized oxidation and/or pyrolysis. Direct-fired rotary desorbers, indirect-fired rotary desorbers, and direct or indirect-heated conveyor systems are three typical types of thermal desorption systems.

2.3.2.1 Direct Fired Rotary Desorber. The direct-fired rotary desorber technology is based on technologies used in such processes as asphalt and cement production, calcination, and common industrial drying processes. The use of mobile or stationary systems utilizing rotating drums to process granular materials is well established, and direct-fired rotary desorbers are often similar to conventional industrial units designed for these processes. There is a general uniformity in design and operation since many direct-fired rotary desorbers are adaptions of existing equipment.

The typical direct-fired rotary desorber system consists of three components: the pretreatment and material handling systems, the desorption unit, and the post-treatment systems for both the gas and the solid. The function of the desorption unit, the rotary desorber, is to heat the medium to a sufficient temperature and maintain it for a sufficient period to desorb the moisture and the contaminants from the medium. Material is passed through the rotating cylinder and is heated by direct heat exchange with a support flame and/or combustion products. The burner is usually fired with natural gas, propane, or fuel

oil. Combustion in the unit provides heat required to maintain the thermal desorber temperature. Direct-fired thermal desorber heat duties commonly range from 7 to 100 MM Btu/hr [7]. It is estimated that a heat input of 25,000 Btu/hr is the maximum required for each cubic foot of internal kiln desorber volume [6].

The maximum soil temperature that can be obtained in a rotary desorber depends on the materials of construction of the desorber shell. Most rotary desorbers are constructed from carbon steel and operate at soil discharge temperatures of 300 to 600°F, while those made of alloy steels are capable of operating up to 1,200°F.

The residence time of the material in the desorber is controlled by several parameters: rotation rate, the angle of inclination, solid feed rate, and the arrangement of internal lifters. The target residence times of petroleum or semivolatile organic contaminated soils in direct-fired thermal desorber usually range from 10 to 30 minutes. Typical rotation speeds range from 0.25 to 10 rev/min. Lifters which are often termed flights are typically attached to the inside surface of the cylinder to enhance gas/solid contact. Heat and mass transfer are therefore optimized within the unit.

The flow of solids may be either cocurrent or countercurrent to the direction of exhaust gas flow. The equipment downstream of a countercurrent rotary desorber is a cyclone, a baghouse, an ID fan, an afterburner, and a stack (see Figure 2.4). One advantage of the countercurrent system is that the exhaust gas can go directly to the baghouse without adding water or air for cooling, since the gases leaving the desorber will generally be cool enough to flow directly from the cyclone into the baghouse. The size of all process equipment downstream of the rotary desorber thus can be reduced in this

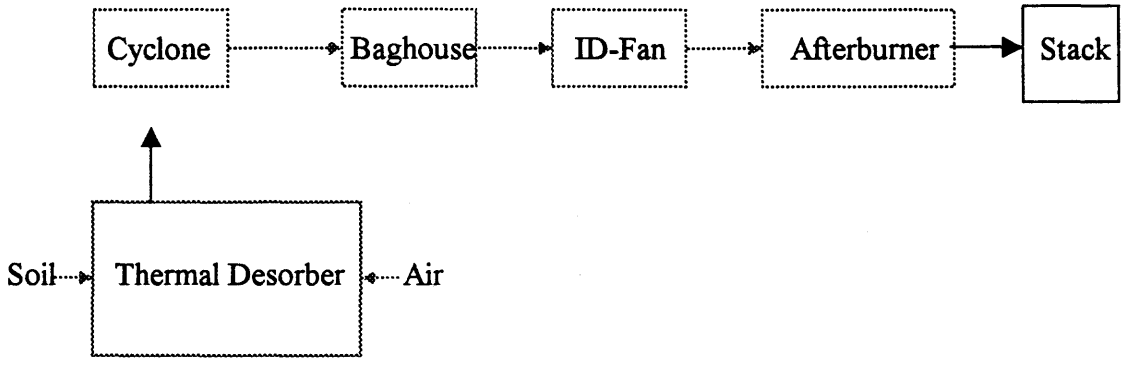

Figure 2.4 Counter-current rotary desorber system process flow diagram.

counter flow system. However, there is the potential of heavier organics to condense in the baghouse and blind the bags due to the relatively low baghouse operating temperature. Heavier organics are therefore not treated with this arrangement.

The equipment arrangement downstream of a cocurrent rotary desorber is a cyclone, an afterburner, an evaporative cooler, a baghouse, an ID fan, and a stack (see Figure 2.5). These cocurrent rotary desorber systems can treat heavy petroleum products, since baghouse blinding by condensed organic compounds is not a major consideration (due to afterburner).

Direct-fired thermal desorbers produce the largest volume of offgas per ton of treated material of any of the thermal desorbers. This is the pressure of combustion products from the fuel used to provide heat for the process. Excessive flow rates should be avoided in order to allow for the use of smaller air pollution control equipment and to minimize dust problems. The typical offgas velocities range from 5 to 15 ft/sec [7].

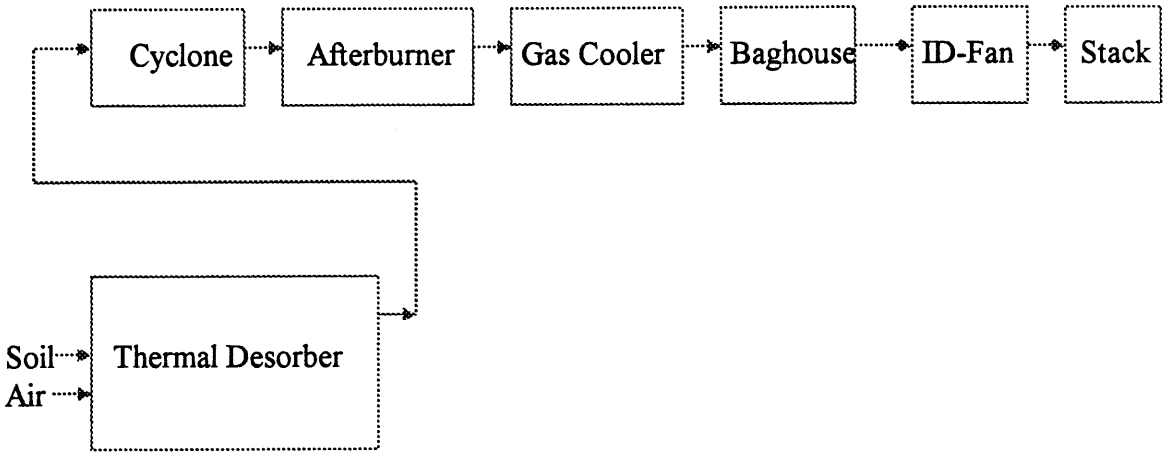

Figure 2.5 Co-current rotary desorber system process flow diagram.

2.3.2.2 Indirect Fired Rotary Desorber. Indirect-fired rotary desorbers were developed from equipment designed for materials drying techniques. Problems such as contamination of the heated material by the combustion gases or handling with explosive gases can be avoided by applying indirect heating to remove contaminants from soils. The indirect-fired rotary desorber system consists of three components: the pretreatment and material handling systems, the desorption unit, and the post-treatment systems for both the gas and the solid. Many of the operational requirements and considerations of indirect-fired rotary desorber are similar to those of the direct-fired rotary desorber.

The removal of combustion gases without contacting the waste material for indirect-fired rotary desorber makes a major difference between indirect-fired and direct-fired rotary desorber. The metal rotary shell is heated on the outside by the combustion of natural gas or propane. The hot shell indirectly heats the solids tumbling on the inside via

conduction through the metal shell. Refractory lining is not used because it would impede the heat transfer to the solids and it is not needed for low temperature operation. A sweep gas is used to transfer the volatilized organics and water to the offgas treatment system. The thermal desorber is under negative pressure that is induced by a fan downstream of the desorber.

Thirty to 120 minutes is the typical range of retention times. Rotation speeds can be as high as 2.5 rev/min. Angle of inclination varies from 1 to 2 degrees downward, moving the solids toward the exit end of the desorber. Feed rates vary depending on the waste characteristics and the contaminant residual levels required. Nominal feed rates for the process vary from 1.3 kg/sec to 2 kg/sec.

One major advantage of indirect-fired rotary desorber is that the combustion gases used in the heating do not pass through the associated air pollution control devices. Air permits for vent stacks from propane or natural gas combustors are easily obtained, usually without any required air pollution control (APC) devices. This allows the APC devices for the system to be one tenth to one hundredth of the size of that for an equivalent capacity incinerator. In addition, the amount of sweep gas which has been in contact with the waste is much less than that of direct-fired desorber and results in much lower cost of cleaning.

2.3.2.3 Heated Conveyor. Heated conveyors technology is based upon technologies used in mineral processing industries and in bulk solid chemical processing. The systems are in various stages of development depending on the specific conveyor and heating method. Conveyors used in thermal desorption applications consist of screw conveyors,

paddle or mixing conveyors, and belt conveyors. Direct or indirect heat is applied to the contaminated soil while it is transported or moved in a process conveyor.

In direct-heated conveyor, heat is transferred from a source in direct contact with the material being treated. Sources of heat consist of electric resistance heaters imbedded in the conveyor or a source located in the open space above the contaminated media in the conveyor (fuel combustion or radiant heaters). When electric heating is used, offgases generated during processing are greatly reduced. Direct-heated systems generate a greater volume of sweep gas than do indirect-heated systems. High dust generation and entrainment of particulate from the conveyor can be avoided by maintaining low-sweep gas velocities.

In indirect-heated conveyor systems, the heat is generated outside of the main process desorber in a separate, secondary process unit and is conducted by a media in contact with the desorber conveyor. The source of heat can be the combustion of a common fuel or waste process heat from another process system. Indirect systems employ various media to transfer the heat to the conveyor: steam, special heat transfer fluids, and eutectic salts. The heat transfer fluid heating system may be fired with propane, natural gas, or No. 2 fuel oil. The majority of the combustion gas does not contact the contaminated soils and can be discharged directly to the atmosphere without emission controls. A fraction of the flue gas from the hot oil heating system is recycled to the conveyor system. This recycled flue gas maintains the exhaust gas exit temperature above 300°F so that volatilized organics and moisture do not condense. The recycled flue gas has a low oxygen content (less than 2 percent by volume oxygen) and provides an inert atmosphere to minimize oxidation of organics. The maximum soil temperature that can be

attained in a conveyor system is limited by the temperature of the heat transfer fluid and the materials of construction of the system. Hot oil heated systems can achieve soil temperatures of up to 500°F and steam heated systems can heat soil up to 350°F.

The volume of exhaust gas from the primary thermal treatment unit operation of indirect-heated system may be a factor of 2 to 10 times less than the volume from a directly heated system with an equivalent soil processing capacity. The size of gas treatment systems therefore can be much reduced. Higher organic content soils can be treated with indirect system since the flame does not directly contact with the contaminants.

The retention time of the conveyor system is determined by the volumetric feed rate of the media and conveying velocity of the system. The retention time of belt conveyor system is based upon bed depth, due to volatilization limitations and belt speed. Throughput of screw conveyors can be varied with rotational speed, diameter, and flight pitch.

The conveyor system can heat soils to temperatures ranging from 300 to 800°F. Treated soil exits the conveyor system will be sprayed with water for cooling and dust control. The exhaust gas exits the conveyor reactor and is treated in an exhaust gas treatment system that consists of an afterburner, quench chamber, and venturi type scrubber. Water discharged from the scrubber is used to cool the decontaminated soils.

2.3.3 Pyrolysis

Pyrolysis is the chemical decomposition of waste brought about by heating the material in the absence of oxygen. This thermal destruction process is performed in a two-chamber

system. The wastes are heated in the primary chamber, resulting the volatile components being separated from the nonvolatile ash, such as metals and salts. Hazardous organic materials are transformed into gaseous components, small quantities of liquid, and a solid residue (coke) containing fixed carbon and ash. Pyrolysis of organic materials produce combustible gases, including carbon monoxide, hydrogen and methane, and other hydrocarbons. Volatile components are burned afterwards in the secondary chamber under the proper air, temperature, time, and turbulence to destroy any remaining hazardous components. Particulate can be removed using equipments such as filters or wet scrubbers. This two-step process occurs in the pyrolysis chamber typically under pressure and at temperatures of 800 to 2,100°F.

An advantage of pyrolysis is the potential for resource recovery. The hot combustion gases from the secondary chamber can be passed through a boiler to recovery energy. Several factors however may limit the applicability and effectiveness of the process. One limiting factor is the requirements of specific feed size and materials handling that impact applicability or cost at specific sites. The technology also requires drying of the soil to achieve a low soil moisture content which is less than one percent. High moisture content of soil thus increases treatment costs. In addition, highly abrasive feed can potentially damage the processor unit. Treated media containing heavy metals may require stabilization. Pyrolysis at very high temperatures can result in undesirable char and tar formations. The pyrolysis rate and temperature can be limited to control this.

Pyrolysis is an emerging technology. The basic concepts of the process although have been validated, the performance data for an emerging technology have not been evaluated according to methods approved by EPA and adhering to EPA quality

assurance/quality control standards. Performance data are currently available only for vendors.

2.4 Waste Applicability

The physical and chemical properties of the feed soils determine the performance of treatment systems. These physical/chemical properties include: heat value, soil particle size, moisture content, concentration and distribution of contaminants, and acid forming elements such as sulfur and the halogens. A thorough characterization of the site and a well-designed and conducted treatibility study are required to perform a contaminated site soil remediation.

2.4.1 Incineration

Incineration is used to remediate soils contaminated with explosives and hazardous wastes, particularly chlorinated hydrocarbons, PCBs, and dioxins [4]. Constituents of the waste data must be evaluated to achieve an efficient combustion. Sulfur or chlorine content influences sulfur dioxide and hydrogen chloride levels released from the combustion process and requires secondary recovery and neutralization. Significant levels of toxic trace metals, such as lead, cadmium, or arsenic, in the waste may prevent it from being incinerated. The incineration of such metals may require stringent, specialized air pollution control measures and result in classification of the ash as a hazardous waste, which can make its disposal prohibitively expensive.

Heating value of the feed material affects both feed capacity and fuel usage of the incinerator. Information on the heating value of the feed is required in operating an

incineration system and in determining the need for auxiliary fuel. A minimum heat content of 17 to $22*10^6$ BTU per ton is generally necessary to sustain combustion [11]. The heat value of a waste decrease with an increase in moisture and/or chlorine content. An increased heating value of feed material however can raise incinerator temperature, which can become uncontrollable. The use of water injection has been used to control the operation of incineration for the feeds with high heat content such as brominated hydrocarbon sludge.

Moisture content can either improve or impede incinerator performance depending upon the heat content of the waste. Moisture acts as a heat sink to control reactor temperature for the feeds with high heat value. Moisture increases auxiliary fuel requirements while using feeds with low heat content, results in the decrease of afterburner residence time. Feed rate must be decreased to maintain afterburner residence time.

2.4.2 Thermal Desorption

The target contaminants for thermal desorption are volatile organic compounds (VOCs), semivolatile organic compounds (SVOCs), polychlorinated biphenyls (PCBs), and pesticides [4]. The technology is usually not effective in separating inorganics from the contaminated medium. Volatile organic compounds and fuels also may be treated, but treatment may be less cost-effective. Extremely volatile metals may be removed by higher temperature thermal desorption systems. The presence of chlorine can affect the volatilization of some metals, such as lead. The process is applicable for the separation of

organics from refinery wastes, coal tar wastes, wood-treating wastes, creosote-contaminated soils, hydrocarbon-contaminated soils, mixed (radioactive and hazardous) wastes, synthetic rubber processing wastes, and paint wastes.

Moisture content is important because of the energy required to heat and vaporize the water in the solid. Moisture is a major heat sink in the thermal desorber. Solids typically with less than 40 percent moisture is desired, 20 percent is considered ideal, and five percent is too low due to prehandling dust problems [6]. High moisture levels (> 40 percent) require more fuel and larger residual liquid handling systems and present additional materials handling problems. Processing rates are also lowered.

2.4.3 Pyrolysis

The target contaminant groups for pyrolysis are SVOCs and pesticides [4]. The process is applicable for the separation of organics from refinery wastes, coal tar wastes, wood-treating wastes, creosote-contaminated soils, and hydrocarbon-contaminated soils.

Pyrolysis systems may be applicable to a number or organic materials that undergo a chemical decomposition in the presence of heat. Pyrolysis has shown promise in treating organic contaminants in soils and oily sludges. Chemical contaminants for which treatment data exist include PCBs, dioxins, PAHs, and many other organics. Pyrolysis is not effective in either destroying or physically separating inorganics from the contaminated medium. Volatile metals may be removed as a result of the higher temperatures associated with the process but are similarly not destroyed.

2.5 Feasible Treatment Processes and Site Demonstration

Thermal technologies are classified and described for each component of the treatment technology, as indicated in chapter 2 and chapter 3. A detailed description of specific feasible treatment processes will be discussed in this chapter. Pretreatment, reactor design, and post-treatment systems are described. Site demonstration examples including site information, waste characterization, operation parameters used and performance results are presented as case studies of the treatment process.

2.5.1 Incineration Systems

Several feasible incineration systems are described in the following sections.

2.5.1.1 Weston Rotary Kiln System - Rotary Kiln Incinerator. Weston Rotary Kiln System, developed by Weston Inc., West Chester, PA, uses a transportable rotary kiln incinerator for PCB destruction. This system is comprised of a 7.5 ft by 25 ft long rotary kiln furnace, hopper/screw feed system, secondary combustion chamber (after-burner), multifuel burner, ash handling, heat recovery, exhaust gas fabric filtration (baghouse) system, optional gas scrubbing, induction fans and exhaust stack.

The kiln is a rotating cylindrical steel shell, refractory-lined and is mounted on a slight angle from horizontal. The burner is mounted above the feed inlet and combustion gas flow is concurrent with movement of the feed. The kiln operates at a temperature up to 2,500°F with a throughput of 2 to 8 tons per hour. Solid retention time is 15 to 90 minutes. Off-gases are treated in the secondary chamber for two seconds at 2,300°F.

Exhaust gases from the kiln are passed to an after-burner, then water-cooled to

1000°F in a spray tower. Particulate fallout is transferred to the ash collection system. The exhaust gas then enters the baghouse filters which remove the particulates. Exhaust gases from the baghouse are directed to the horizontal packed tower scrubber. The acidic gases are neutralized and scrubbed from the flue gas with a caustic solution. The final gases are released to the atmosphere through a stack.

2.5.1.2 Circulating Bed Combustor (CBC) System - Fluidized Bed Incinerator.

The Ogden Circulating Bed Combustor System was developed by Ogden Environmental Services Inc, Houston, TX. This system is composed of a combustion chamber, cyclone collector, flue gas cooler, baghouse and stack. Combustible solids or sludges and auxiliary fuel are individually introduced into the bottom of the 30 ft high combustion chamber, along with a sorbant (limestone) and inert material. Forced draft fans provide high velocity atmospheric gas to the bottom of the combustion chamber. The heavier non-combustible solid materials settle towards the bottom of the combustion chamber forming the bed, which is fluidized by high velocity gas. Lighter solids are carried upwards in the combustion chamber. Additional air is injected into the combustion chamber to enhance combustion and to reduce NO_x and CO emissions. The lighter solids are separated from the gases in a hot cyclone collector, and returned to the combustion chamber via a loop seal. The off-gases are cooled and passed through baghouse collectors to remove fine particulates (fly ash). Residence times of the solids and gases are approximately 30 minutes and two seconds, respectively.

2.5.1.3 Shirco Infrared Incineration System - Infrared Incinerator

Process Description. The transportable Shirco Infrared Thermal destruction System was developed by Shirco Infrared Systems Inc, Dallas, Texas [12]. This system consists of a waste preparation system and weigh hopper, infrared primary combustion chamber, supplemental propane-fired secondary combustion chamber, emergency bypass stack or diesel generator and auxiliary emergency shutdown system, venturi/scrubber exhaust system, and data collection and control system -- all mounted on transportable trailers.

Solid waste feed material is processed by waste preparation equipment designed to reduce the waste to the consistency and particle sizes that can be processed by the unit's primary combustion chamber. The primary combustion chamber is a rectangular box insulated by layers of ceramic fiber. Combustion air is supplied to the primary combustion chamber through a series of air ports at points along the length of the chamber. The gas flow in the incinerator is countercurrent to the conveyed feed material. Electric infrared heating-elements installed above the conveyor belt heat the waste to the designated temperature (typically 1,400-2,600°F), which results in desorption or incineration of organic contaminants from the feed. Rotary rakes gently turn the material to ensure adequate mixing and complete desorption. The waste soil reaches the discharge end of the chamber after thermally treated, then is cooled with a water spray and discharged by a crew-auger/conveyor to ash hopper.

Exhaust gas containing the desorbed contaminants exits the primary combustion chamber into an afterburner (or secondary combustion chamber) where propane-fired

burners combust residual organic compounds into CO_2, CO, HCl, and H_2O. The afterburner is typically operated at 2,200°F and gas residence time exceeding 2 seconds. Secondary air is supplied to ensure adequate excess oxygen levels for complete combustion. Exhaust gas from the afterburner is quenched and scrubbed by a water-fed venturi-scrubber emissions-control-system to remove particulate matter and acid gases.

Table 2.1 Applicable Range of Waste Characteristics

Characteristics	Applicable Range
Morphology	Soil/solid Semi-solid Oily-sludge/solid
Particle size (diameter)	5 microns - 2 in.
Moisture content	0 - 50 wt % (no free liquids or free-flowing sludges)
Density	30 - 130 lb/ft^3
Heating value	0 - 10,000 Btu/lb
Organics	0 - 100 wt % (determined by preoperation testing)
Chlorine	0 - 5 wt %
Sulfur	0 - 5 wt %
Phosphorous	0 - 300 ppm
pH	5 - 9
Alkali metals	0 - 1 wt %
Heavy metals	0 - 1 wt % (determined by preoperation testing)

An induced draft fan transfers the gas to the exhaust stack for discharge to the atmosphere.

Waste Applicability. Information on both the physical and chemical characteristics of the waste matrix is necessary to determine the suitability of that waste for thermal processing using the Shirco technology and the possible need for waste preparation and pretreatment. Table 2.1 presents a range of waste characteristics suitable for processing in the Shirco unit.

Materials greater than 2 in. or less than 5 microns cannot be processed by the Shirco system. Wastes with a size greater than 2 in. or clumpy sludge-like materials, diffusion of contaminants through the particles and through the bed to expose contaminants to the infrared heat is diminished. Wastes with a size less than 5 microns lead to the possibility of very light fines being generated that would be carried through the system and possibly cause an overload on the emissions control system or problems with the ash handling system.

Acid gases are formed when waste feed containing chlorine, fluorine, bromine, sulfur, and phosphorous are thermally treated. The Shirco unit design thus places maximum limits on the halogen, sulfur and phosphorous content. It is recommended that the range of pH 5 to 9, and chlorine and sulfur contents not exceeding five percent. Heavy metal concentrations less than one wt % are processed in the Shirco unit.

Site Demonstration. The SITE (Superfund Innovative Technology Evaluation) program demonstration of the Shirco Pilot-Scale Infrared Incineration System for thermal treatment was conducted at the Demode Road Superfund Site in Rose Township, Mich. The demonstration was conducted from November 2-13, 1987 and treated 1,799 kg of

contaminated soil under various test conditions. The site soil used for demonstration was highly contaminated by PCBs and lead, with concentrations up to 600 ppm and 3,000 ppm, respectively.

The Shirco Infrared System operated with a residence time of 15-25 minutes, a primary combustion chamber temperature of 900-1,600°F, and a secondary combustion chamber temperature of 1,800-2,200°F. The Shirco unit achieved a DRE for PCBs greater than 99.99 percent. The test demonstration of the pilot-scale unit showed that, based on the test results, the Shirco system is a viable technology for application at the Demode Road Superfund site.

2.5.2 Thermal Desorption Systems

Several feasible thermal desorption systems are described in the following sections.

2.5.2.1 LTTA System - Direct-Fired Thermal Desorber:

Process Description. The Low Temperature Thermal Aeration (LTTA) process was developed by Canonie Environmental Services Inc., Porter, Indiana, as a treatment system that desorbes contaminants from soils by heating the soils up to 800°F. The main components of the LTTA process include a materials dryer, a pug mill, two cyclonic separators, a baghouse, a wet Venturi scrubber, a liquid-phase granular activated carbon (GAC) column, and two vapor-phase GAC beds.

Contaminated soils are introduced into the materials dryer by a conveyor belt. Contaminated soils are heated by a parallel-flow hot air stream heated by a propane/fuel oil burner. The materials dryer is a rotating drum 8 ft in diameter and 40 ft long equipped with longitudinal flights for soil mixing.

Processed soil is discharged to an enclosed pug mill, where water is added to cool it and to control fugitive dust emissions. The exhaust air stream from the materials dryer is treated with a series of standard air pollution control devices before being vented to the atmosphere. The exhaust air stream is first vented into cyclonic separators followed by a baghouse to remove coarse particulates, then directed to a wet Venturi scrubber to remove fine particulates and to neutralize acid vapors. Two vapor-phase GAC beds remove any remaining organic contaminants before the treated exhaust air stream is vented to the atmosphere.

Waste Applicability. The LTTA process can remove volatile organic compounds (VOC), semivolatile organic compounds (SVOC), volatile and semivolatile organochlorine pesticides (OCP), organophosphorous pesticides (OPP), and total petroleum hydrocarbons (TPH) from soils, sediments, and sludges. Canonie reports removal efficiencies of greater than 99 percent for VOCs at concentrations up to 5,400 mg/kg, greater than 92 percent for pesticides up to 1,500 mg/kg, and 67 to 96 percent for SVOCs up to 6.5 mg/kg.

Site Demonstration. The LTTA demonstration was conducted in September, 1992, as part of ongoing remediation of a pesticide-contaminated site in western Arizona. Feed soil consisted of a dry, clay or clay-like loam and had been impacted with toxaphene, DDT, its derivatives DDD and DDE as well as other pesticides. Soils were heated to 730°F. A feed rate ranging between 34 and 38 tons/hr was utilized during the demonstration.

The LTTA process met the specified cleanup criteria for the site. Residual levels of all the pesticides in the treated soil were generally below or close to the laboratory

detection limit. The LTTA process did not generate observable levels of dioxins or furans as products of incomplete combustion or thermal transformation.

2.5.2.2 SoilTech ATP System - Indirect-Fired Thermal Desorber:

Process Description. The SoilTech Anaerobic Thermal Processor (ATP) system is licensed by SoilTech ATP Systems Inc, Porter, Indiana [13]. The ATP technology involves a physical separation process that thermally desorbes organics such as polychlorinated biphenyls (PCBs) from soil and sludge. The processor consists of four separate thermal zones: the preheat, retort, combustion, and cooling zones.

Contaminated soils are sprayed with a diesel fuel and oil mixture containing alkaline polyethylene glycol (APEG) reagents before entering the preheat zone.. Water and volatile organic compounds (VOC) initially vaporize in the preheat zone (400-650°F). The reagents dehalogenate or chemically break down chlorinated compounds, including PCBs. The vaporized contaminants and water are removed by a vacuum to a preheat vapor cooling system. The noncondensed light organic vapors are then fed into the combustion chamber of the processor.

The remaining hot, granular solids pass through a sand seal to the retort zone (900-1,150°F). Heavy oils vaporize, and thermal cracking of hydrocarbons forms coke and low molecular weight gases. The vapor stream from the retort zone passes through a pair of cyclones to remove entrained particles, and cooled by a two-stage direct contact condenser for the higher boiling point compounds. The remaining vapors are then cooled in a water-cooled noncontact condenser and pass through a 3-phase separator.

The coked soils pass through a second sand seal into the combustion zone (1,200-1,450°F). The coked soils are combusted and either recycled to the retort zone or sent to

be cooled in the cooling zone. Flue gas from the combustion zone is treated in a system consisting of a cyclone and baghouse that remove particulates; a scrubber that removes acid gases; and a carbon adsorption bed that removes trace organics. The treated flue gas is then discharged to the atmosphere through a stack. Treated soils exiting the cooling zone (500-800°F) are quenched with water and are then transported by conveyor to an outside storage pile.

Waste Applicability. The ATP system is used to dechlorinate and burn carbon residues from PCBs and chlorinated pesticides in soils and sludges; to separate oils and water from refinery wastes and spills; and to remove hazardous VOCs and semivolatile organic compounds (SVOC) from soils and sludges. The ATP unit is capable of processing about 10 tons of contaminated soil or sediment per hour. The optimal moisture content of the waste to be treated is between five percent and ten percent by weight. Wastes with a moisture content greater than 20 percent may need to be dewatered to optimize process economics.

Site Demonstration. The SoilTech Anaerobic Thermal Processor mobile treatment system was demonstrated at the Wide Beach Development Superfund site in Brant, New York from October 1990 to September 1991. Contamination of soil at the Wide Beach site resulted from the spraying of waste oil containing polychlorinated biphenyls (PCBs) over the roadways in the community to control dust. Approximately 42,000 tons of stockpiled soil contaminated with PCBs, mainly Arochlor 1254, at concentrations ranging from 10 to 5,000 mg/kg, were treated.

Performance results showed that about 98 percent of the PCBs were removed using the SoilTech ATP System. The concentrations of PCBs in treated soil were

generally at or below the reported detection limit (0.5 mg/kg). Treatment of 42,000 tons of soil was completed in a one year period. Stack gas emission requirements were met for PCBs, PEG, and particulates during the demonstration test.

2.5.2.3 MT's Indirect System - Indirect-Fired Thermal Desorber:

Process Description. The Indirect System, which was developed by Maxymillian Technologies (MT), Inc., Pittsfieod, Massachusetts, is an indirectly heated thermal desorption system for decontaminating soils contaminated with PCBs [14]. This system is mobile and trailer-mounted for easy transport to remediation sites to treat contaminated soils. The system is designed to effectively decontaminate PCB soil to below 2 ppm at a rate of 10 to 20 tons per hour. MT developed the Indirect System to meet a growing need for cost-effective, mobile, high-throughput technologies that effectively remediate soils contaminated with PCBs.

MT's Indirect System is an indirect-fired rotary desorber, with collection of organics in the off-gas by condensation and adsorption. A steam process enhances desorption efficiency. Condensed contaminants and water are processed through MT's mobile Series IIIA water treatment system where contaminants are removed, concentrated and collected.

The system indirectly heats soil in an enclosed rotary drum volatilizer where contaminants are desorbed from the soil. The system is designed to operate over a range of soil discharge temperatures from 250°F to 1000°F. Contaminants are both filtered and condensed from the effluent carrier gas, and are then treated and removed from the liquid stream. Vapors are carried through a HEPA filter for particulate removal, then through vapor phase carbon, and then another HEPA filter/polymer tray system.

One specific design feature of the Indirect System is a proprietary technique of using steam to strip residual contaminants from the soil. Steam stripping is a separate process that occurs after thermal desorption in the rotary drum volatilizer.

Waste Applicability. The Indirect System can handle a variety of soil types and consistencies at a high throughput for a mobile desorption system. The system is not limited by Btu value or contaminant concentrations of the soil. The unit is designed to treat material with a moisture content of up to 20 percent.

Site Demonstration. A Research & Development (R&D) Test was conducted using the Indirect System in the South Glens Falls Drag Strip Site, from December 1995 to early 1996. The Indirect System successfully treated several hundreds tons of PCB contaminated soil. A range of soil throughput from 6.3 to 15.5 tons per hour was used and 625-904°F of soil exit temperature reached in this application. Soil cleanup levels of less than 2 ppm were achieved for all test runs.

2.5.2.4 Low Temperature Thermal Desorption (LT^3) System - Indirect-Fired Thermal Desorber:

Process Description. The low temperature thermal treatment (LT^3) system was developed and demonstrated by Weston Inc., West Chester, PA [10, 15]. This system thermally desorbs organic compounds from contaminated soil without heating the soil to full combustion temperatures. The LT^3 system consists of four major components: a solids handling system, a hot oil indirect heating system, an effluent gas handling system, and a water effluent treatment system. The system is comprised of equipment assembled on three flat-bed trailers and requires an area of about 75 feet (23 meters) square.

Contaminated soil is excavated and screened before treatment. Screened material is transported by an enclosed drag conveyor to a hopper that directly feeds the thermal processor. The thermal processor is an indirectly heated auger type heat exchanger for solids and slurries. The processor mixes, conveys, agitates, and heats the contaminated soils allowing the moisture and volatiles to vaporize and escape from the soil. Hot oil circulates through the hollow screws and through jackets and acts as a heat transfer fluid. A burner heats the circulating oil to an operating temperature of 400 to 650°F. Combustion gases released from the burner are used as sweep gas in the thermal processor, and served to limit direct combustion in the treatment process.

The vaporized contaminants are swept from the thermal processor using a sweep gas mixture of air and exhaust gases from the hot oil system. The oxygen content in the sweep gas is controlled by the quantity of exhaust gases from the hot oil system to provide the efficiency and safety of the system. The sweep gas carries the volatiles through a fabric filter (baghouse) for particulate emissions control and then into a condensor. The condensor reduces the water load on the subsequent afterburner and often condenses volatiles.

Condensate from the condenser is composed of water and condensed volatile organics. The two-phase condensate is separated in an oil/water separator. The water is then treated in a two-stage carbon absorption system.

Waste Applicability. The LT^3 system can process a wide variety of soils with differing moisture and contaminant concentrations. This system is best suited for soils with a moisture of less than 20 percent and VOC concentrations of up to 1 percent. SVOCs with boiling points greater than 500°F can also be treated, but treatment must be evaluated

based on cleanup objectives. Wastes with a moisture content between 20 and 50 percent can be treated at a reduced capacity basis. Wastes with a moisture content greater than 50 percent need to be dewatered to enable treatment in the LT^3 system.

Site Demonstration. The LT^3 system was demonstrated at the Anderson Development Company (ADC) site located in Adrian, Lewanee County, Michigan, from January 1992 to June 1993. The ADC site was used for the manufacture of 4,4-methylene bis (2-chloroaniline) or MBOCA, a hardening agent used in plastics manufacturing. The contaminant characterization result showed that 4,4-ethylene bis (2-chloroaniline) (MBOCA) was identified as the primary constituent of concern. Other VOCs present in the site soil included toluene and degradation products of MBOCA. High levels of metals (e.g., manganese at levels up to ten percent) were also present at the site.

The LT^3 thermal processor operated with a residence time of 90 minutes and a soil/sludge temperature of 500-530°F in this application. Performance results showed that cleanup goals for treated soil and sludge in this application were met for 4,4-ethylene bis (2-chloroaniline) (MBOCA) and six other VOCs, eight of nine SVOCs with a range of 20 ppb (e.g., for benzene) to 80,000 ppb (e.g., for phenol). Elevated levels of manganese were measured in the treated soil; as a result, ADC was required to dispose of treated soils in an off-site landfill. This cleanup of 5,100 tons of soil and sludge was completed in a 17 months period.

2.5.2.5 X*TRAX System - Indirect-Fired Thermal Desorber:

Process Description. The X*TRAX Model 200 Thermal Desorption System was developed by Chemical Waste Management, Inc., subsequently operated by Rust Remedial Services, Inc. and currently by OHM Remediation Services, Inc [16]. This system involves

a low temperature desorption process designed to remove organic contaminants from soils, sludges, and other solid media.

The X*TRAX system is a thermal/physical separation process. Contaminated materials are fed into an externally heated dryer in which water and organic contaminants are volatilized from the solids. Processed solids exit the dryer at between 450 and 850°F and are cooled with water to eliminate dusting. The treated solids can be returned to their original location and compacted in place.

The organic contaminants and water vapor that are volatilized from the solids are transported out of the dryer by an inert carrier gas. the carrier gas is ducted to the gas treatment system, where it passes through a cyclone (for fine particulate removal) and then a high-energy eductor scrubber. the scrubber removes high boiling point organic compounds, cooling the gas to 180°F. Carrier gas exiting the scrubber then passes through two condensers in series where it is cooled to less than 50°F. Most of the conditioned carrier gas is reheated and recycled to the dryer. Approximately 10 percent of the carrier gas is vented through a high efficiency particulate air (HEPA) filter and a carbon adsorption train before it is discharged.

Site Demonstration. Full scale operation of the X*TRAX system was performed in 1993 at the Re-Solve Superfund site in North Dartmouth, Massachusetts. Initial 45,000 Tons of PCB-contaminated soil required treatment. PCB levels in the feed soil ranged from 25 ppm to 13,000 ppm. The system was operated at continuous feed rates of up to 11 tons/hr and consistent operation was achieved with the product temperature between 500 and 750°F, product soil typically contained less than 2 ppm PCBs. PCB levels in the

feed ranged from 181 to 515 ppm. The treated soil samples typically contained less than 1 ppm PCB.

2.6 Technology Status

Incineration, either off-site or on-site, has been selected or used as the remedial action at more than 150 Superfund sites. Table 2.2 lists the site experience of the various mobile/transportable incinerator systems. It includes information on the incinerator type/size, site location, and contaminant source or waste type treated [2].

Soil treatment costs at off-site incinerators range from $220 to $1,100 per metric ton ($200 to $1,000 per ton) of soil, including all project costs [4]. Mobile units that can be operated on-site will reduce soil transportation costs. Soils contaminated with PCBs or dioxins cost $1,650 to $6,600 per metric ton ($1,500 to $6,000 per ton) to incinerate. The cost of incineration includes fixed and operational costs. Fixed costs include site preparation, permitting, and mobilization/demobilization. Operational costs such as labor, utilities, and fuel are dependent on the type of waste treated and the size of the site.

Thermal desorption has been selected 51 times for superfund remedial actions, according to Records of Decision (RODs) for fiscal years 1982-1994 [17]. Seventeen projects are completed; another 13 are operating. Thermal desorption projects take less time to implement, from 1 to 18 months for the 13 remedial projects completed, compared to another frequently selected innovative technology- soil vapor extraction. Contaminants treated are shown in Figure 2.6. This technology is used to treat SVOCs as well as VOCs.

Table 2.2 Mobile/Transportable Incinerator Technology Status

Treatment System/ Vendor	Thermal Capacity (MM BTU/Hr)	Site, Location	Contaminant Source or Waste Type
Rotary Kiln /Ensco	35	Sydney Mines, Valrico, FL Naval Construction Battalion Center, Gulfport, MS Smithiville, Canada	Waste oil Dioxin/soil PCB transformer leaks
	100	Bridgeport Rental, Bridgeport, NJ	Used oil recycling
Rotary Kiln / IT	56	Motco, Texas City, TX	Styrene tar disposal pits
Rotary Kiln / Vesta	8	Fairway Six Site, Aberdeen, NC	Pesticide dump
	12	Nyana/Nyacol Site, Ashland, MA American Crossarm & Conduit Site Chehalis, WA	Dye manufacturing Wood treatment
Rotary Kiln / Weston	35	Lauder Salvage, Beardstown, IL Paxton Ave., Chicago, IL	Metal scrap salvage Waste lagoon
Rotary Kiln / AET	20	Valdez, AK	Crude oil spill
Rotary Kiln / Boliden	40	Oak Creek, WI	Dye manufacturing
Rotary Kiln / Harmon	82	Bog Creek, Howell Township, NJ	Organics
Rotary Kiln / Bell	30	Bell Lumber & Pole, New Brighton, MN	Wood treatment
Rotary Kiln / Kimmins	100	Lasalle, IL	PCB capacitor manufacturing
Rotary Kiln / USEPA	10	Denney Farm, MO	Dioxin Soils
Rotary Kiln / Vertac	35	Vertac, Jacksonville, AR	Chemical manufacturing
Shirco Infrared /Haztech	30	Peak Oil, Tampa, FL	Used oil recycling, PCBs/Lead
Shirco Infrared / GDC Engr.	NA	Rubicon, Geismar, LA	Chemical manufacturing
Shirco Infrared / OH Materials	30	Florida Steel, Indiantown, FL	Steel mill used oils
	12	Gas Station Site, Cocoa, FL	Petroleum tank leak
Shirco Infrared / U.S. Waste	10	Private Site, San Bernadino, CA	Hydrocarbons
Circulating Bed Combustor /Ogden	10	Arco Swanson River Field, Kenai, AK Stockton, CA	Oil pipeline compressor oil Underground tank oil leak

NA - Not available

Table 2.3 presents the status of selected Superfund sites employing the thermal desorption technology [3].

The overall range of costs using thermal desorption technology varies from approximately $50 to $400, based on per ton of contaminated soil processed [3]. Cost estimates include excavation, quantity of waste to be processed, moisture content, organic constituency and concentration of the contaminants, and cleanup standard to be achieved.

While basic concepts of operation for pyrolytic systems have been validated and shown capable, the actual field operation and demonstration of performance, that is in accord with EPA approved methods and quality control/assurance standards are more limited. Limited performance data are available for pyrolytic systems treating contaminated soils containing PCBs, dioxins, and other organics. The overall cost for remediating approximately 20,000 tons of contaminated media is approximately $330 per ton [4].

Table 2.3 Superfund Sites Specifying Thermal Desorption as the Remedial Action

Site	Location (Region)	Primary Contaminant(s)	Status
Cannon Engineering (Bridgewater Site)	Bridgewater, MA (1)	VOCs (Benzene, TCE, Toluene, Vinyl Chloride)	Project completed 10/90
McKin	McKin, ME (1)	VOCs (TCE, BTX)	Project completed 2/87
Ottati & Goss	New Hampshire (1)	VOCs (TCE, PCE, 1,2-DCE, Benzene)	Project completed 9/89
Wide Beach Development	Brandt, NY (2)	PCBs	Project completed 9/91
Metaltec/Aerosystems	Franklin Borough, NJ (2)	VOCs (TCE)	Design completed
Caldwell Trucking	Fairfield, NJ (2)	VOCs (TCE, PCE, TCA)	Design completed
Outboard Marine/Waukegan Harbor	Waukegan Harbor, IL (5)	PCBs	Pilot study completed 6/92
Reich Farms	Dover Township, NJ (2)	VOCs (TCE, PCE, TCA), SVOCs	Pre-design
Re-Solve	North Dartmouth, MA (1)	PCBs	Pilot study completed 5/92
Waldick Aerospace Devices	New Jersey (2)	VOCs (TCE, PCE), Metals (Cadium, Chromium)	Design completed
Anderson Development Company	Adrian, MI (5)	VOCs, SVOCs	Project completed 6/93

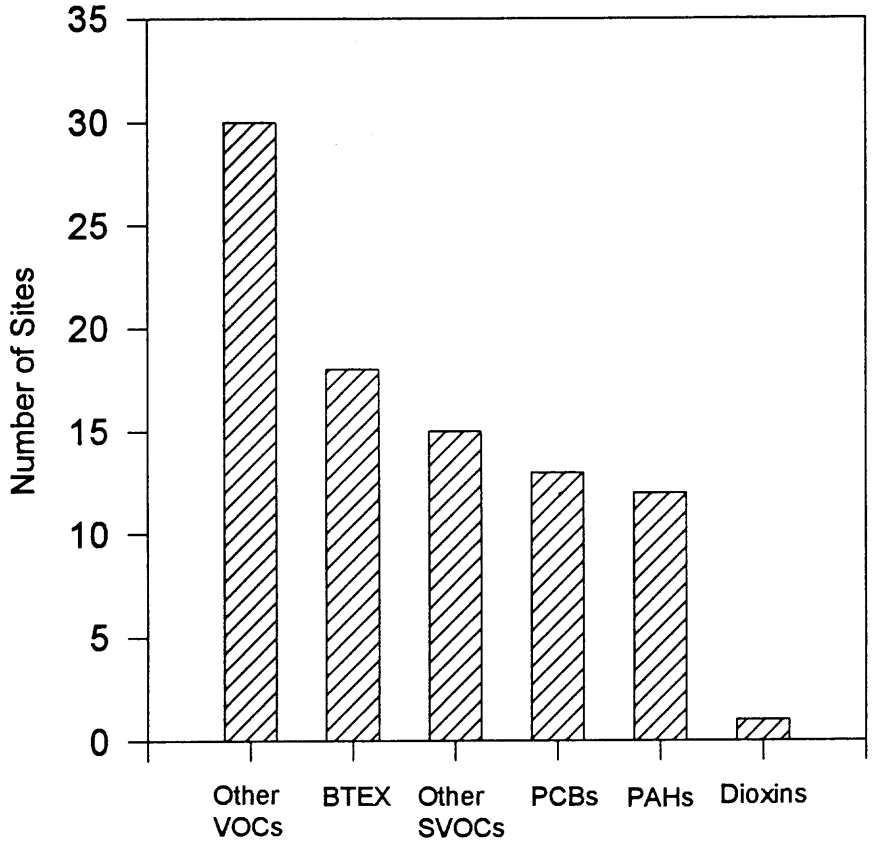

Figure 2.6 Superfund remedial actions contaminants treated by thermal desorption.

CHAPTER 3

ENERGY CONSIDERATIONS

Nomenclature

Cp	heat capacity, kcal/kg.K
ds	density, kg/m^3
F	mass flowrate, kg/sec
FF	mass fraction of water or contaminant in soil feed, %
FV	volumatric flowrate, m^3/sec
H_{des}	heat of desorption, kcal/kg
H_{vap}	heat of vaporization, kcal/kg
Q	heat flow, kcal/sec
T	temperature, K

Subscripts

bp	boiling point
des	desorption
vap	vaporization
env	environment
f	final
g	gas
i	initial

org	organic contaminant
s	soil
wtr	water
wtr-vpr	water vapor

3.1 Introduction

The removal of organic hydrocarbons and other organic chemicals from soils and sludges by relatively low temperature processes such as thermal desorption, where temperatures are not high enough for incineration to occur, is economical and is becoming a popular remediation technology.

One problem does exist: organic compounds can enter into exothermic combustion or oxidation reactions which can serve to supply energy into the overall process. In some cases this exotherm can result in a runaway thermal gradient in the reactor and thus an incident.

This initiation can occur by a number of different processes, which include: catalysis, chemical reaction, spark...etc. If the exothermic energy is more than can be absorbed and dissipated by the reactor system then dramatic increases in temperature may occur - thermal runaway and /or incineration behavior. It is important in evaluating applications of this technology to consider possible safety implications and/or implement precautions to prevent thermal runaway or other incidents.

Several attempts have been made to establish an evaluation and control strategy for thermal runaway reaction condition. Hoppe et al [18] developed a method using a bench scale calorimeter to evaluate the runaway reaction probability for process design

applications. This method was a systematic approach which collected the thermodynamic data, such as temperature, heat of reaction, heat capacity and heat-generation rate, under both the conditions of desired and undesired reactions, such as explosion. The critical limits for the safe operation were then determined from the data and a risk analysis procedure established.

Gygax [19] outlined the performance of risk assessment by extending Chemical Engineering Principles to the study of potential runaway reactions. The focus is on thermal aspects of process design such as designing safer processes, and avoiding heat accumulation conditions. Gygax [20] developed this into an approach to assess thermal runaway risks. At first, routine procedures such as the determination of : the energy potentials (thermodynamic properties), ranges of thermal activities, heat production rates, and prediction of runaway scenarios by using a simulation and/or calculation are used to assess and identify cases most sensitive with respect to thermal safety. He proposed that extensive efforts are then directed to theses high risk cases in the explicit scale-up considerations on the basis of thermochemical-kinetic models and heat balances. He stated that this thorough approach not only successfully assessed thermal runaway risks on the cases being analyzed but safety-assessment procedures are also easier and well defined.

Smith [21] presented theory of thermal explosion as a guiding principle for predicting / controlling runaway reactions. Thermodynamic property data, kinetic parameters, and physical properties are basic components of the required information; these must be determined to assess the thermochemical hazardous. The situation of "criticality", where thermal equilibrium is not possible, was derived mathematically and

used to predict the occurrence of runaway reactions. Smith [22] also assessed the hazardous of runaway reactions by setting up criteria for evaluating critical condition in which a thermal explosion will occur. These criteria were used to evaluate critical conditions of a zero-order exothermic reaction and a first order reaction. The parameters to determine critical conditions needed are: heat of reaction, reaction rate as a function of temperature and concentration, thermal conductivity, heat transfer coefficient and the shape of the heat transfer area. The author suggested that simulations should be based on experiments conducted under temperature and concentration extremes, because there is risk in extrapolating kinetic models to conditions not studied experimentally.

The main objective of this study is to determine (identify) the levels of specific organic pollutants where the heat of reaction exceeds the heat capacity of the reactor system. This is applied in the thermal desorption processing of solids and soils contaminated with organic compounds. Organic concentration conditions are delineated, example calculations are performed and calculational procedures are illustrated. Calculations include heat capacity and heat losses of a rotary kiln desorber unit, input heat and heat balance from possible combustion processes. Specific heat acceptor components include heat capacity of the kiln, heat transfer to the atmosphere via conduction, radiation and convection, de-sorption energies, vaporization energies of both the organics and water, heating of the contaminated soil, heating of purge gas. Heat input includes chemical reaction, and energy to the kiln for the normal desorption process.

3.2 Energy Requirements from Operation

The thermal desorption process, which is an endothermic reaction process, requires energy for heating soil, air, water content and organic contaminants in the soil and to maintain the kiln reactor at the target operation temperature. Heat losses include: heat to raise soil to operation temperature; heat to raise carrier and purge air to operation temperature; heat to desorb water from soil, to vaporize and then raise water content to operation temperature; heat to desorb organic contaminants from soil , plus to vaporize and raise organic contaminants to operation temperature; and heat loss from the kiln shell to environment. The summation of these heat loss quantities is the total energy input required to the kiln for operation at a target temperature. Should combustion occur, the heat released from combustion, would reduce the energy required to maintain constant temperature operation.

Energy for Heating Soil. Energy to heat soil from operation involves energy to raise soil from its initial temperature to operation temperature. Energy for heating soil to kiln desorption temperature are determined as follows:

$$Q_{soil} = Fs \; Cps \; (T_{s,f} - T_{s,i}) \tag{3.1}$$

Energy for Heating Purge Air. Energy to heat purge air from operation involves heat loss to raise purge air from its initial temperature to operation temperature. Energy for heating air to kiln temperature is determined as follows:

$$Q_{air} = Fvg \; ds_g \; Cpg \; (T_{g,f} - T_{g,i}) \tag{3.2}$$

Energy for Heating Water Content. Energy to heat the water content in the soil involves the heat required in the mechanisms of desorption of water content from soil, vaporization and heating of the water vapor to kiln temperature. The heat of desorption depends on the physical properties of soil holding the water and the water itself. These physical properties include boiling point, heat capacity, heats of vaporization for the water and heat of desorption for removing water from the soil surfaces and pores. Energies for desorption of water from soil, vaporization and heating of the water vapor to kiln temperature are determined as the equations shown below:

$$(Q_{des})_{wtr} = (H_{des})_{wtr}\ Fs\ FF_{wtr} \tag{3.3}$$

$$(Q_{vap})_{wtr} = (H_{vap})_{wtr}\ Fs\ FF_{wtr} \tag{3.4}$$

$$Q_{wtr\text{-}vpr} = Fs\ FF_{wtr}\ (Cp)_{wtr}\ [(T_f)_{wtr\text{-}vpr} - (T_{bp})_{wtr\text{-}vpr}] \tag{3.5}$$

The final temperature of water vapor refers to the target temperature of reactor.

Energy for Heating Organic Contaminants. Energy to heat the organic contaminants in the soil involves the mechanisms of desorption of organic contaminants from soil, vaporization and heating of the organic contaminants vapor to kiln temperature. The heat of desorption depends on the physical properties of soil and organic contaminants. These physical properties include boiling point, heat capacity, heats of vaporization for the organic contaminants and heat of desorption for removing organic contaminants from the soil surfaces and pores. Heat loss for heating organic contaminants vapor to kiln temperature is determined as follows:

$$(Q_{des})_{org} = (H_{des})_{org} \quad Fs \quad FF_{wtr} \tag{3.6}$$

$$(Q_{vap})_{org} = (H_{vap})_{org} \quad Fs \quad FF_{wtr} \tag{3.7}$$

$$Q_{org\text{-}vpr} = Fs \quad FF_{wtr} \quad (Cp)_{org} \quad [(T_f)_{org\text{-}vpr} - (T_{bp})_{org\text{-}vpr}] \tag{3.8}$$

The final temperature of organic vapor refers to the target temperature of reactor. The heat capacity of organic contaminant is estimated from thermodynamic properties using group additivity which will be discussed in next section.

Heat Transfer to the Environment. Heat loss from the kiln shell to environment is calculated as convection to the surrounding air plus radiation to the environment.

$$Q_{loss}(\text{kiln shell} \rightarrow \text{environment}) = h \quad A \quad (T_{\text{kiln shell}} - T_{env}) + \sigma \, A[(T_{\text{kiln shell}})^4 - (T_{env})^4]/(1.0/\epsilon) \tag{3.9}$$

where h is heat transfer coefficient of air, 3.0 W/m^2K. A is surface area of kiln shell, m^2. σ is Stefan-Boltzman constant 5.676E-8 W/m^2K^4, and ϵ is emissivity of the kiln shell, 0.8.

The summation of these heat loss quantities is the total energy required into the kiln for operation at a target temperature. Should combustion occur, the heat released from combustion, would reduce the energy required to maintain operation.

3.3 Heat Released from Combustion

Heat released from combustion should be considered during thermal desorption process as part of overall operation safety. Organic contaminants may continue to be volatilized

from the soil being treated inside the kiln desorber until they are completely removed. These vapors may ignite if conditions exist to support combustion. Once the organics in the soil have been identified and their concentration is determined, the heat released from combustion can be calculated based on the worst case scenario: all the organics desorbed can react (oxidation) and are converted to minerals, CO_2 and H_2O. This energy is compared to the energy required for continuous operation at constant temperature. Results of this comparison then can provide an overall evaluation on the risk for possible runaway of the treatment process.

A computer code called **THERM** (THermo Estimation for Radicals and Molecules) developed by Ritter and Bozzelli [23] is used in this chapter to determine the heat (enthalpy) released from specific combustion reactions. This computer code can be used to estimate, edit, or enter thermodynamic property data for gas phase radicals and molecules using Benson's group additivity method. This method assumes that the properties for a chemical substance are the sum of the contributions from each group or polyvalent atom (central atom) in that molecule. Benson's group estimation technique is an accurate method for the estimation of ideal gas phase heat capacities, heat of formation, and entropies of molecules.

An example is presented here considering benzene as specified species to illustrate the estimation of thermodynamic properties of molecule and thermodynamic analysis for combustion reaction of benzene using THERM. One group contribution is considered for benzene. Benzene is comprised of 6 CB/H groups. Table 3.1 is a sample of the documentation generated when estimating thermodynamic properties of benzene species. $\Delta Hf°(298K)$ for benzene (C_6H_6) is estimated as 19.8 kcal/mol. $S°(298\ K)$ and

Table 3.1 Thermo Estimation for Benzene. An Example of Documentation File Entry

```
SPECIES
 BENZENE
Thermo estimation for molecule

 BENZENE                                        C6H6
 UNITS:KCAL
 GROUPS  1
  Gr # -  GROUP ID  - Quantity
    1 - CB/H        - 6
   Hf       S  Cp 300   400   500   600   800   1000  1500
 19.80  67.80  19.44   26.64 32.76 37.80 45.24 50.46 58.38
       CPINF =  67.56
 SYMMETRY        2
 CREATION DATE:  7/29/96
 ENDSPECIES
```

Cp (300-1500 K) for benzene are also estimated. Elemental formula (C_6H_6), Cp_∞ (high temperature limit heat capacity), symmetry number and optical isomer corrections (if any) for entropy, and the number of rotors in the molecule (if any) are recorded in the documentation file.

Thermo property tables can be generated using the THERMLST procedure. These tables contain species name, $\Delta Hf°(298K)$, $S°(298\ K)$, and Cp at 300-1500 K. An example of this format is presented in Table 3.2. This format provides a convenient list for reviewing or referencing the thermodynamic property data.

Table 3.2 An Example Thermodynamic Property Table Created by THERMLST Procedure

UNITS:kcal
THERMO LISTING

Species	HF(298)	S(298)	CP300	CP400	CP500	CP600	CP800	CP1000	CP1500
CO2	-94.01	51.00	8.92	9.83	10.61	11.26	12.26	12.95	13.86
H2O	-57.80	45.10	8.23	8.41	8.64	8.91	9.51	10.14	11.50
O2	.00	49.00	6.93	7.22	7.46	7.68	8.02	8.29	8.71
C6H6	19.80	64.24	19.44	26.64	32.76	37.80	45.24	50.46	58.38

THERM contains a chemical reaction interpreter to calculate thermodynamic property changes for chemical reactions as functions of temperature. Thermodynamic analysis for a chemical reaction can be therefore determined over a temperature range specified by the user. All species appearing in a reaction must be defined in the database. The thermodynamic properties which are calculated are equilibrium constant (Kc), heat release (required heat, ΔHr), entropy changes (ΔSr), Gibbs free energy changes (ΔGr), and the ratio of forward to reverse Arrhenius A-factors (for elementary reactions). The reaction of benzene with oxygen to CO_2 plus H_2O products is illustrated in Table 3.3. This oxidation reaction is illustrated to be exothermic by about 1,514-1,527 kcal/mol for 300-2,000 K.

3.4 Example Calculations Evaluating Enthalpies for Thermal Runaway

The following example calculations demonstrate the usefulness of incorporating the equations evaluating energy required for operation, THERM program evaluating energy released from oxidation of organic contaminants, and the computer approach determining thermal runaway. Both bench and full scale reactors are illustrated as examples. Comparison of bench to full scale operation conditions is also discussed. Ranges of operation temperature and mass fraction of different organic contaminants in the soil are considered to evaluate the critical conditions of thermal runaway.

3.4.1 Bench Scale Reactor

A bench scale size rotary kiln with 0.1 m internal diameter and 0.432 m length is used as the first example to evaluate the total heat loss during steady state operation: continuous

Table 3.3 Thermodynamic Property Analysis for Reaction of Benzene with Oxygene - An Example of the Output from THERMRXN

THERMODYNAMIC ANALYSIS for REACTION:

Rx 2 BENZENE + 15 O2 = 12 CO2 + 6 H2O
Hf {Kcal/mol} 39.600 0.000 1128 -346.800
S {cal/mol K} 128.400 735.000 612.000 270.600

dHr {kcal/mol} (298K) = -1514.40 dHr avg (298., 1500. K) = -1517.43
dU (dE) {kcal/mol} (") = -1514.99 dUr avg (298., 1500. K) = -1519.22
dSr {cal/mol K} (") = 19.20 dSr avg (298., 1500. K) = 17.89
dGr {kcal/mol} (") = -1520.12 dGr avg (298., 1500. K) = -1533.51
Kc (") = > 1.0E+119
Fit Af/Ar : A = 1.070E-10 n = 4.34 alpha = 8.492E-03 avg error 48.25 %
Fit Af/Ar w/ddU: A = 8.383E-14 n = 5.98 alpha = 1.342E-02 avg error 134.78 %

T (K)	dH(Kcal/mol)	dU(Kcal/mol)	dS(cal/mol K)	Kc(liter/mol.s)	dG(Kcal/mol)
300.00	-1.514E+03	-1.515E+03	1.929E+01	*********	-1.520E+03
400.00	-1.513E+03	-1.514E+03	2.238E+01	*********	-1.522E+03
500.00	-1.513E+03	-1.514E+03	2.355E+01	*********	-1.525E+03
600.00	-1.513E+03	-1.514E+03	2.372E+01	*********	-1.527E+03
800.00	-1.513E+03	-1.515E+03	2.267E+01	*********	-1.532E+03
1000.00	-1.515E+03	-1.517E+03	2.096E+01	*********	-1.536E+03
1200.00	-1.517E+03	-1.519E+03	1.915E+01	*********	-1.540E+03
1500.00	-1.520E+03	-1.523E+03	1.658E+01	*********	-1.545E+03
2000.00	-1.527E+03	-1.531E+03	1.283E+01	*********	-1.553E+03

feed, thermal treatment and effluent of a contaminated soil in a thermal desorber. Values of the operation parameters are listed in Table 3.4. The kiln desorber temperature is targeted to be 400°C (673 K). Soil feed rate, purge gas flow and soil particle residence time are adjusted over a range values. The soil residence time and solid fill fraction inside the reactor once are decided, the soil feed rate can be determined combining the volume of solid fill fraction, density of soil and soil residence time. The soil feed rate is determined to be $9.0*10^4$ kg/sec in this case as the soil residence time is 1,200 sec and a 21 percent of solid fill fraction of the kiln space is expected to be achieved. Purge gas

Table 3.4 Kiln Size and Operating Parameters of Bench Scale Reactor

Kiln I.D., meter	0.1
Kiln length, meter	0.432
Kiln temperature, K	673
Soil residence time, sec	1,200
Soil fill fraction in the kiln, % (by volume)	21 %
Soil feed, kg/sec	9.0E-4
Purge gas flowrate, m^3/sec	2.5E-4
Moisture content in soil feed, %(by mass)	10
Organic contaminant	Benzene, C6H6
Organic contaminant concentration in soil feed, %(by mass)	10

flowrate is set to be 2.5E-4 m^3/sec to reach a linear velocity of 0.032 m/sec. A 10 percent mass fraction of water content in the soil feed is assumed. The organic contaminant is assumed to be benzene, with a concentration of 10 percent mass fraction in the soil. Operation parameters such as soil feed rate and kiln temperature however still need to be reconsidered carefully after initial trial run using contaminated soil owing to the concentration of water and contaminants effect the performance of reactor tremendously.

The Woodburn Soil [24], which is assumed to contain 10 percent water content and 10 percent mass fraction of benzene, is used as the soil to be treated in this example. The composition of the soil on a dry-weight basis is 1.9 percent organic matter, 9 percent sand, 68 percent silt, and 21 percent clay. The heat capacity of soil is estimated to be 995 J/kg.K. The molar heat of desorption of benzene is 9.61 kca/mol, and the molar heat of desorption of water is 12.44 kcal/mol, respectively.

The calculation for heat loss during thermal desorption process at 673 K in the bench scale reactor is performed following the procedure described in the previous section. The energy required for heating soil from initial temperature 298 K to target final

temperature 673 K is calculated from Eq.(3.1). The inlet purge air flow is assumed to be preheated to 473 K. The energy required for heating air from initial temperature 473 K to target final temperature 673 K is calculated from Eq.(3.2), using 0.2375 cal/g.K for heat capacity of air and 600 g/m^3 for air density at given temperature range.

The energy required for heating and desorbing water involves the heat of desorption of water from soil, vaporization and heating of the water vapor to kiln temperature. Heat of desorption of water content from soil is calculated from Eq.(3.3), based on the molar heat of desorption of water 12.44 kcal/mol [24] and water content amount in the soil. Heat of vaporization of water is calculated from Eq.(3.4), based on ΔHvap of water 2.257E+03 J/g and water content amount at given temperature range. Energy required for heating water vapor from it's boiling point to target kiln temperature is calculated from Eq.(3.5). Heat capacity of water is estimated to be 8.8 cal/mol.K for the temperature range 373-673 K, using the data of Thermodynamic Property Table in Table 3.2.

The energy required for heating organic contaminant benzene involves the heat of desorption of benzene from soil, vaporization and heating of the benzene vapor to kiln temperature. Heat of desorption of benzene from soil is calculated from Eq.(3.6), based on the molar heat of desorption of benzene 9.61 kcal/mol [24] and benzene concentration in the soil. Heat of vaporization of benzene is calculated from Eq.(3.7), based on heat of vaporization of benzene 7.352 kcal/mol and total benzene moles number at given temperature range. Energy required for heating benzene vapor from it's boiling point to target kiln temperature is calculated from Eq.(3.8). Heat capacity of benzene is estimated

to be 32.26 cal/mol.K for the temperature range 351-673 K, using the data of Thermodynamic Property Table in Table 3.2.

Heat transfer from kiln shell to the environment is calculated from Eq.(3.9), assuming the temperature of surrounding environment is 323 K. Combining bench scale kiln surface area 0.152 m^2, Stefan-Boltzman constant and emissivity of the kiln shell, plus the heat transfer coefficient of air noted in the previous section, a value of 0.321 kcal/s is calculated for heat loss to the environment when kiln temperature is at 673 K.

The calculation result is summarized in Table 3.5 and Figure 3.1. The total energy required from operation is 0.571 kcal/s at 673 kiln operation temperature by summing each heat requirement: soil, air, water content, contaminant, and heat loss to the environment. It can be seen from Figure 3.1 that the heat loss from kiln shell to environment demands major fraction, over 50 percent of total heat loss among the all heat acceptor components. The heat requirement for treatment of water, which combines heat of desorption of water from soil, vaporization and heating of water vapor to the kiln

Table 3.5 Heat Loss during Thermal Desorption Process in Bench Scale Reactor at 673 K

	Initial Temperature, K	Final Temperature, K	Heat Loss, kcal / s
(i)Heating Soil	298	673	0.08
(ii)Heating Air	473	673	0.07
(iii)Heat of Desorption (H2O)			0.062
Heat of Vaporization (H2O)	298	373	0.049
Heating H2O Vapor	373	673	0.013
(iv)Heat of Desorption (C6H6)			0.018
Heat of Vaporization(C6H6)	298	351	0.0085
Heating C6H6 Vapor	351	673	0.012
(v)Heat Loss from Kiln Shell to Environment	673	323	0.321
Total Heat Loss			0.571

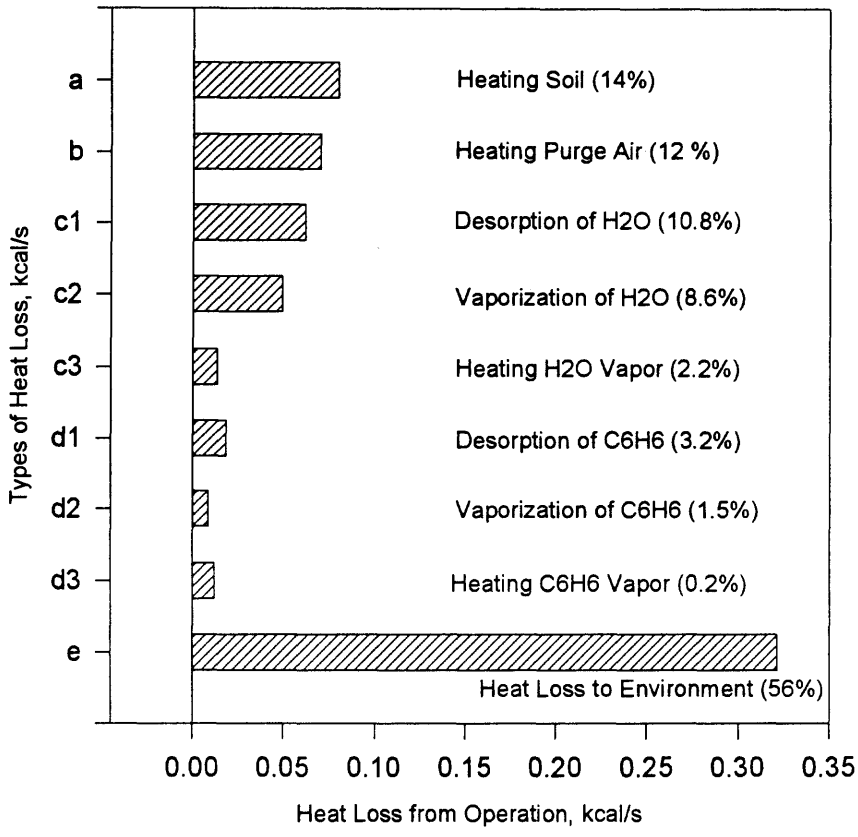

Figure 3.1 Heat loss in bench scale reactor
(Total heat loss: 0.571 kcal/sec).

operation temperature, is the next largest fraction of all. The heat requirement for treatment of contaminant benzene, although assumed as a high concentration of 10 percent mass fraction in the soil, is still low compared to which of soil and purge air.

Thermodynamic property analysis for combustion of benzene is listed in Table 3.3. The heat released from combustion of benzene, which is shown as Eq.(3.10), is calculated to be 0.87 kcal/s. This heat released rate from combustion reaction is approximately one and half times of the heat required from thermal desorption, 0.571 kcal/s . A significant potential risk of thermal runaway from the operation process can be therefore expected.

$$C_6H_6 + 7.5\ O_2 \rightarrow 6\ CO_2 + 3\ H_2O \qquad (3.10)$$

3.4.2 Full Scale Reactor

A rotary kiln with 2 m internal diameter and 10 m length is used here as a full scale reactor to evaluate the total heat loss during steady state operation. Continuous feed of a contaminated soil to the thermal desorber is treated. Values of the operation parameters are listed in Table 3.6. The kiln desorber temperature is targeted to be 400°C (673 K). Soil feed rate, purge gas flow and soil residence time are adjusted over a range

Table 3.6 Kiln Size and Operating Parameters of Full Scale Reactor

Kiln I.D., meter	2
Kiln length, meter	10
Kiln temperature, K	673
Soil residence time, sec	1,200
Soil fill fraction in the kiln, % (by volume)	21 %
Soil feed, kg/sec	8.3
Purge gas flowrate, m^3/sec	0.1
Moisture content in soil feed, %(by mass)	10
Organic contaminant	Benzene, C6H6
Organic contaminant concentration in soil feed, % (by mass)	10

values. The soil feed rate, 30,000 kg/sec is used so that approximately 21 percent fill of kiln volume is achieved. Purge gas flowrate is set to be 0.1 m^3/sec to reach a linear velocity of 0.032 m/sec. A 10 percent mass fraction of water content in the soil feed is assumed. The organic contaminant is assumed to be benzene, with a 10 percent mass fraction of concentration in the soil, to simplify evaluation of total heat loss.

The result of calculation for total energy requirement for the thermal desorption process at 673 K in the full scale reactor is shown as Table 3.7 and Figure 3.2. The same calculation procedure which is described for bench scale reactor is applied. The total heat

Table 3.7 Heat Loss during Thermal Desorption Process in Full Scale Reactor at 673 K

	Initial Temperature, K	Final Temperature, K	Heat Loss, kcal / s
(i) Heating Soil	298	673	742
(ii)Heating Air	473	673	2.9
(iii)Heat of Desorption (H2O)			575
Heat of Vaporization (H2O)	298	373	450
Heating H2O Vapor	373	673	123
(iv)Heat of Desorption (C6H6)			167
Heat of Vaporization(C6H6)	298	351	78.3
Heating C6H6 Vapor	351	673	111
(v)Heat Loss from Kiln Shell to Environment	673	323	148
Total Heat Loss			2,397

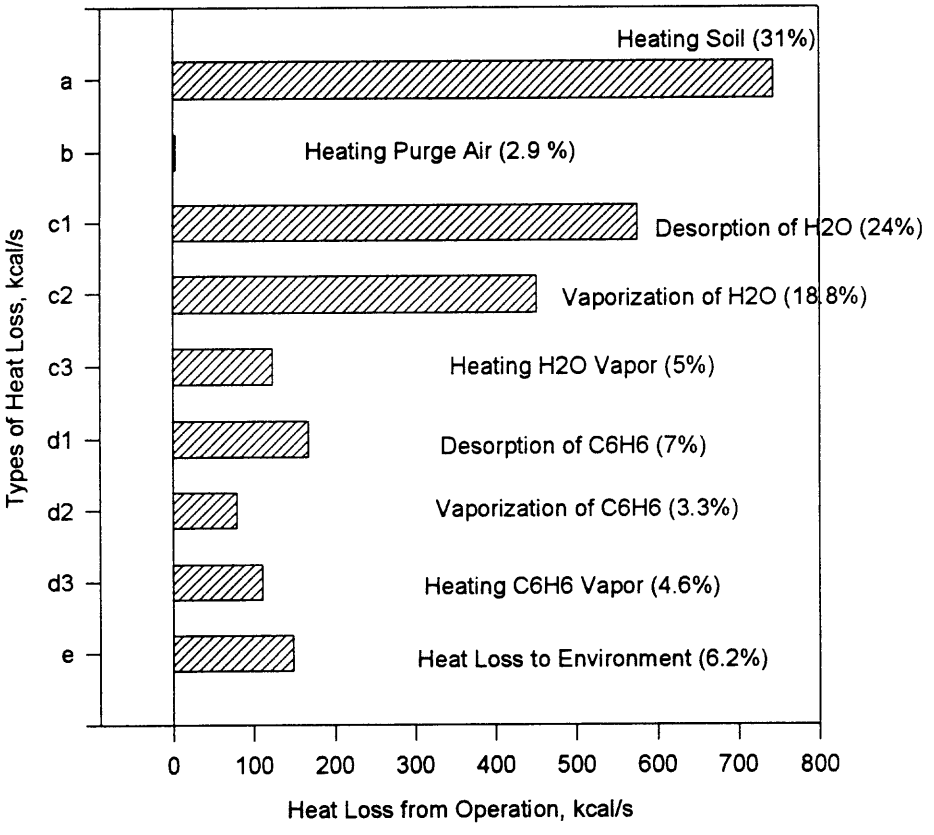

Figure 3.2 Heat loss in full scale reactor
(Total heat loss: 2,397 kcal/sec).

required from operation is 2,397 kcal/s. The heat required for treatment of water consumes approximately 48 percent fraction of all. A fraction of 31 percent and 15 percent of total heat required are demanded for heating of soil and treatment of organic contaminant benzene, respectively. Heat loss from kiln shell to environment, however, requires only 6percent of total heat requirement. This reveals a quite different data than which in bench scale, where the heat loss from kiln shell to environment takes the major fraction of total heat required.

The heat released from combustion of benzene, 8,072 kcal/s, is calculated also using the thermodynamic data of Table 3.3. This heat released from combustion at full scale reactor is over three times of the heat loss from thermal desorption, 2,397 kcal/s.

3.4.3 Comparison of Bench to Full Scale Operation Calculations

It is valuable to be able to relate the bench scale and full scale reaction data under similar operating conditions so that resulting data from a bench scale analysis, as a test run, can be used to simulate the full scale reaction. There are however substantial difference in conditions between the bench and full scale thermal desorption processes. A meaningful method of comparison is therefore important for analysis of the different scales of reactions.

It was suggested by Lester and co-workers [25] to use temperature, kiln rotation rate and solids fill fraction in the kiln as scaling criteria. We choose temperature, fill fraction, solid residence time and linear velocity of purge gas flow as more complete scaling criteria in this work. The residence time and solid fill fraction determine the solid feed rate, and the linear velocity determines the purge gas flowrate under the conditions

of different scale reactors. Other operation parameters such as water content, organic contaminant and it's concentration are assumed to be the same in bench as in full scale. The data of both endothermic and exothermic reaction from bench scale and full scale reactor can then be compared as under similar operating conditions.

Both the bench scale and full scale data show that the potential risk of thermal runaway exists at conditions of operating parameters which are listed in Table 3.4 and Table 3.6, based on the difference of the heat required from operation and the heat released from combustion of organic contaminant. The risk of thermal runaway at full scale reaction indicates a stronger potential than at bench scale reaction under similar operating conditions. This result thus suggests a higher safety factor should be applied while scaling up the design of reaction.

It should be noted that while scaling up from bench to full scale reactor, the diameter of kiln is enlarged by a factor of 20, and the length of kiln is enlarged by a factor of 23. The heat loss of each heat acceptor components therefore increase by different number of factor due to the different dimensions of reactor being considered. Heating purge air increases by a factor of 400, due to the scaling up of linear velocity. The heat loss from kiln shell to the environment increases by a factor of 460, considering the scaling up of contact surface area between kiln shell and outside environment. The heat loss of other three heat acceptor components, which includes heating of soil, treatment of water and organic contaminants, however increase by a factor of 9,250, considering scaling up of kiln volume. This explains the reason why much less heat loss for heating purge air and from shell to the environment compared to those of heating soil, water and organic contaminants while scaling up from bench scale to full scale reactor.

The risk of thermal runaway while scaling up from bench scale to full scale reactor as previous data result can be also understood for the different fraction of heat loss increased. The fraction of heat loss for treatment of organic contaminants would increase tremendously for scaling up to full size reactor since the heat loss from kiln shell to the environment decreases largely. Precaution should be therefore taken for the increasing of thermal runaway of scaling up reactor.

CHAPTER 4

MASS BALANCE ANALYSIS ON PCDD/F IN WASTE INCINERATION

4.1 Overview

Data on concentrations of PCDD/F in the feed, and in the effluent from modern municipal solid waste incinerators (MSWI) are surveyed and evaluated to determine if more PCDD/F are destroyed than formed in the Municipal Solid Waste (MSW) incineration process. PCDD/F concentrations in the feed of MSW incinerators are assigned into different waste categories with associated PCDD/F levels. Comparison of the input and output levels shows that for 7.2 g(I-TE) PCDD/F, which is calculated from the average value of PCDD/F range 0.8 to 87 pg (I-TE)/g in the feed to a MSW incinerator per year (data from Europe and Asia); the output in the combined gas and solid streams (bottom ash, boiler ash and air pollution control residues) ranges from 0.11 to 12 g (I-TE) per year. The total PCDD/F levels in the waste feed to a US MSWI is estimated to be higher. Overall, the total PCDD/F input and effluent levels appear to be similar or perhaps slightly more is destroyed than emitted. The PCDD/F in the effluent gas is high relative to ambient air by a factor of 8-18,000. Further studies on PCDD/F in MSW feed materials as well in the effluent gas and solid streams are recommended to validate these results.

4.2 Introduction

The presence of polychlorinated dibenzo-p-dioxins (PCDD) and dibenzofurans (PCDF) has been detected in fly ash from municipal solid waste incinerators (MSWI) as early as 1977 [26] and dioxin levels are consistently observed as a product from current MSW

incineration, albeit at reduced levels relative to older combustors. There is a recent enhancement in worldwide concern over emissions of PCDD and PCDF from combustion and industrial sources [27] because of recent reports on its toxicity. Levels of dioxins are often monitored in some countries [28], with strict limitations regulated on effluent levels. The emission of dioxins from industrial sources are reported to be reduced by ca. 75percent between 1987 and 1995 [29]. The US EPA's ability to understand risk and the EPA's evaluation of this risk over roughly the same time frame has also improved. One demonstration of this is a draft EPA report recently referenced by the media [30], which concludes (for the first time) that dioxin is a human carcinogen. This latest dioxin reassessment indicates that developing advanced methods of control of PCDD/F emissions remains important, even given the substantial reduction in industrial emissions.

Reductions in PCDD/F emissions (~75percent) over the past decade, can be attributed to improved incinerator design, resulting from research which has shown that the process characterized as *de novo synthesis* is the dominant mechanism of formation [31]. The improved understanding on the physical characteristics leading to this *de novo synthesis*, which is operative in the combustor's air pollution control devices, has led to design changes for reduced formation. The *de novo synthesis* is considered to be direct PCDD/F formation from a carbon matrix that has been chlorinated and oxidized [32]. This PCDD/F formation is primarily associated with waste heat boilers and dust collectors in the air pollution control equipment of MSW incinerators [33-36]. Modification to several of the air pollution control device operating parameters, such as temperature, has typically resulted in significant emission reductions. Combustors with

waste heat boilers have also had to install additional air pollution control equipment to reduce dioxin concentrations to regulatory levels.

Mass balance studies involving input versus output for PCDD/F concentrations in a number of combustion systems have been reported [37-43]. These data which were published in 1984-1988, showed that significantly more PCDD/F was detected in the effluent of the combustor than was detected in the feed. This was interpreted as PCDD/F species were synthesized in the overall combustion process.

A significant and different result relating the ratio of PCDD/F in the effluent versus the feed of MSW incinerators was recently reported by Velhow et al [44]. This estimation was performed assuming a low dioxin operation (effective combustion control with high burnout and low dust release) in modern efficient MSW incinerators. It was estimated for an input of 10 g I-TE (International Toxic Equivalents) PCDD/F in an annual throughput of 2×10^8 kg waste for a MSW incinerator, the cumulative output via gas and solid mass streams was less than 0.2 g (I-TE). Velhow indicated approximately 50 times more dioxin (PCDD/F) is destroyed in the MSW than is produced and is effluent to the environment.

The research group of Rivera performed several mass balance evaluations for PCDD/Fs in municipal waste incinerator plants (in Spain) between 1997 and 2000 [45-47]. Both negative and positive balances were obtained from the evaluations. Our interpretation of their overall data indicate that for MSW plants which have modern operation parameters and control equipment, the PCDD/Fs in the effluent are similar to the levels in the feed.

This article continues this analysis on the input versus output of PCDD/F in MSW incinerators using available data. Input PCDD/F concentrations in the feed of MSW incinerators are categorized into four different waste fractions (paper + cardboard; plastics, wood, leather, textiles etc; fine debris less than 8 mm in particle size; food and garden wastes and debris greater than 8 mm in particle size) [48]. Additional input PCDD/F data measured in the feed of municipal solid waste incinerators include the PCDD/F concentrations in actual waste samples of Berlin and Bielefeld, FRG [48], the PCDD/F in sewage sludge and milled waste in the input of MWI Bielefld-Herford, FRG[49], and PCDD/F in compost from the waste consisting of vegetable and plant material [49]. The PCDD/F levels are further applied to mass distributions for the categories of waste reported for the US by the US EPA to obtain the input level of PCDD/F in MSW feed for the additional evaluation. The PCDD/F concentrations in inlet air are also considered as part of total PCDD/F input into MSWI.

Estimation of PCDD/F concentrations in the output of MSW incinerators considers the production rate of gaseous PCDD/F emissions plus levels in the solid effluent streams (bottom ash, boiler ash and air pollution control residues) which result from a contemporary design MSW incinerator with prevailing, control equipment. Data of the input and output PCDD/F levels are evaluated to determine whether the modern MSW incinerators actually destroy more PCDD/F than they produce.

4.2.1 Toxicity Equivalent Factors

This group of compounds, often symbolized by the terms "dioxins and furans" or PCDD/F's, consist of 75 isomers of polychlorinated dibenzo-p-dioxins and 135 isomers

of polychlorinated dibenzofurans. The common units of their concentration measurement is somewhat unique. It is termed "Toxic Equivalent (TE)" and is calculated based on an assigned factor (TEF - Toxic Equivalency Factor) for the potential toxicity of each specific isomer in relation to 2,3,7,8 - tetrachloro-dibenzo-p-dioxin and the isomer's concentration. The most common schemes for applying PCDD/F toxicity factors are shown in Table 4.1. The International Toxic Equivalent Factors "I/TEF" are the most widely used [50]. A Toxic Equivalent (TE) value of a mixture is calculated by multiplying the concentration (pg/g or ng/m^3) of individual congeners by their respective TEF. The sum of the TE concentrations for the individual congeners is the TE concentration for the mixture. The TE values, which are calculated based on the I/TEF factors, are termed as "I-TE". The TE values which are calculated based on the recommendation of the Bundesgesundheitsamt (BGA, [51]) are termed "TE BGA".

Table 4.1 Toxicity Equivalent Factors (TEFs) for Specific PCDD/F Congeners [50]

Isomer	I/TEF[53]	US EPA	BGA[51]
2,3,7,8 - TetraCDD	1	1	1
1,2,3,7,8 - PentaCDD	0.5	0.2	0.1
1,2,3,4,7,8 - HexaCDD	0.1	0.04	0.1
1,2,3,6,7,8 - HexaCDD	0.1	0.04	0.1
1,2,3,7,8,9 - HexaCDD	0.1	0.04	0.1
1,2,3,4,6,7,8 - HeptaCDD	0.01	0	0.01
OctaCDD	0.001	0	0.001
2,3,7,8 - TetraCDF	0.1	0.1	0.1
1,2,3,7,8 - PentaCDF	0.05	0.1	0.1
2,3,4,7,8 - PentaCDF	0.5	0.1	0.1
1,2,3,4,7,8 - HexaCDF	0.1	0.01	0.1
1,2,3,6,7,8 - HexaCDF	0.1	0.01	0.1
1,2,3,7,8,9 - HexaCDF	0.1	0.01	0.1
2,3,4,6,7,8 - HexaCDF	0.1	0.01	0.1
1,2,3,4,6,7,8 - HeptaCDF	0.01	0.001	0.01
1,2,3,4,7,8,9 - HeptaCDF	0.01	0.001	0.01
OctaCDF	0.001	0	0.001
Other PCDD/PCDF	0	0–0.01	0.001–0.01

4.2.2 Control of PCDD/F

Reduction of PCDD/F compounds generated in the combustion process can be achieved by minimizing the formation of these products during the process and applying efficient removal and destruction technologies [44, 52]. An optimized (complete) burnout is one effective way to limit the formation of PCDD/F by reducing the unburned carbon species in the raw gas. Minimization of adsorption of incomplete combustion products on fly ash surfaces in the air pollution control equipment, where catalyzed formation of PCDD/F occurs is a second method for effectively limiting their formation. Control of dust release and prevention of large dust deposits in the boiler are also helpful to limit the PCDD/F formation.

PCDD/F removal in modern incinerators is performed by several techniques: adsorption on charcoal in a bed filter, adsorption on activated carbon injection into the flue gas, or by catalytic destruction in treatment of the flue gas [54]. Injection of oxidizing agents into the raw gas between the boiler and filter is also utilized [55].

4.3 PCDD/F Concentrations in MSW Feed

The distribution of PCDD/F concentrations in MSW Feed was studied by categorizing the waste into four different municipal waste fractions [48]:

A = paper + cardboard;

B = plastics, wood, leather, textile etc;

C = fine debris < 8 mm;

D = food and garden wastes > 8 mm (in particle size).

Representative waste samples were reported from five sites in Germany (FRG): Land Baden-Württemberg, Land Northrhine-Westfalia, Lands Lower Saxony and Bremen, Land Bavaria, and Cities Bochum and Lüdinghausen. The concentration ranges in each waste fraction are shown in Table 4.2. The average PCDD/F concentration of dried (analytical) waste amounted to 104 pg(I-TE)/g, or 50.2 pg(I-TE)/g of the wet total waste.

Table 4.2 Range and Typical Concentrations of PCDD/F in Different MSW Fractions - Samples Collected in 1980 [48]

Waste Fraction	Concentration range, pg(I-TE)/g	Concentration range, pg(TE BGA)/g	Typical concentration, pg(TE BGA)/g
A - Paper, cardboard	18–383	21–510	177
B - Plastics, wood, leather, textile	29–1370	31.5–1600	484
C - Fine debris (dust and particles) < 8 mm	8–468	8.8–619	214
D - Food and garden wastes > 8 mm (in particle size)	7–100	7.9–89.4	44

A listing of concentrations in waste samples is summarized in Table 4.3 [48]. The average PCDD/F concentrations range from 2 to 50 pg(TE-BGA)/g in data which were reported in 1989-1991. Published data like this on PCDD/F in waste feed is limited; but available data indicate that concentrations in waste feed are about 50 pg(I-TE)/g [43, 49,56].

Table 4.3 PCDD/F Concentrations in Actual Waste Samples (1989 - 1991) [48]

Location	pg(TE BGA)/g
Berlin, FRG* (1 sample) [57]	7.8
Berlin, FRG (green waste, 5 samples) [57]	2.1 – 13.6
Bielefeld, FRG (2 samples) [49]	33 – 41
FRG (average of 6 samples) [58]	50

* FRG = Former Federal Republic of Germany

Lahl et al [49] collected and analyzed input samples of municipal waste from the MWI (Municipal Waste Incinerator) Bielefeld-Herford at 1989-1990. The results from analysis of sewage sludge and milled waste in the input which were collected over two sample collection episodes, summer versus winter, are summarized in Table 4.4. The input showed a severe burden of PCDD/F in which a range of 10 to 41 pg(TE-BGA)/g PCDD/F was found. Several high concentrations (up to 7,655 ng/g) of PCDD/F precursors like PCB, chlorobenzenes and chlorophenols were also identified in the feed (waste included sewage sludge).

Lahl et al [49] also analyzed PCDD/Fs in compost from the waste consisting of vegetable and other plant materials; these materials typically comprise about 30 to 40 percent of municipal solid waste. The result of PCDD/F contents in four different materials (green waste, plant waste, mixed waste, and bark) are shown in Table 4.5. The PCDD/F toxicity equivalents range from 0.8 to 35.7 pg(I-TE)/g.

Table 4.4 Results of Two Sample Collection Periods at the MWI Bielefeld-Herford [49] - S: Summer (27.7.1989), W: Winter (23.1.1990); ng/g Referring to Dry Substance

PCDD/PCDF	sewage sludge ng/g S	sewage sludge ng/g W	milled waste ng/g S	Milled waste ng/g W
Sum PCDD	5.15	2.552	13.21	7.939
Sum PCDF	< 0.01	0.757	0.3	1.397
PCDD+PCDF	5.15	3.309	15.51	8.79
TE (BGA)	0.01	0.021	0.03	0.041
PCB	139	47	514	527
Chlorobenzenes	86	18	154	128
Chlorophenols	3090	435	7655	1070

Table 4.5 PCDD/PCDF Content in Different Compost Samples [49]

		PCDD ng/g	PCDF ng/g	PCDD + PCDF ng/g	PCDD + PCDF pg(I-TE)/g
A	Mixed waste compost	12,530	40	12,570	22.6
B	Mixed waste compost	19,100	40	19,140	32.1
C	Plant waste compost	1,620	< 10	1,620	1.8
D	Plant waste compost	2,940	160	3,100	5.2
E	Plant waste compost	1,880	< 10	1,880	2.2
F	Bark compost	2,150	50	2,150	3.6
G	vegetable waste compost	15,910	50	15,960	19.4
H1	vegetable waste compost	4,680 - 21,280	140 – 1,760	5,390 – 21,670	7.1 – 35.7
H2	vegetable waste compost	11,060	40	11,100	13.4
I1	vegetable waste compost	17,920	110	18,030	21.8
I2	vegetable waste compost	276	285	562	7.7
I3	vegetable waste compost	734	443	1,177	15.4
I4	vegetable waste compost	338	56	394	0.8
K1	Source not specified	8,543	884	9,427	30.8
K2	Source not specified	4,782	523	5,305	19.7
K3	Source not specified	5,394	534	5,928	24.2

4.4 PCDD/F Concentrations in Inlet Air

It is reported by J. Koning et al [59] that the PCDD/F concentrations in ambient air are 0.048-0.146 pg(I-TE)/m^3 in Germany. R. Lohmann et al [60] reported the PCDD/F concentration in ambient air are 0.0055-0.22 pg(I-TE)/Nm^3. The PCDD/F concentrations in ambient air are estimated to 0.0055-0.22 pg(I-TE)/m^3 based on these data.

The PCDD/F concentrations in inlet air are also considered as part of total PCDD/F input into MSWI. Assume air flow input into MSWI is 4.5 m^3/kg waste, which is the rate of flue gas production from waste [50]. The PCDD/F concentration in inlet air is calculated to 0.000025-0.00099 pg(I-TE)/g waste. This value is less than 0.01 percent of the other sources of PCDD/F in the MSW feed, and can be ignored.

4.5 PCDD/F Concentrations in Modern MSW Incinerator Effluent and Solid Streams

Emission levels of PCDD/F in the effluent of a MSW incinerator have been reduced over the past decade, due to improved combustion conditions, modern furnace designs, and adequate APC (air pollution control) devices. The international air emission standards are summarized in Table 4.6. A value of 0.05 ng(I-TE)/m^3 PCDD/F concentration for stack emission is reported in typical MSW incinerators in Germany [44].

Table 4.6 Municipal Solid Waste Incinerator PCDD/F Emission Limits (in ng(I-TE)/Nm^3)

EU*	0.1
Germany	0.1
The Netherlands	0.1
USA	0.14 – 0.21
Japan	0.5 (for existing MSWIs) 0.1 (for newly installed MSWIs)

* EU = European Union

The PCDD/F concentrations in the different ash streams are also reduced in modern MSWI relative to older units. PCDD/F concentrations of 0.001 - 0.01 ng(I-TE)/g are found in the bottom ash [44]. This concentration level is as low as the PCDD/F levels which are found in soils of Western Europe that are considered uncontaminated (5 ng(I-TE)/kg) [50]. The concentration of PCDD/F in boiler ash and APC residues from a modern MSWI are also low; a typical boiler ash concentration 0.023 ng(I-TE)/g and APC residue concentration 0.213 ng(I-TE)/g are reported [50].

The author describe a number of different modern incinerators and summarize their reported effluent PCDD/F levels below.

Takuma et al [61] developed a new incineration technology using oxygen enriched primary air (27 percent oxygen) for MSW to reduce Dioxins emission. The MSW incineration facilities are large-scale incineration plants with daily waste throughputs of 146 and 264 metric tons/day. The dioxin concentrations in bottom ash, fly ash and emission gas for conventional and for oxygen-enriched operations are shown in Table 4.7. The dioxin concentrations for conventional (non oxygen enriched) operation is 0.032 ng(I-TE)/Nm^3 in emission gas, which is one third the 0.1 ng(I-TE)/Nm^3 limit. The data on dioxin concentration in the bottom ash and the fly ash show that the dioxin concentration can be reduced by approximately one half using oxygen-enrichment.

Table 4.7 The Dioxin Concentrations in Output of a Large-Scale Incinerator for Conventional and Oxygen-Enriched Operations (Japan) [61]

	Conventional operation	Oxygen-enriched operation
Bottom ash	0.012 ng(I-TE)/g	0.0059 ng(I-TE)/g
Fly ash	1.03 ng(I-TE)/g	0.49 ng(I-TE)/g
Emission gas	0.032 ng(I-TE)/Nm^3	0.0083 ng(I-TE)/Nm^3

Joschek et al [62] described and demonstrated rotary kiln incinerators of BASF Inc., Germany. These plants have kilns of 10 m length, 3.8 m inner diameter and a capacity of 35,000 tons/year. A BASF catalyst which is installed behind the electrostatic precipitator and in front of the scrubber is used for removal of PCDD/F. The PCDD/F in the flue gas is removed by reacting with oxygen to yield carbon dioxide, water and hydrochloric acid. It is reported that the PCDD/F emissions are reduced to values below 0.1 ng(I-TE)/Nm^3.

Sakai [63] investigated and compared the emission release of PCDD/Fs from a number of MSW incinerators at a 30 ton/day operating scale in Japan. The conventional

incinerators were equipped with one of two treatment devices: i. residue melting furnace, ii. thermal dechlorination device. A third system described as initial gasification (pyrolysis) was also studied. This system removed the pyrolysis gases from inorganic solids and metals, with thermal conversion of the solids/inorganics into slags and combustion of the pyrolysis gases. The results are shown in Table 4.8. The PCDD/F concentration in fly ash was reduced from 0.35 ng(I-TE)/g to 0.049 ng(I-TE)/g by the thermal dechlorination treatment, and from 2.05 ng(I-TE)/g to 0.033 ng(I-TE)/g by melting furnace.

Table 4.8 The PCDD/Fs Concentration in Combustion Residues from a MSW Incinerator Using Treatment Technologies [63]

Treatment	Combustion residues	PCDD/Fs concentration (ng(I-TE)/g ash)
Melting furnace	Bottom ash	0.017
	Fly ash	2.05
	Melting fly ash	0.033
Gasification	Melting fly ash	0.17
Thermal dechlorination	Bottom ash	0.002
	Fly ash	0.35
	Dechlorination fly ash	0.049

4.6 PCDD/Fs Mass Balance in MSWIs (Spain)

Several mass balance evaluations for PCDD/Fs in Spanish municipal waste incinerator (MWI) were performed by the research group of Rivera between 1997 and 2000. The PCDD/F levels in the effluents (stack emission, fly ash, and slag) were compared to those in the feed of different MWIs to determine the mass balances for Dioxin. The analysis of

PCDD/F in different components of MSW feed was also presented. The results of the mass balances from these incinerators are described in this section.

4.6.1 Dioxin Mass Balance in Eight Municipal Waste Incinerator (MWI) Plants of Spain

The levels in emission gas, plus those in fly ash and slag as solid residues and the PCDD/Fs in the feed (input) from the urban solid waste (USW) for eight different MWI plants in Spain were analyzed by B. Fabrellas et al. in the period from January 1997-November 1999 [45]. The results are shown in Table 4.9. Total PCDD/Fs emitted were 49-78 g(I-TE)/yr, which were lower than PCDD/Fs in USW feed 53-101 g(I-TE)/yr. An overall PCDD/Fs destruction was reported over the data collected from eight Spanish incinerators in this mass balance evaluation.

Table 4.9 PCDD/Fs in USW, Stack Gas and Fly Ash from Eight Spanish Incinerators [45]

	PCDD/F level	no. of samples analyzed
PCDD/Fs in USW, pg(I-TE)/g	46- 87	10
PCDD/Fs in USW, g(I-TE)/yr	53-101	
PCDD/Fs in stack gas, ng(I-TE)/Nm^3		78
MWI- 4, 5	0.03-1.08	
MWI- 1, 2, 3, 6, 7, 8	0.002-0.1	
PCDD/Fs in slag, ng(I-TE)/g	0.007-0.062	15
PCDD/Fs in fly ash, ng(I-TE)/g	0.69-0.9	50
Total PCDD/F emitted, g(I-TE)/yr	49-78	

Of the eight MWI plants only MWI 4 and 5 exceeded the emission limit 0.1 ng(I-TE)/Nm^3. These two incinerators only had electrostatic precipitators as particulate filters.

Fabrellas et al indicated that their APC systems needed to be upgraded to comply with present standards.

4.6.2 Dioxin Mass Balance in One Spanish MWI and Analysis of Different Waste Materials in the Feed

A dioxin mass balance evaluation in one Spanish MWI in 1998 was presented by E. Abad et al [46]. This MWI was retrofitted with a modern gas cleaning system to comply with the effluent limit of 0.1 ng(I-TE)/Nm^3. Input and output data from two sampling collection episodes including the analysis of PCDD/F in urban solid waste (USD), stack gas emission, fly ash and slag (i.e. bottom ash) were reported and are shown in Table 4.10. The mass balance results showed that the levels of PCDD/Fs in the effluent were 3.31 g(I-TE)/yr higher, compared with those in the feed in one sample collection; while a second sample set showed that the levels of PCDD/Fs in the effluent were 7.7 g(I-TE)/yr lower, compared with those in the feed.

Table 4.10 PCDD/F Levels in Urban Solid Waste, and Effluents (Stack Gas, Fly Ash and Slag) from An Spanish MWI [46]

	Input		**Output**				
sample collec -tion	USW (pg(I-TE)/g)	USW (g(I-TE) /yr)	stack gas (ng(I-TE) /Nm^3)	fly ash (ng (I-TE) /g)	slag (ng(I-TE) /g)	total emitted (g(I-TE) /yr)	Output - Input (g(I-TE) /yr)
1	8.84 (range: 4.4-13.27)	1.33	0.004	0.65	0.06	4.64	+3.31
2	64.15 (range: 45.73-87.48)	9.62	0.004	0.37	0.013	1.92	-7.70

In addition, the analysis of PCDD/F in each category (textiles, wood, organics, paper and plastics) of MSW feed was performed. The metal and glass samples were not analyzed on the assumption that these matrices did not have significant levels of PCDD/F. Table 4.11 gives the levels of PCDD/Fs detected in the waste feed materials. The textile samples were found to present the highest PCDD/F levels, varying between 140 and 170 pg (I-TE)/g.

Table 4.11 Levels of PCDD/Fs in Different Component of Waste Materials

Material	PCDD/F (pg(I-TE)/g)	No. of samples analyzed
Paper	6.26	2
Plastic	21.77	2
Textile	157.35	2
Wood	2.71	2
Organic	2.71	2
Metals	-	-
Glass	-	-

4.6.3 Dioxin Mass Balance in Two MWI Plants of Tarragona (Spain)

E. Abad et al. compared the levels of PCDD/Fs of all input and output contributors (MSW, stack gas emission, fly ash, and slag) in two large-scale MWI plants of Tarragona (Spain) [47]. Eight data sets were analyzed over 1998-1999 and three additional data sets were analyzed in 2000 for PCDD/F in the input feed. Total 8,000 kg of MSW was taken from the waste bunker over a three week period to be analyzed for PCDD/Fs content. A total of eight data sets were obtained and the results are shown in Table 4.12. The PCDD/F levels in the input feed samples ranged from 1.5 to 87 pg(I-TE)/g.

Three types of samples (stack gas emission, fly ash, and slag) collected over the eight data sets in 1998-1999 in the output of MWI plants were analyzed for the total

Table 4.12 Overall Results of PCDD/Fs in MSW Feed, Stack Gas Emissions, Fly Ashes, and Slags (1998-2000)

			Input [a]	
sampling period	sample collection	no. of samples	MSW feed (pg(I-TE)/g)	MSW feed (g(I-TE)/yr)
1998-1999	1	9	64.15	9.3
	2	2	3.24	0.47
	3	2	2.73	0.4
	4	2	4.07	0.59
	5	1	2.29	0.33
	6	2	7.09	1.03
	7	2	2.23	0.32
	8	2	2.36	0.34
2000 [b]	1	6	3.47	0.5
	2	6	4.94	0.72
	3	6	15.31	2.22

				Output			**Output - Input**
sampling period	sample collection	no. of samples	stack gas emission (ng(I-TE)/Nm^3)	fly ashes (ng(I-TE)/g)	slags (ng(I-TE)/g)	total emitted (g(I-TE)/yr)	**(g(I-TE)/yr)**
1998-1999	1	1	0.004	0.37	0.013	1.62	-7.68
	2	1	0.02	0.51	0.011	1.98	1.51
	3	1	0.003	0.55	0.007	1.97	1.57
	4	1	0.01	0.67	0.009	2.42	1.83
	5	1	0.006	0.5	0.004	1.7	1.37
	6	1	0.006	0.27	0.010	1.19	0.16
	7	1	0.009	0.51	0.013	2.05	1.73
	8	1	0.008	0.72	0.010	2.62	2.28

a: Overall Dioxin content in MSW: 1.5-87.5 pg(I-TE)/g.
b: Reevaluation of Dioxin content in MSW (March 2000).

emissions. The data are summarized in Table 4.12. Results determined from the fly ash ranged from 0.27 to 0.72 ng(I-TE)/g; where stack emission gas ranged from 0.004 to 0.02 ng(I-TE)/Nm^3.

The mass balance results showed that the levels of PCDD/Fs in the effluent were higher than those in the feed in seven sample results. Only one sample data showed the PCDD/Fs in the effluent were lower than in the feed.

4.6.4 Partial Summary

Figure 4.1 summarizes the overall PCDD/F levels as described above in the feed and in the effluent of Spanish MWI plants. The results indicate that the PCDD/Fs in the effluent are similar to the levels in the feed.

4.7 PCDD/F Concentrations in United States MSW Feed

The input PCDD/F concentration in the MSW feed is also calculated based on the material weight of each category. A breakdown of the materials generated in each category of MSW in the U.S. 1997 is reported by the USEPA as shown in Figure 4.2 [64]. The concentration values of PCDD/F in each waste fraction shown in Table 4.2 and Table 4.10 are used in this evaluation. The PCDD/F level in MSW is calculated to 55.5 - 521 pg(I-TE)/g, as shown in Table 4.13.

4.8 Data Summary: PCDD/F Concentrations in MSW Feed and in Effluent and Solid Streams

The overall results show that a range of 0.8 to 87 pg(I-TE)/g or 2 to 50 pg(TE BGA)/g PCDD/F is present in the feed to a MSW incinerator in Europe. Table 4.14 summarizes the concentration of PCDD/F in the feed to a MSWI in Europe. A total of nine data are collected from literature. The standard deviation for the average of PCDD/F

concentration is calculated as Equation 4.1. The average concentration of PCDD/F in the feed to a MSWI is calculated to 36 ± 22 pg(I-TE)/g.

Table 4.13 PCDD/F in Different MSW Fractions

Waste fraction	Range of PCDD/F concen -tration (pg(I-TE)/g) [48]	Range of PCDD/F concen -tration (pg(I-TE)/g) [46]	Overall Range	Mater -ials in MSW 1997 (in 10^9 kg)	Weight percent in MSW [64]	PCDD/F in each fraction of MSW (g (I-TE))
A - Paper, cardboard	18–383	6.3	6.3–383	76.0	38.6 %	479 – 29,108
B - Plastics, wood, leather, textile	29–1370	179.2	29–1370	43.3	22 %	1,260 – 59,321
C - Fine debris (dust and particles) < 8 mm	8–468	-	8–468	2.0	1.0 % [a, b]	16 – 936
D - Food and garden wastes, screen remainders > 8 mm	7–100	5.4	5.4–100	45.1	22.9 %	334 – 4,510
E - Other Remainings	290 [c]	-	290	30.5	15.5 %	8,845
Total				197.0		10,934 - 102,720

* a: Weight percent of fine debris in MSW is assumed to be 1.0 %.
* b: Calculation of weight percent of fine debris attached to metal and glass in the MSW is shown in Appendix A.
* c: PCDD/F concentration in fraction E (Other Remainings) is assumed to be the average concentration of total PCDD/Fs in fractions A, B, C, and D.
* The PCDD/F in MSW = (10,934 to 102,720 g(I-TE))/(1.97E+11 kg)
  = 55.5 pg(I-TE)/g to 521 pg(I-TE)/g

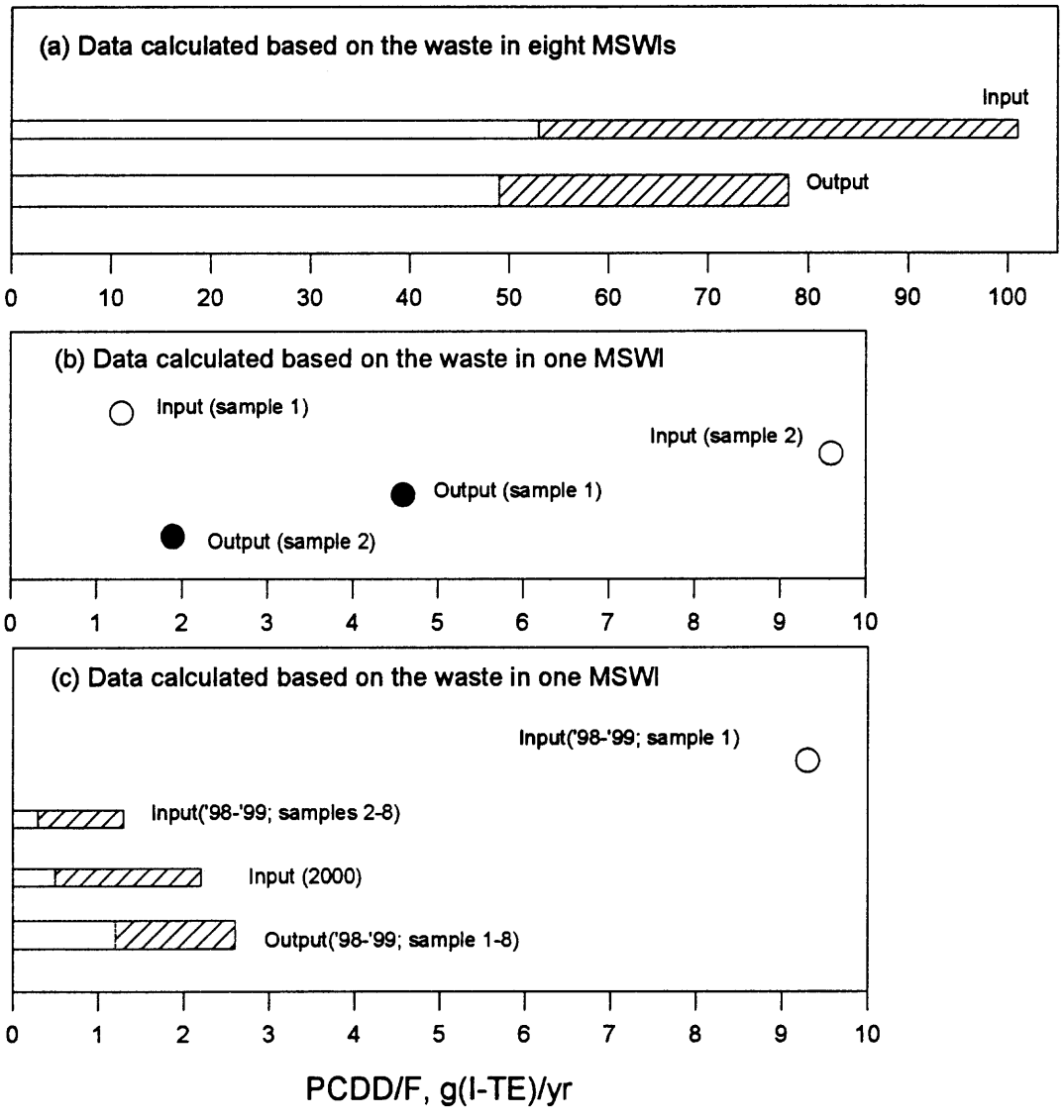

Figure 4.1 Mass balance for PCDD/F in Spanish MSWIs.
(a) Data collected from eight Spanish MSWIs in 1997-1999.
(b) Data collected from one Spanish MSWI in 1998.
(c) Data collected from two Spanish MSWIs (Tarragona) in 1998-2000.

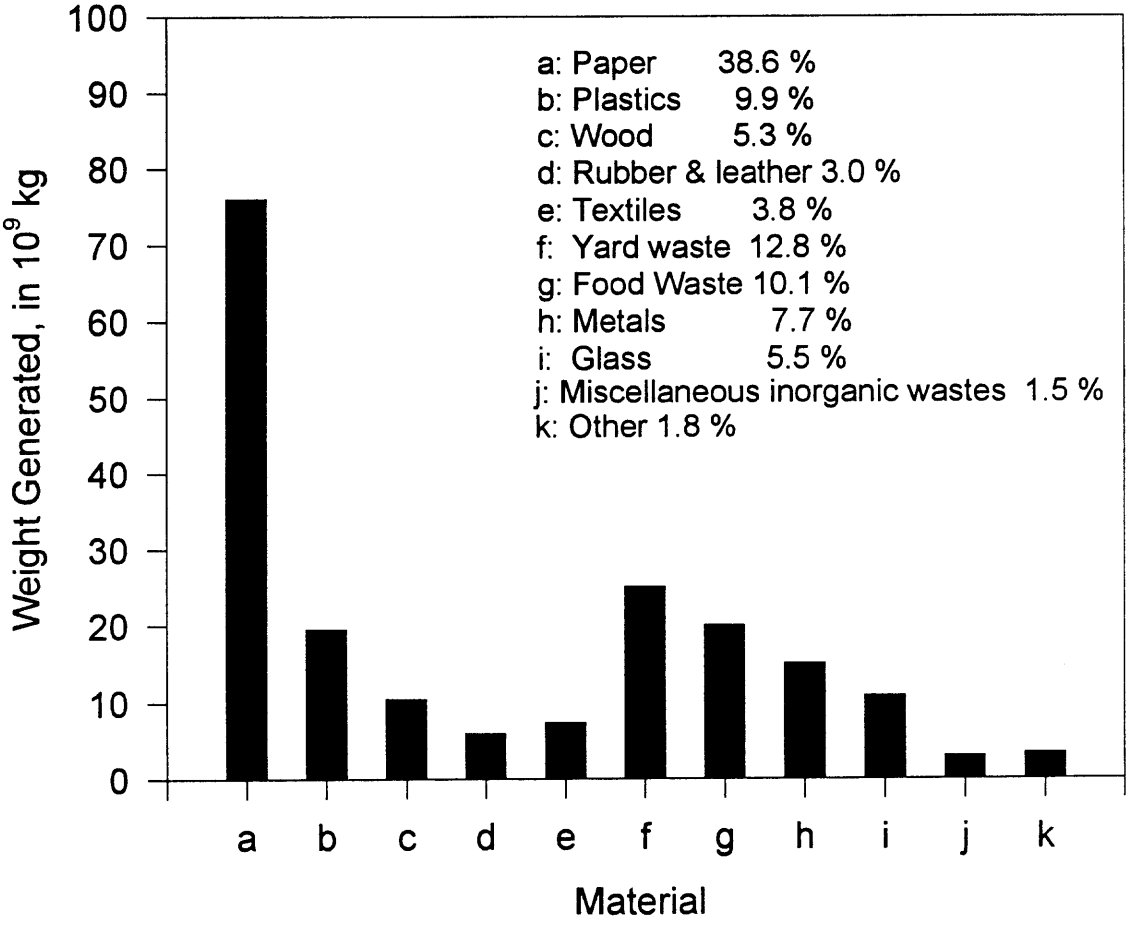

Figure 4.2 Materials in the municipal solid waste of the United States, 1997 as reported by US EPA (Total waste generation before recycling: 197 million metric tons).

Table 4.14 Summary of PCDD/F Concentrations in the Feed to MSWI in Europe

Reference	PCDD/F concentration (pg(I-TE)/g)	
1. M. Wilken (1992) [48]	50.2	
2. M. Wilken (1992) [48]	50	
3. U. Lahl (1991) [49]	10-41	avg. = 25.5
4. U. Lahl (1991) [49]	0.8-35.7	avg. = 18.3
5. E. Abad (2000) [46]	(a) 8.8	
	(b) 64	
6. B. Fabrellas (2001) [45]	46-87	avg. = 66.5
7. E. Abad (2001) [47]	(a) 2.2-64.15	avg. = 33.2
	(b) 3.47-15.31	avg. = 9.4
Mean		36.2
Standard Deviation		22
Average		36 ± 22

The author has classified the waste feed as consisting of different categories (fractions). PCDD/F levels in the different categories are estimated, then the fraction of each waste category is used as categories reported for the US by the US EPA. The total PCDD/F levels in the United States waste feed to MSWI (55.5 ~ 521 pg(I-TE)/g) is estimated to be much higher than the estimates in Europe. This data is strongly dependent on data in Figure 4.1 and it is believed to need further evaluation.

The PCDD/Fs concentration ranges in the emission gas and ash streams (bottom ash, boiler ash, and fly ash or APC residues) in a typical modern MSW incinerator as described above, are summarized in Table 4.15.

Table 4.15 Summary of PCDD/Fs Concentration Ranges in the Emission Gas and Ash Streams in a Typical Modern MSW Incinerator

	PCDD/Fs concentration
Bottom ash, ng(I-TE)/g	0.001 – 0.062
Boiler ash, ng(I-TE)/g	0.023
Fly ash or APC residues, ng(I-TE)/g	0.033 – 2.05
Emission gas, ng(I-TE)/Nm^3	0.002 – 0.1

4.9 Do Modern MSW Incinerators Actually Destroy More PCDD/F Than They Produce?

Data evaluations are performed for the PCDD/F in the feed and in the effluent of MSWIs to determine if more PCDD/F are destroyed than formed in the Municipal Solid Waste (MSW) incineration process. Data evaluation-Europe refers to the data of PCDD/F in MSW feed, which are collected from studies in Europe. Data evaluation-US refers to the data of PCDD/F in MSW feed, which are representative of waste in the US.

4.9.1 Data Evaluation-Europe (Assume 36 pg(I-TE)/g PCDD/F in the Feed)

It appears that input and output levels of PCDD/F in modern, efficient Municipal Solid Waste Incineration are in similar magnitude. One estimates that an averaged annual quantity of 7.2 grams(I-TE) PCDD/F is in the feed (input) to a MSW waste incinerator that has an annual throughput of 2×10^8 kg. This 7.2 gram value is based on a representative average value of 36 pg(I-TE)/g of PCDD/F concentrations in the feed which are based on our available data range 0.8 to 87 pg(I-TE)/g. The PCDD/F output mass ranges are determined based on the MSW output production rates and PCDD/F concentrations in the effluent gas and ash streams, which are shown in Equations (4.1)-(4.2) and Table 4.16. The data evaluation for PCDD/F input mass and emission mass are shown in Figure 4.3. The accumulated annual output in both the gas and the solid mass streams (bottom ash and fly ash/air pollution control residue) are 0.11 - 12 g(I-TE), by assuming operation similar to that reported [44] for modern efficient MSW incinerators. This operation is designed for optimum combustion and for low emission of dioxins.

Table 4.16 PCDD/F in Output Solid Stream and Flue Gas of a Modern MSW Incinerator - The Calculation for MSW and PCDD/F Masses is Based on Annual Input 2×10^8 kg/yr

waste stream	MSW output production rate	ash mass	flue gas volume	PCDD/F Concen -tration	PCDD/F mass in ash or flue gas
bottom ash	0.25 – 0.42 kg/kg waste	(5.0 – 8.4) $\times 10^7$ kg		1 – 62 ng(I-TE) /kg ash	0.05 – 5.21 g(I-TE)
boiler ash	0.002 – 0.012 kg/kg waste	(0.4 – 2.4) $\times 10^6$ kg		23 ng(I-TE) /kg ash	0.009 – 0.055 g(I-TE)
APC residue	0.007 – 0.016 kg/kg waste	(1.4 – 3.2) $\times 10^6$ kg		33 – 2,050 ng(I-TE) /kg ash	0.046 – 6.6 g(I-TE)
flue gas	4 – 4.5 m^3/kg waste		(8.0 – 9.0) $\times 10^8$ m^3	0.002 – 0.1 ng(I-TE)/Nm^3 flue gas	0.0016 – 0.09 g(I-TE)
Total output PCDD/F					0.11 – 12.0 g(I-TE)

Effluent gas volume or ash stream mass, m^3 or kg

= (kg input per year) × (MSW output production rate, m^3/kg or kg/kg) (4.1)

PCDD/F mass in ash or emission gas, ng(I-TE)

= (Effluent gas volume or ash stream mass, m^3 or kg)

× (PCDD/F concentration, ng(I-TE)/m^3 or ng(I-TE)/kg) (4.2)

The effective removal may actually be higher than this. If one assumes that the bottom ash, the boiler ash and the APC ash material are all removed from access by the environment, that is they are stored in a well sealed and managed land fill; then only the effluent gases carry PCDD/Fs back into the environment for further exposure. These

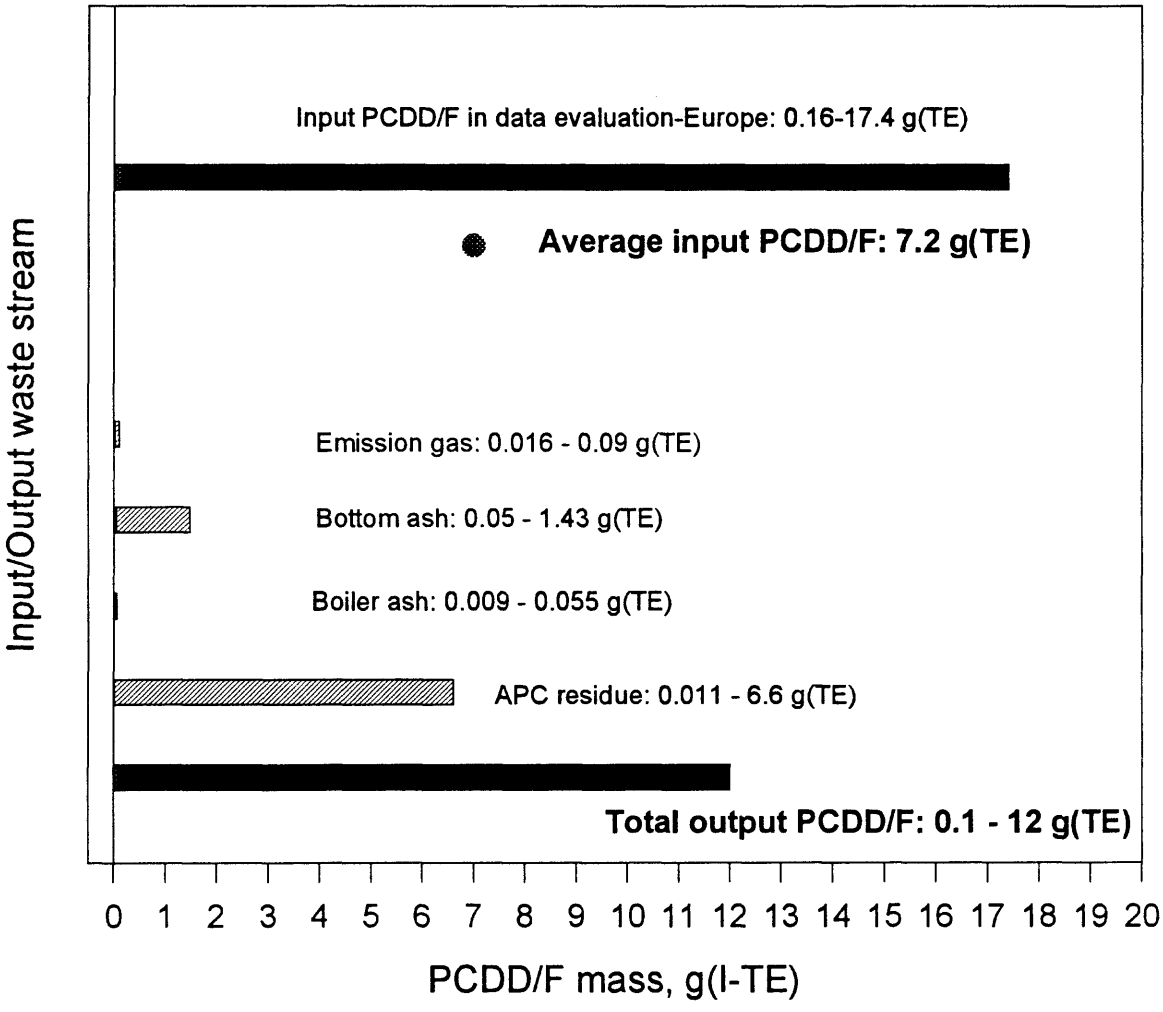

Figure 4.3 Data evaluation-Europe: PCDD/F input mass and emission mass (The calculation for input and emission masses is based on $2*10^8$ kg MSW per year).

effluent gases are reported in Table 4.16 to incorporate an average of 0.05 g(I-TE) PCDD/Fs. This is a reduction in over a factor of 144 from the input (7.2 g(I-TE) PCDD/Fs).

4.9.2 Data Evaluation-US (Assume 288 pg(I-TE)/g PCDD/F in the Feed)

The PCDD/F input mass versus emission mass are evaluated using 288 pg(I-TE)/g PCDD/F input concentration, which is estimated as an average value based on the PCDD/F levels in different categories of MSW reported by the US EPA. It is estimated an annual quantity of 57.6 grams (I-TE) PCDD/F is in the feed (input) to a MSW incinerator that has an annual throughput of 2×10^8 kg. This data show that 5 to 524 times more dioxin (PCDD/F) is destroyed in the MSWI than is produced in effluent to the environment. A reduction in over a factor of 1152 from the input (57.6 g(I-TE) PCDD/Fs) is obtained, considering that only the effluent gases carry PCDD/Fs back into the environment for further exposure.

A data summary for total PCDD/F mass in input and output of MSWI is shown in Table 4.17, which includes the results of data evaluation-Europe and evaluation-US. The results show that the annual PCDD/F mass can be reduced by a factor of 72 (at evaluation-Europe) or higher. This reduction factor can be even higher considering only the effluent gases carry PCDD/Fs back into the environment. It is probably desirable to reduce these effluent levels further.

Data for PCDD/F mass in input and output air is shown in Table 4.18. The PCDD/F in the effluent gas is high relative to ambient air at a factor of 8-18,000.

Table 4.17 Total PCDD/F Mass in Input and Output - PCDD/F Mass are Calculated Based on Total Waste 2×10^8 kg)

	Input Mass g(I-TE)	Emissions Mass g(I-TE)	Reduction Factor (Emissions Gas + Solid Streams)	Reduction Factor (Emissions Gas only*)
Evaluation-Europe	7.2	0.11 – 12	0.6 – 72	144
Evaluation-US (USA)	57.6	0.11 – 12	5 – 524	1152

* Reported average PCDD/F in effluent gases is 0.05 g(I-TE).

Table 4.18 PCDD/F Mass in Input and Output Air - PCDD/F Mass are Calculated Based on Total Waste = 2×10^8 kg

Input Mass	Output Mass*	Output/Input
$5 \times 10^{-6} - 2 \times 10^{-4}$ g(I-TE)	0.0016 – 0.09 g(I-TE)	8 – 18,000

*Output Concentration = 0.002 – 0.1 ng(I-TE)/Nm^3

In summary, data on concentrations of PCDD/F in the feed, and in the effluent from modern municipal solid waste incinerators are collected and evaluated to determine if more PCDD/F are destroyed than formed in the municipal solid waste incineration process. PCDD/F concentrations in the feed of MSW incinerators are categorized into four different waste fractions. Additional PCDD/F data actually measured in the feed to municipal solid waste incinerators are also included. This data is primarily from the international community. The results show that a range of 0.8 to 87 pg(I-TE)/g or 2 to 50 pg(TE BGA)/g PCDD/F is present in the feed to a MSW incinerator. The PCDD/F levels are further applied to mass distributions for the categories of waste reported for the US by the US EPA. The estimates show total PCDD/F levels in the waste feed to a US MSWI is higher, 55.5 to 521 pg(I-TE)/g.

Estimation of PCDD/F concentrations in the output of MSW incinerators considers the production rate of gaseous PCDD/F emissions plus levels in the solid effluent streams (bottom ash, boiler ash and air pollution control residues). The levels are relevant to a contemporary design MSW incinerator with prevailing control equipment. An annual throughput of 2×10^8 kg MSW is used in evaluation of the input and output levels of the modern MSW incinerator.

One evaluation is based on the data of PCDD/F in MSW feed, which are collected from studies in Europe and Japan. The results of this evaluation suggest that a range of 0.8 to 87 pg(I-TE)/g or 0.16 – 17.4 grams(I-TE) PCDD/F in 2×10^8 kg waste is present in the feed to a MSW incinerator. A representative average value of 36 pg(I-TE)/g is chosen for comparison to effluent levels.

Comparison of the input and output levels shows that for 7.2 g(I-TE) PCDD/F in the feed to a MSW incinerator per year; the output in the combined gas and solid streams ranges from 0.11 to 12 g(I-TE) per year. This data indicates that input and output levels of PCDD/F in modern, efficient Municipal Solid Waste Incineration are in similar magnitude.

A higher ratio of input versus output PCDD/F for MSWIs is obtained at the evaluation based on the input fractions representative of waste in the US. This evaluation however is dependent on limited literature results. Further relevant data are still needed for an accurate evaluation.

Do modern waste incinerators actually destroy more PCDD/F than they Produce? Overall, the available data show that the total PCDD/F in input and effluent levels appear to be similar or perhaps slightly more PCDD/F is destroyed than emitted. The PCDD/F

in the effluent gas is high relative to ambient air by a factor of 8-18,000. Further studies on PCDD/F in MSW feed materials as well in the effluent gas and solid streams are recommended to validate these results.

CHAPTER 5

EXPERIMENTAL STUDY ON THERMAL DESORPTION OF ORGANIC CONTAMINANTS FROM SOILS

5.1 Overview

Thermal desorption treatment of field contaminated soils was studied using a bench scale rotary kiln. The soil sample was fed into the rotary kiln desorber at several sets of predetermined variables including kiln temperature, solid residence time, soil feed rate, purge gas flow rate, and humidity in the purge gas. A statistical experimental design was applied to set up the series of experimental runs in order to investigate the effect of operation parameters on removal of organic contaminant from soils. The effect of different design configurations such as co-current and counter-current flow operation was examined in selected experimental runs. The concentrations of carbon in the input soil and in the effluent streams including treated soil and vapor effluent is monitored to determine the mass balance for carbon. Sampling and instrumental analysis methods included ultrasonic and soxhlet extraction, Gas Chromatography Mass Spectrometer, Fourier Transfer Infrared Spectroscopy, Infrared and Gas Chromatographic Flame Ionization Detector, to identify and quantitatively compare mass balances on carbon and organic contaminant removal of the target soil. The experimental results show that temperature, solid residence time and purge gas flow rate, in this order, were the most important parameters in the desorption process. Most of the carbon recovery ranged from 45-115 percent in the result of mass balance for carbon.

5.2 Introduction

Thermal desorption is a physical separation process that inputs low or moderate amounts of energy with a purge gas flow to desorb and vaporize the volatile and semi-volatile organic contaminants from soil. Subsequent incineration or concentration (collection) of organic contaminants in the vapor effluent can then be accomplished more easily and economically. This technology is viable, it uses less energy than complete incineration of the soil mass, allows recycle of the soil, and reduces the volume of the contaminants [66].

Among the types of commercially available thermal desorption systems, such as rotary dryers, thermal screws, and indirectly-heated calciners, rotary kiln thermal desorber is the most commonly used type [67]. A rotary kiln can process larger amounts of soil or waste, due to its continuous operation, compared to other types of desorber systems. A rotating desorber with purge gas flow and uniform continuous feed of contaminated soils provides a well mixed contaminated soil treatment system. It can operate at steady state of temperature and solid residence time, and with the uniform feed, the formation of puffs therefore can be prevented [68].

Thermal desorption has been demonstrated in commercial units for the effectiveness of organic contaminated soil remediation. The organic compounds which were thermally desorbed from soil include volatile organics, semi-volatile organics, and PCB [9, 14, 15, 69].

Several studies have considered the desorption and evaporation of organic contaminant or moisture from soil in a rotary kiln under different operation parameters. The studied operation parameters included temperature, solid residence time, purge gas flow, soil feed rate, solid fill fraction in kiln, kiln rotation speed, moisture content in soil,

and initial concentration of organic contaminants [70-75]. Several empirical and fundamentally based models were developed, along with the experimental studies, in order to aid in interpretation of experimental results and to effect predictions..

Lighty et al. [72] presented a mass-transfer/desorption model to predict desorption of contaminant from soils. P-xylene was used as target contaminant in batch type reactors. Model predictions and experimental results showed the agreement that among the evaluated parameters, which included temperature, solid bed depth, and solid residence time, the temperature was the primary factor to affect the P-xylene remaining in the solids.

Cundy et al. [75] presented a model describing the heat transfer processes within a rotary desorber where the model was validated by comparing the predicted and experimental results. The model was validated by comparing the predicted soil bed temperature profiles and evaporation rates of moisture to those found experimentally. Effects of solid particle size, initial moisture content in solids, and kiln rotation speed were evaluated on the solid bed temperature profiles and evaporation rates of moisture.

Gilot et al. [76] studied the removal of pyrene from a clay soil using thermogravimetric analysis. The experimental results supported the model which predicted 70 percent or more of the pyrene was removed through evaporation. The effects of temperature and treatment time were found to be more significant than other studied parameters such as flow rate of ambient gas and initial mass of soil and pollutant, on the pyrene removal from a clay soil.

Smith et al. [77] used a batch type thermal desorber to study the removal of PAHs from soil. The effect of sample porosity, contaminant molecular weight, desorber

residence time, and desorber temperature on thermal desorption efficiency was investigated. The experiment results were to fitted to an exponential desorption equation to calculate the contaminant desorption rates.

The number of reported fundamental studies on the desorption of organics from soil, which include a heat transfer analysis in the thermal desorber in addition to reported data on contaminated site (soil) cleanup is, however, quite limited. Publications are either based on batch feed type desorber, or use only one compound as target organic contaminant; these cannot be fully considered as representative of the cleanup process on the remediation of field contaminated soils. A clear need exists to incorporate experimental results with a fundamental model on decontamination of soil using a continuously feed thermal desorber, in order to validate a model for prediction use.

The objective of the experimental study in this chapter is to collect data on thermal desorption of organic contaminants from field contaminated soil using a continuous feed rotary kiln thermal desorber. Sampling and instrumental analysis methods are developed and applied for identification and quantitative analysis on organic contaminants in the target soil before and after treatment.

A statistical experimental design method is applied, in which the operation parameters are varied to determine their relative effects on the soil decontamination based on the experimental results. The effect of different design configurations such as co-current and counter-current flow runs was also examined in selected experimental runs. The carbon mass in the input soil and in effluent streams is evaluated to determine the mass balance for carbon in the chosen runs. The experimental results are used to validate a mathematical model which incorporates heat and mass transfer between gas, soil,

moisture and organic contaminants in the thermal desorber. Details of the modeling study will be discussed in next chapter.

5.3 Experimental

5.3.1 Rotary Kiln Thermal Desorber

A bench scale rotary kiln thermal desorber is constructed and tested using lab or field contaminated soils or sand as the evaluation matrices. The bench scale rotary kiln, shown schematically in Figure 5.1, is 16 inches in length and 4.5 inches in outside diameter. Contaminated soil is continuously loaded into the rotary kiln by a pulsating wall screw feeder and desorbed for a predetermined residence time. The screw feeder is equipped with remote controller for turning spline rotation and bed pulsation rates.

Two cartridge heaters, Model MWF * 30275-1 KF, from Ogden Manufacturing Co., Arlington Heights, Illinois, are used to control the temperature. These heaters are the primary heat source for the system and are 0.3 inch in diameter by 18 inches in length. They operate with control of power input and a maximum combined power of up to 2,880 watts.

The temperature for heater control of the reactor is monitored in the center point of the kiln using a type K thermocouple equipped with an Omega Model temperature controller. This thermocouple is placed within a 5 mm ID quartz tube for protection. Another type K thermocouple is also placed in the quartz tube and to be moved along the kiln to measure the kiln temperature profiles once the experimental runs have reached steady state condition.

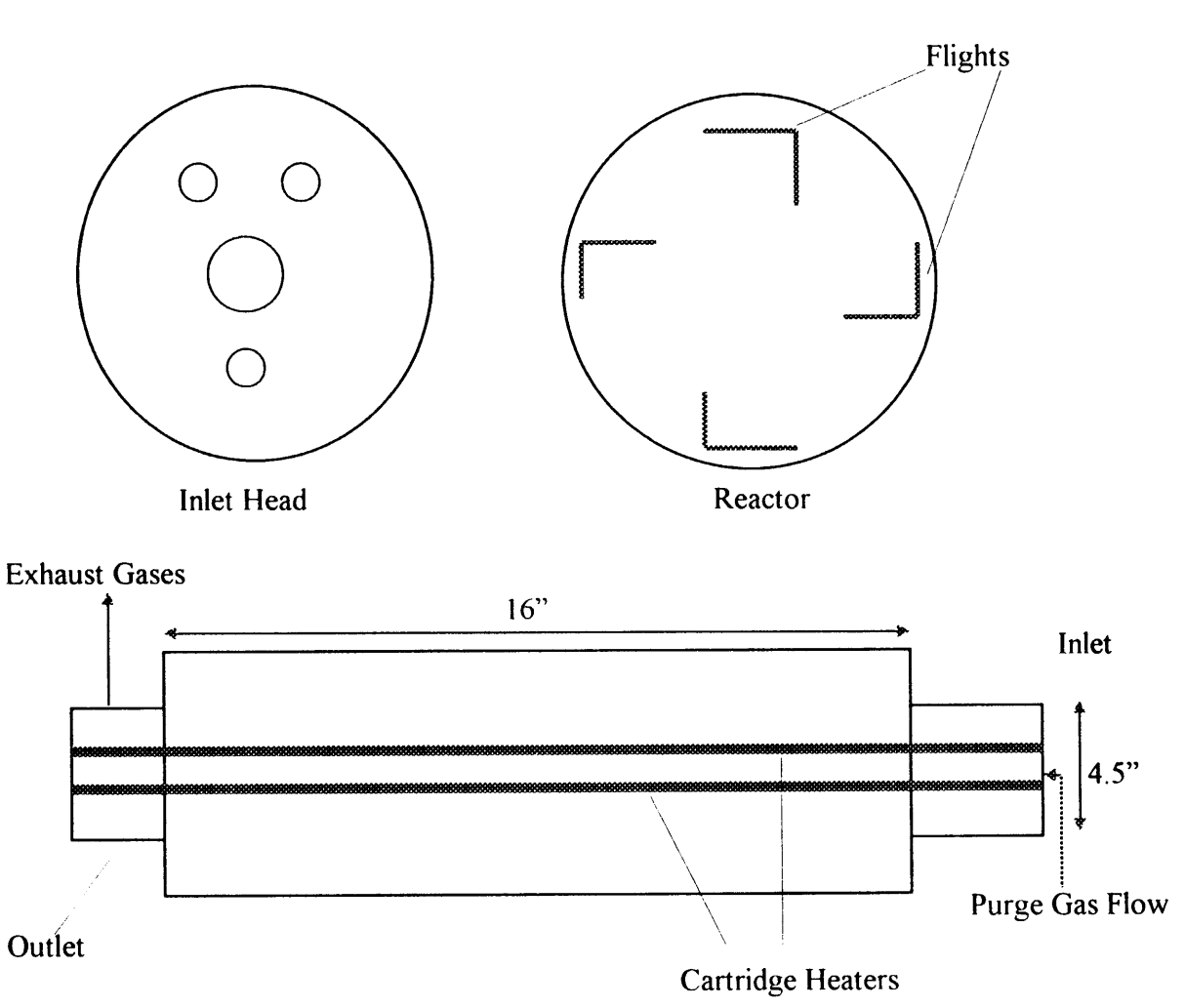

Figure 5.1 Rotary kiln thermal desorber.

An inert air flow is used to purge the reactor and to help remove the organic compounds from the sand and soil in the kiln. The air flowrate is monitored by a rotameter calibrated with a soap bubble meter.

5.3.2 Field Contaminated Soils

The soil studied in this experimental work was obtained from an industrial site thought to be contaminated with hydrocarbons including polynuclear aromatic hydrocarbons. The soil was in dark, brown color. The site soil was sieved to remove the gravel and sand with a particle size more than 2mm. The composition of sieved soil on a dry weight basis was 59 percent sand, 29 percent silt, and 12 percent clay. Soil samples were dried in aluminum trays in fume hood at ambient temperature for 12 hours to reduce the moisture content. A test for moisture in the soil was performed after the dried soil was mixed uniformly. A 10 percent of moisture content in the soil samples was obtained. The organic contaminants in the soil samples were extracted by solvent and analyzed before and after thermal desorption treatment for identification and quantitatively analysis, which will be discussed in next section.

5.3.3 Experimental Design for Operation Parameter Analysis

A statistical experimental design was used to reduce the number of experimental runs required to determine the effect of operation parameters. The experimental runs were performed based on the low, intermediate, and high settings of the operational parameters (variables). The selected operation parameters for the thermal desorption on

Table 5.1 Experimental Design for Thermal Desorption Experimental Runs[a]

Run	Kiln Rotary Speed (rpm)	Kiln Tilt Angle (degree)	Soil Feed Rate (g/min)	Purge Gas Flow Rate (L/min)	Humidity in Gas Flow (mole fraction)	Solid Residence Time[b] (min.)
1	2.5	5.5	80	10	0.1	7.0
2	2.5	5.5	80	10	0.1	8.2
3	4.5	9	120	20	0.16	2.3
4	0.5	2.7	35	5	0.16	36.0
5	4.5	2.7	120	20	0.03	17.0
6	0.5	9	120	20	0.03	14.3
7	4.5	2.7	35	5	0.03	20.0
8	0.5	9	35	5	0.03	15.0
9	4.5	9	35	20	0.03	3.3
10	4.5	9	120	5	0.03	2.3
11	2.5	5.5	80	10	0.1	8.3
12	4.5	9	35	5	0.16	3.3
13	0.5	2.7	35	20	0.03	36.0
14	0.5	2.7	120	5	0.03	32.0
15	0.5	9	120	5	0.16	14.3
16	0.5	2.7	120	20	0.16	33.0
17	4.5	2.7	120	5	0.16	17.0
18	0.5	9	35	20	0.16	15.0
19	4.5	2.7	35	20	0.16	34.0
20	2.5	5.5	80	10	0.1	9.0
21	4.5	5.5	80	10	0.03	5.4
22	1.0	5.5	120	10	0.03	13.3

a: Temperature setting for runs 1 to 20 are: 200, 250, and 300°C, for runs 21 and 22 are 200, 250, 300, and 350°C

b: Residence time is incorporated in the combination of parameters of kiln rotation speed, kiln tilt angle, and soil feed rate.

contaminated field soils is shown in Table 5.1. An experiment matrix consisting of a total of 20 planned plus 2 additional experimental runs was chosen based on the fractional factorial experimental design method to verify the statistical analysis. Four center point runs (run 1, 2, 11, and 20), which used mid-value of each parameter range, were proposed

to help examine the variation of overall result data. A higher kiln temperature 350°C was targeted in two additional runs 21 and 22 to examine the result at a higher temperature setting.

A total of six variables were chosen and the effects of the variables on soil decontaminant were determined based on the experimental data using a statistical analysis method. These variables include kiln temperature, kiln rotation speed, kiln tilt angle, soil feed rate, purge gas rate, and humidity in gas flow. The kiln operation temperature was varied between 200 and 300°C. The kiln rotation speed was varied between 0.5 and 4.5 RPM, kiln incline tilt angle was varied between 2.65 and 9 degrees, and the soil feed rate was varied between 35 and 120 grams per minute. The soil feed rate, in combination with kiln rotation speed and kiln tilt angle, determines the soil residence time in the kiln. The residence time ranged from 2.3 to 36 minutes which resulted from the ranges of soil feed rate, kiln rotation speed, and kiln tilt angle.

The purge gas flow direction was co-current for all runs. The purge gas flow rate was varied between 5 and 20 liter per minute, reaching a linear velocity at 0.011-0.042 m/s. Humidity in gas flow was varied between 3 and 16 percent mole fraction.

A statistical analysis software program Statgraphics (Statgraphic Corp., Princeton NJ) [78] was used to analyze the data of the experimental results and chosen parameter sets. Statgraphics analysis includes: analysis of variables, experimental parameter set design, and regression analysis. The effect on contaminant removal of each operation parameter was determined using Statgraphics analysis. A regression analysis was also performed to determine the optimum condition of operation parameters based on the observed experimental results.

5.3.4 Experiments to Examine Counter-Flow Run Effect and Mass Balance for Carbon

Experimental runs 5, 9, 10, and 14 were performed with a counter-current flow configuration to compare decontaminating data against co-current run results. The effect of this different design configuration was examined using the same setting ranges of operation parameters. The co-flow run is defined as the purge gas flow entering the kiln with the soil and flows in the same direction as soil flow. The counter-flow run however has the purge gas flow inlet at the exit of the kiln and it travels opposite to the direction of soil flow.

The temperature profiles and removal efficiencies of organic contaminants from soils were compared between these two design configurations. In the co-flow runs the soil and purge gas both experienced heating and thus both increase in temperature as the flows travel through the kiln toward the exit. In the counter-flow runs the purge gas will be heated then it will interact with the incoming, cooler soil at the soil entrance area. Here counter-flow runs the purge gas will transfer some heat to the soil and experience some cooling plus possible contaminant recondensation at the purge exit (which is the soil inlet).

Total hydrocarbons (THC) in the soil, along with CO and CO_2 concentrations in the effluent vapor were sampled and analyzed to determine the mass balance for carbon in co-flow runs 5, 10, 21, and 22, and counter-flow runs 9 and 10.

5.3.5 Sampling and Instrumental Analysis:

Organic Contaminants Identification. Organic contaminants in the field contaminated soils were identified by Gas Chromatography/Mass Spectrometry (GC/MS)

and Fourier Transform Infrared Spectrometry (FTIR). Soil samples were extracted by Dichloromethane using soxhlet extraction for sixteen hours at 313 K. The extracts were then concentrated and analyzed by GC/MS using a Varian 3400 gas chromatograph with a Varian Ion Trap Saturn II MS to try and determine specific organic species in the field contaminated soils. Spectra of extract sample were identified by matching library standard spectra in a Varian Saturn version 5.0 software.

FTIR analysis was performed to provide additional information on functional groups of organic contaminants in the soils. The results of functional groups of organics using FTIR were compared and served as a confirmation of the GC/MS analytical results. The soil samples were extracted using Freon 113 following EPA method 418.1. The extracts were filtered and analyzed by a Digilab FTS-40 FTIR.

Sampling and Quantitative Analysis. Four types of parameter sets of samples were analyzed quantitatively in these thermal desorption experiment runs. These samples included THC (total hydrocarbon) levels in the soil prior to treatment, THC levels after treatment, THC in the effluent vapor, and CO/CO2 levels in the effluent vapor.

Hydrocarbon levels in the soil samples were determined by measuring Total Petroleum Hydrocarbon (TPH) level in the extract solution from soils. A fully halogenated hydrocarbon ethane solvent (Freon 113) was used for ultrasonic extraction of the organics from the soils, based on EPA standard method 418.1 [79]. The extract solution is then subject to Infrared adsorption analysis for quantitative determination of hydrocarbon present as hexanes, using the Carbon -- Hydrogen (C--H) streching absorbance band of the IR spectra, entered at 2930 cm^{-1}. A Perkin Elmer Model 1310 infrared spectrometer was used in this analysis.

Volatile hydrocarbon species in the effluent stream were monitored by collection of the samples in impingers containing organic solvent (Freon 113) at ice bath temperature. The collected volatile hydrocarbons in the solvent were then analyzed by the same Infrared spectrometer for soil sample analysis.

CO/CO_2 concentrations in effluent vapor from the kiln were collected by a pre-vacuumed sampling canister followed by GC/FID analysis from gas sample valve loop injection. A batch of 0.0015 mole air sample was collected for CO/CO_2 analysis in each experimental run.

The mass balance for carbon in the desorption process was determined by comparing the THC levels in the soil matrices prior to treatment versus summation of the THC levels in soil after treatment, THC level in the effluent vapor, and CO/CO2 levels in the effluent vapor. Calculation for the amount of THC and CO/CO_2 levels were based on a period of 20 minutes at the steady-state condition of each thermal desorption run. Figure 5.2 shows an overall diagram of sampling and instrumental analysis for the thermal desorption experiment.

5.4 Results and Discussion

5.4.1 Identification of Organic Contaminants in The Field Soil:

GC/MS Identification of Organic Contaminants. Figure 5.3 shows the chromatograms for the GC/MS analysis of the organic compounds in field contaminated soils. The identified compounds as listed in Table 5.2 are identified by matching their mass spectra in a mass spectral library. The results show that the identified compounds ranged in molecular weight from 106 to 170; boiling point from 136 to 285°C. These

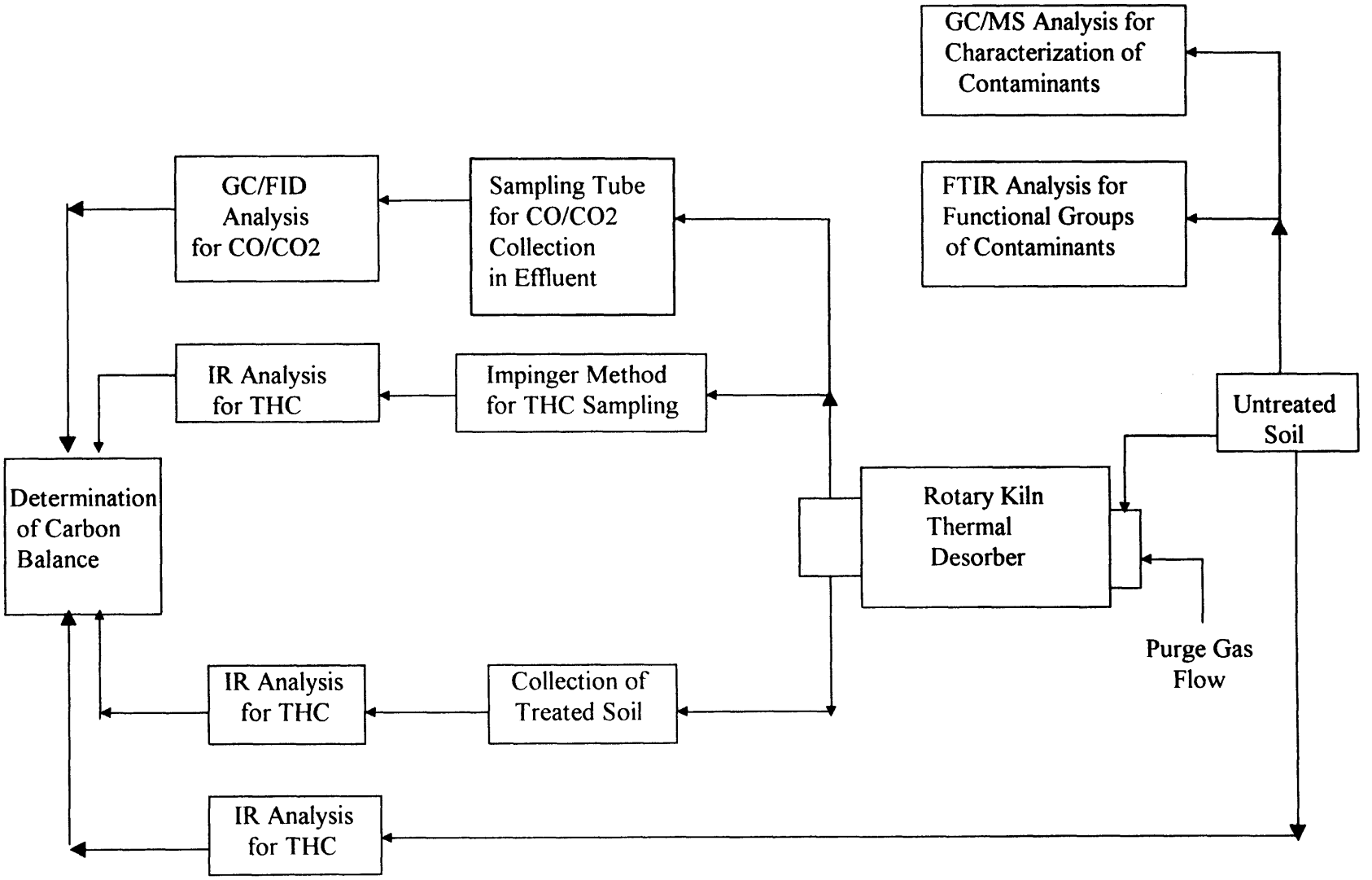

Figure 5.2 Flow diagram of sampling and instrumental analysis for thermal desorption experiment.

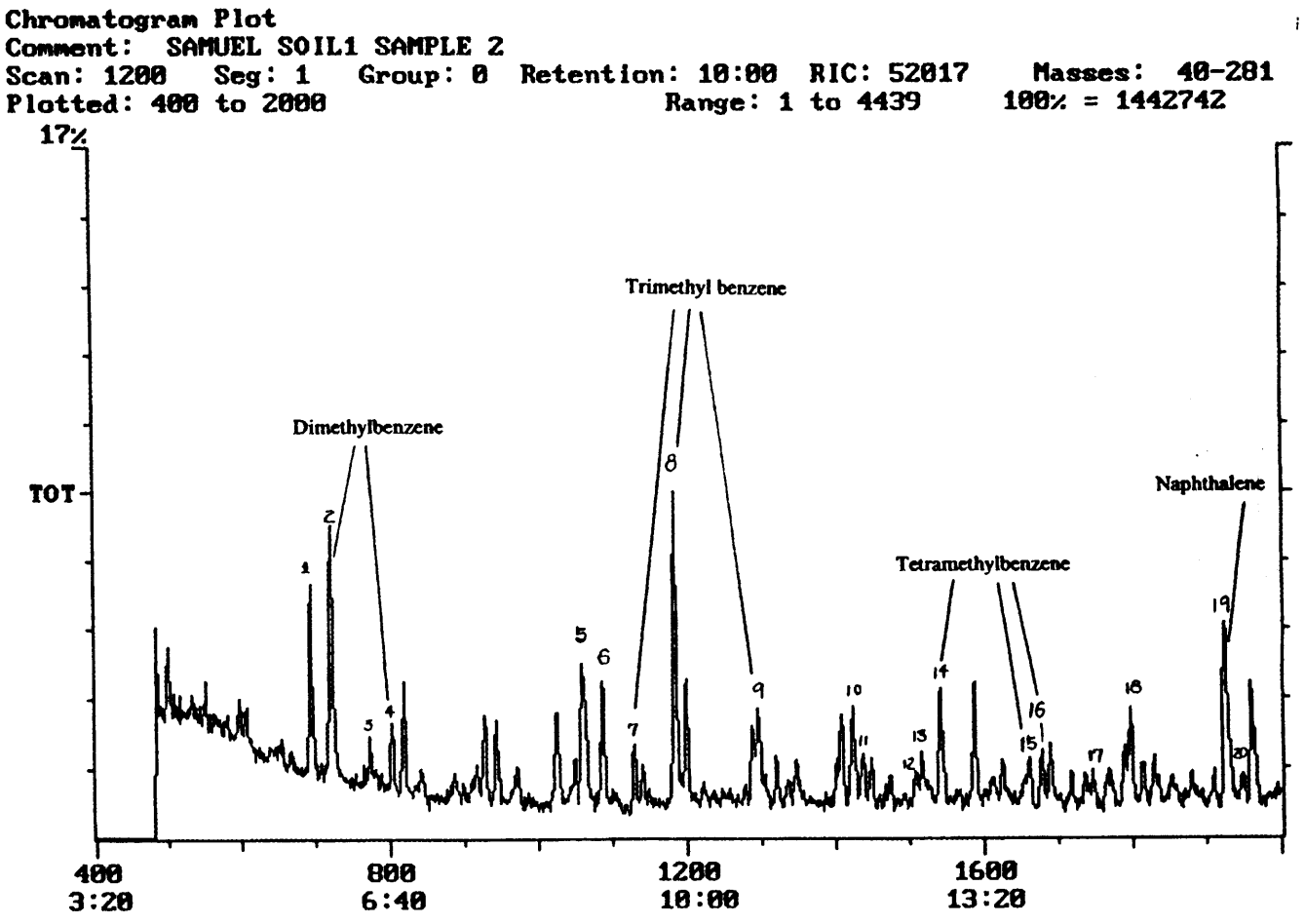

Figure 5.3 Chromatograms of organic compounds analyzed by GC/MS.

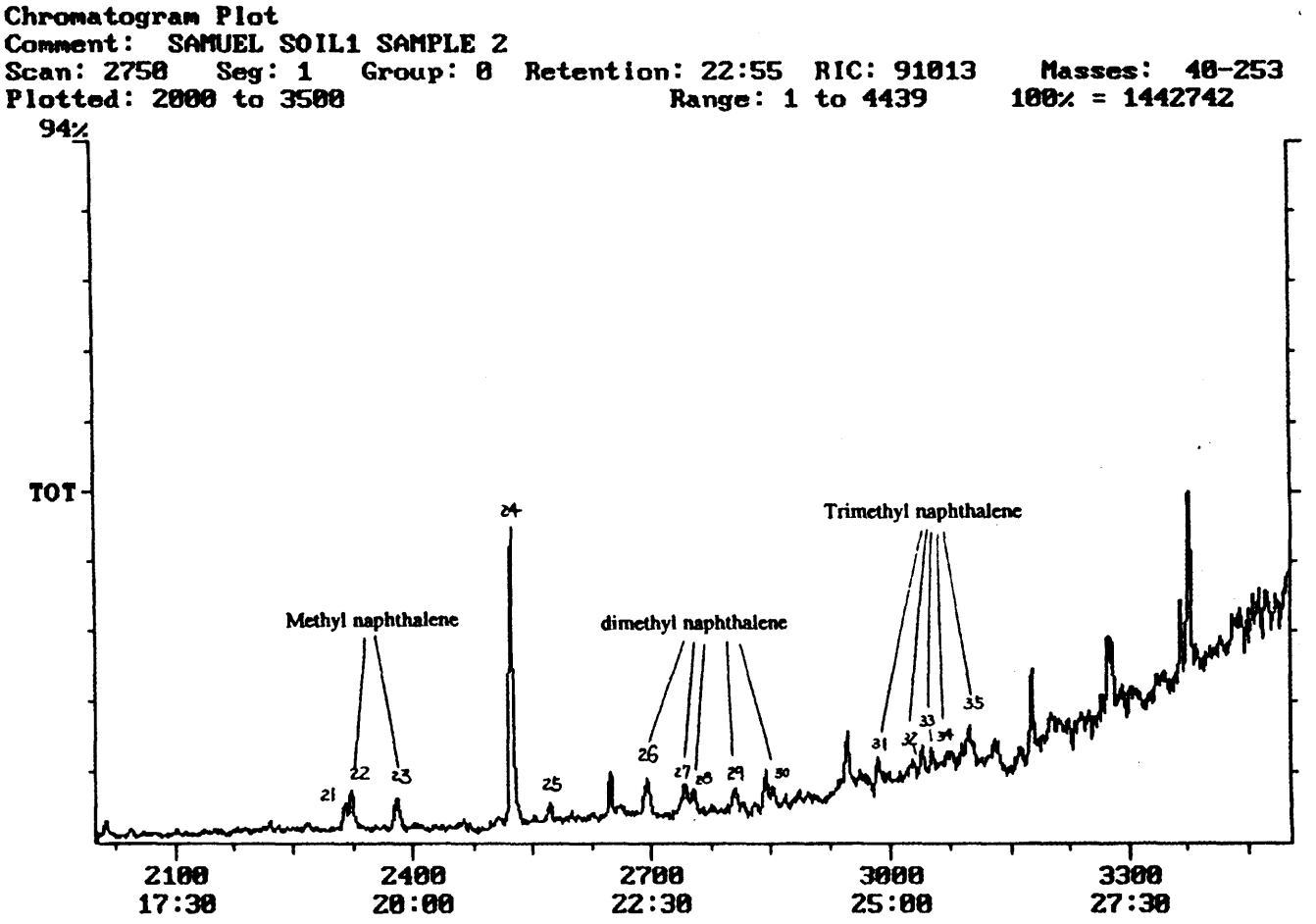

Figure 5.3 Chromatograms of organic compounds analyzed by GC/MS (continued).

Table 5.2 Major Components of Organics in The Field Contaminated Soil

Peak No.	Compound	Formula	Mass	Boiling Point (°C)
1	Ethylbenzene	C8H10	106	136
2	P-xylene (1,4-Dimethylbenzene)	C8H10	106	138
3	2-Isopropyl-1,3-Dimethyl-cyclopentane	C10H20	140	181
4	O-xylene (1,2-Dimethylbenzene)	C8H10	106	144
5	1-Ethyl-3-methylbenzene	C9H12	120	161.3
6	1-Ethyl-2-methylbenzene	C9H12	120	165
7	1,3,5-Trimethyl benzene	C9H12	120	165
8	1,2,4-Trimethyl benzene	C9H12	120	169.5
9	1,2,3-Trimethylbenzene	C9H12	120	176
10	Cycloheptane	C10H14	134	169-183
11	Ethyl-dimethylbenzene	C10H14	134	185
12	1-Ethyl-2,3-dimethylbenzene	C10H14	134	185
13	1-Ethyl-3,5-dimethylbenzene	C10H14	134	185
14	1,2,4,5-Tetramethylbenzene	C10H14	134	191
15	1,2,3,5-Tetramethylbenzene	C10H14	134	196
16	1,2,3,4-Tetramethylbenzene	C10H14	134	204
17	1-Methyl-2-propylbenzene	C10H14	134	185
18	1,2-Diethylbenzene	C10H14	134	183.5
19	Naphthalene	C10H8	128	218
20	2-Methyl-1-butylbenzene	C11H14	146	216
21	Trimethyl-decane	C13H28	184	236
22	2-Methyl naphthalene	C11H10	142	241
23	1-Methyl naphthalene	C11H10	142	245
24	TRIACEN	C9H14O6	218	258
25	trimethyl dodecane	C15H32	212	271
26	dimethyl naphthalene (isomer)	C12H12	156	262-267
27	dimethyl naphthalene (isomer)	C12H12	156	262-267
28	dimethyl naphthalene (isomer)	C12H12	156	262-267
29	dimethyl naphthalene (isomer)	C12H12	156	262-267
30	dimethyl naphthalene (isomer)	C12H12	156	262-267
31	trimethyl naphthalene (isomer)	C13H14	170	285
32	trimethyl naphthalene (isomer)	C13H14	170	285
33	trimethyl naphthalene (isomer)	C13H14	170	285
34	trimethyl naphthalene (isomer)	C13H14	170	285
35	trimethyl naphthalene (isomer)	C13H14	170	285

compounds includes VOC such as p-Xylene as well as SVOC such as naphthalene, dimethyl naphthalene, and trimethyl naphthalene.

FTIR Identification of Functional Groups. The result of FTIR spectra for the organic contaminants in the field contaminated soils is shown in Figure 5.4. An abbreviated table of group frequencies for organic functional groups is included in Table 5.3 [80] for reference purposes and is used for interpretation of the FTIR results. The absorption bands between 2800 and 3100 cm^{-1} are attributable to C-H stretching for

Table 5.3 Relevent Table of Group Frequencies For Organic Groups

Bond	Type of Compound	Frequency Range, cm^{-1}	Intensity
C-H	Alkanes	2850-2970	Strong
		1340-1470	Strong
C-H	Alkenes	3010-3095	Medium
		675-995	Strong
C-H	Alkynes	3300	Strong
C-H	Aromatic rings	3010-3100	Medium
		690-900	Strong
O-H	Monometric alcohols, phenols	3590-3650	Variable
	Hydrogen-bonded alcohols, phenols	3200-3600	Variable, sometimes broad
	Monometric carboxylic acids	3500-3650	Medium
	Hydrogen-bonded carboxylic acids	2500-2700	Broad
N-H	Amines, amides	3300-3500	Medium
C=C	Alkenes	1610-1680	Variable
C=C	Aromatic rings	1500-1600	Variable
C≡C	Alkynes	2100-2260	Variable
C-N	Amines, amides	1180-1360	Strong
C≡N	Nitriles	2210-2280	Strong
C-O	Alcohols, ethers, carboxylic acids, esters	1050-1300	Strong
C=O	Aldehydes, ketones, carboxylic acids, esters	1690-1760	Strong
NO_2	Nitro compounds	1500-1570	Strong
		1300-1370	Strong

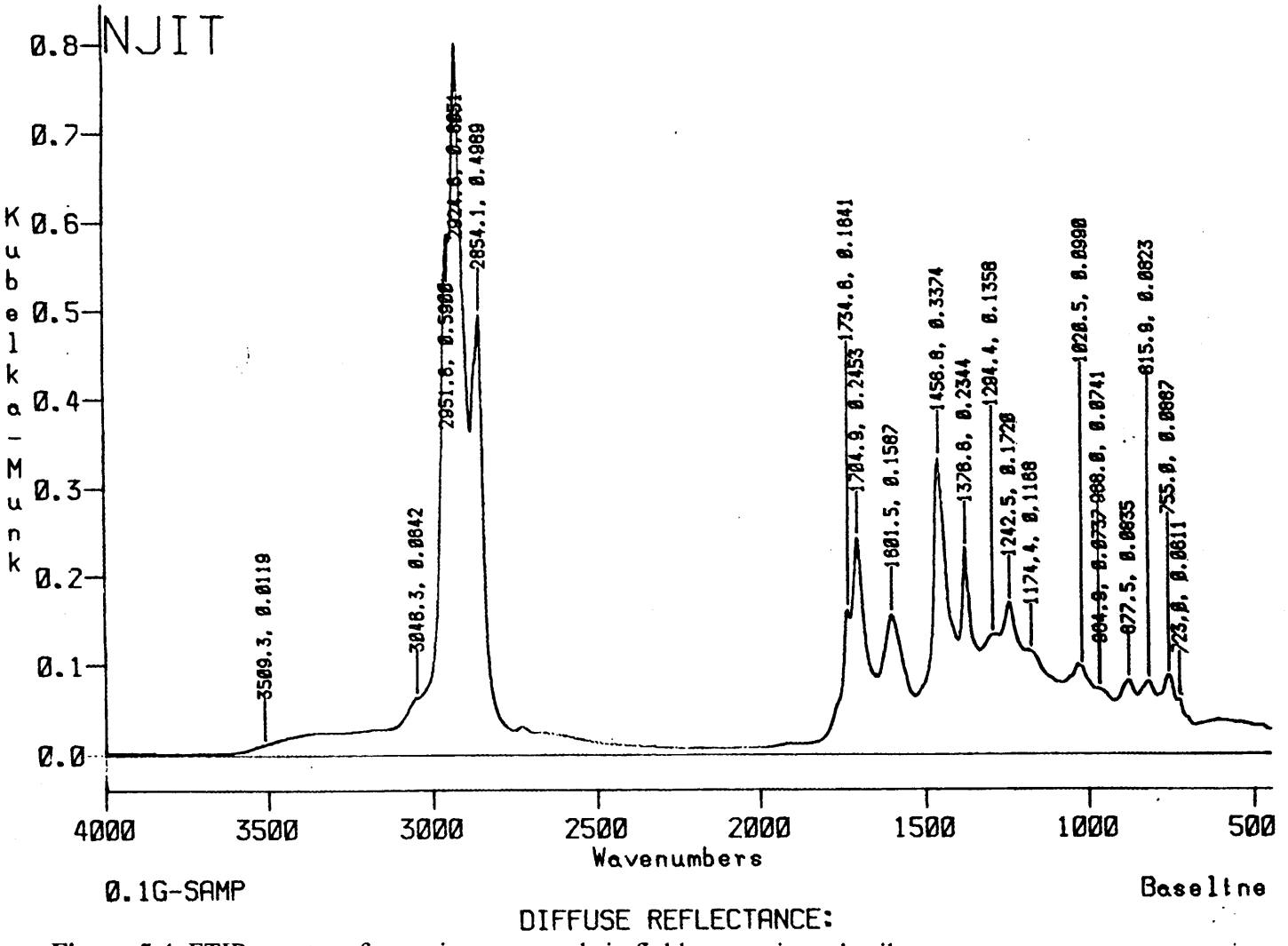

Figure 5.4 FTIR spectra of organic compounds in field contaminated soils.

alkanes, alkenes, and alkyl aromatics. The absorption bands between 1100 and 1800 cm^{-1} are due to C-H bending for alkanes, plus C=C stretching for alkenes and aromatic rings. It is also possible that the bands between 1100 and 1800 cm^{-1} are due to C-O stretching for alcohols, ethers or esters and C=O stretching for aldehydes, ketones, or esters. The bands between 700 and 1100 cm^{-1} are attributed to C-H bending for alkenes and aromatic rings.

5.4.2 Desorption of Hydrocarbons from Field Contaminated Soil - The Experimental Result and Effect of Operation Parameters:

Thermal Desorption Results. THC remainings in soil at 3 percent and 16 percent mole fraction humidity in purge gas flow at 473 K, 523 K, and 573 K kiln temperatures are illustrated in Figures 5.5 and 5.6. The result shows that kiln temperature and solid residence time are found to be the most important parameters to reduce the percent THC remaining in soils. At 473 K kiln temperature and solid residence time less than 4 minutes, the THC remaining in treated soils were over 50 percent. The THC concentration decrease as the temperature and solid residence time increase. At 573 kiln temperature and residence time over 32 minutes, the THC remaining in soil were less than 15 percent.

The purge gas flow also showed positive (i.e. improving removal) on THC removal. Desorption runs with higher purge gas flow showed higher THC removal in the 2.3 and 3.5 minute solid residence time runs and 14.3-17 minute solid residence time runs of Figure 5.5 and 5.6. The humidity in purge gas, which was another evaluated operation parameter; it did not show significant effect on THC removal as compared with the THC remaining result in Figure 5.5 and 5.6.

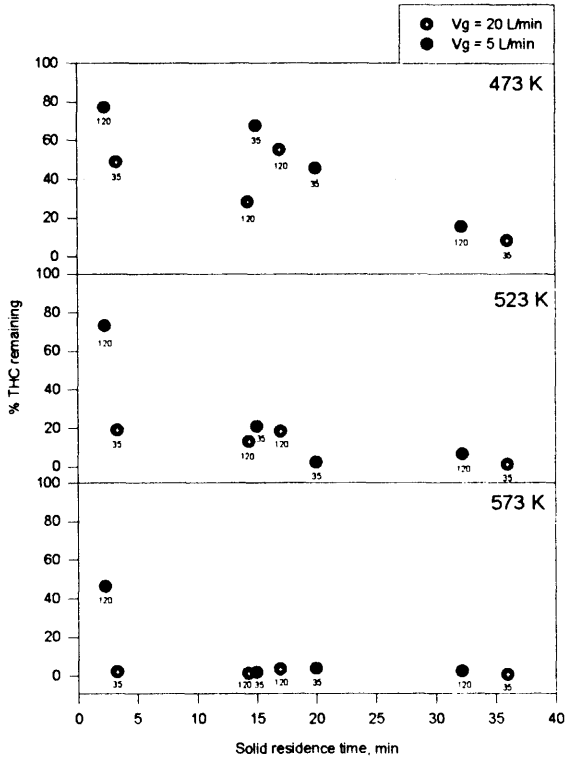

Figure 5.5 THC remaining in soil at 0.03 mole fraction humidity in purge gas flow on 473 K, 523 K, and 573 K kiln temperatures (the numbers denote solid feed rate: 35 or 120 g/min.).

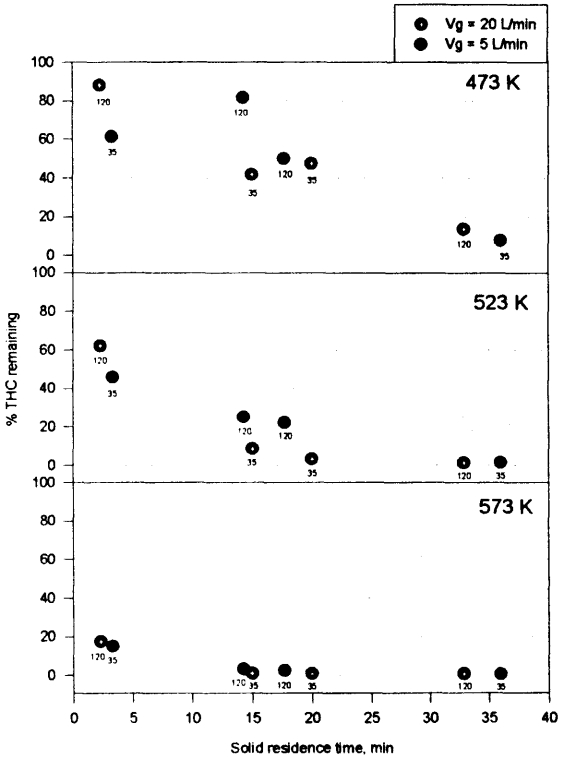

Figure 5.6 THC remaining in soil at 0.16 mole fraction humidity in purge gas flow on 473 K, 523 K, and 573 K kiln temperatures (the numbers denote solid feed rate: 35 or 120 g/min.).

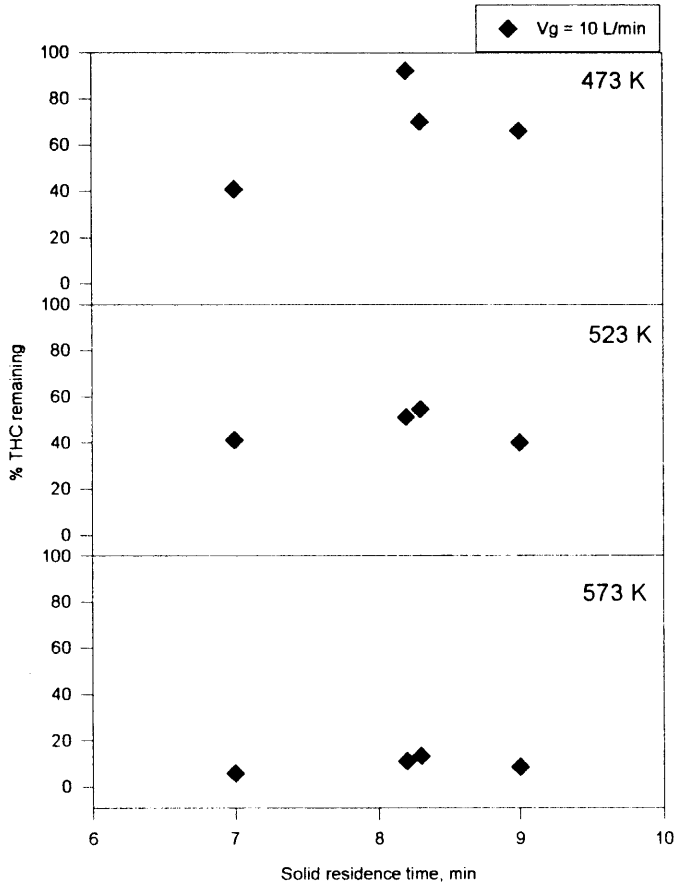

Figure 5.7 THC remaining in soil on 473 K, 523 K, and 573 K kiln temperatures at center point runs 1, 2, 11, and 20.

Figure 5.7 illustrates the result of four center-point runs (run 1, 2, 11, and 20) which used the center value of each operation parameter as shown in Table 5.1. The average and standard deviation values of solid residence time and percent THC remaining in soil are shown in Table 5.4. The result of these four runs shows that a 10 percent variation was obtained for solid residence time, and 15-31 percent variation was obtained for THC remaining in soil. The high variation of percent removal data was due to the organic compounds in the field contaminated soils which were difficult to be uniformly mixed prior to the experiment. The kiln temperature was also not easy to maintain on the target temperature with a narrow range, especially for the runs with high solid feed rate.

Table 5.4 Data Variation of Percent THC Remaining in Field Soils for Four Center-point Runs

Run	Solid residence time (min.)	Kiln temperature (K)		
		473	523	573
1	7	40.8	41.1	5.8
2	8.2	92.1	51	10.9
11	8.3	70	54.5	13.2
20	9	66	40	8.4
Mean	8.1	67	46	10
Standard deviation	0.8	21	7	3
Coefficient of variation*	10 %	31 %	15 %	30 %

* Coefficient of variation = Standard deviation/ Mean

Overall, the results from thermal desorption experiment based on the selected ranges of operation parameters demontrated that this rotary kiln desorber is highly effective in removing organic compounds from field contaminated soils. Temperature and solid

residence time were found to be two primary parameters affecting the desorption results. Increase kiln temperature from 200 to 300°C and increase solid residence time from 2.3 to 36 minutes, can reduce the difficult to remove THC remaining in soils from ca. 80 percent to below 8 percent. Purge gas flow rate also showed a positive but not significant effect on THC removal, compared to effect of temperature and solid residen time.

Effect of Operation Parameters Using Statistical Analysis. Effect of six operation parameters (kiln temperature, kiln rotation speed, kiln tilt angle, solid feed rate, purge gas flow, and humidity in purge gas) on removal of THC from field contaminated soils are illustrated in Figure 5.8. This result was obtained using Statgraphics software based on the experimental result. Six operation parameters were normalized at their ranges to determine their relative effect on THC removal in the 20 runs. The result showed that kiln temperature and purge gas flow had positive effect on THC removal. This was because high temperature increase the volatilization, and diffusion out of pores and desorption from soil surface. The other parameters including kiln rotation speed, kiln tilt angle, solid feed rate, and humidity in purge gas flow however show negative effect (i.e. decreased removal) on THC removal. Increase kiln rotation speed and increase kiln tilt angle results in the decrease of soil residence time in kiln and therefore it also decreased soil exposure time to high temperatures. Increase solid feed rate resulted in the decrease of overall soil residence time and this time exposure to high temperatures. The parameters of kiln rotation speed, kiln tilt angle, and the solid feed rate therefore show a negative effect on THC removal from soils. Increasing these parameter values all result in shorter time and lower temperatures in the kiln operation.

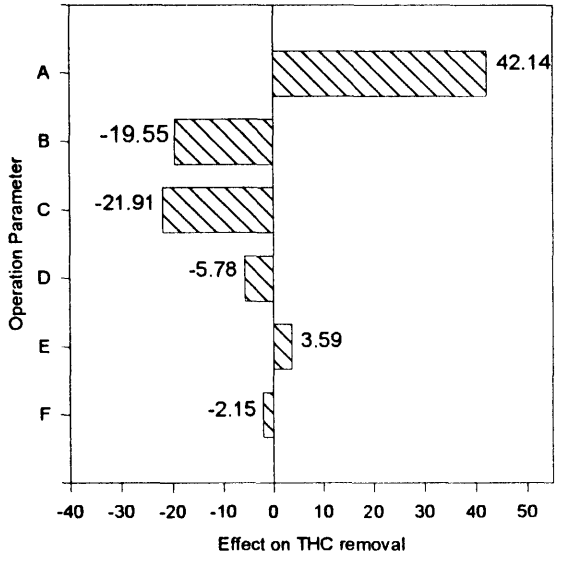

Figure 5.8 Effect of 6 operation parameters on removal of THC from field contaminated soil

(A: kiln temperature, B: kiln rotation speed, C: kiln tilt angle, D: solid feed rate, E: purge gas flow rate, F: humidity in purge gas flow).

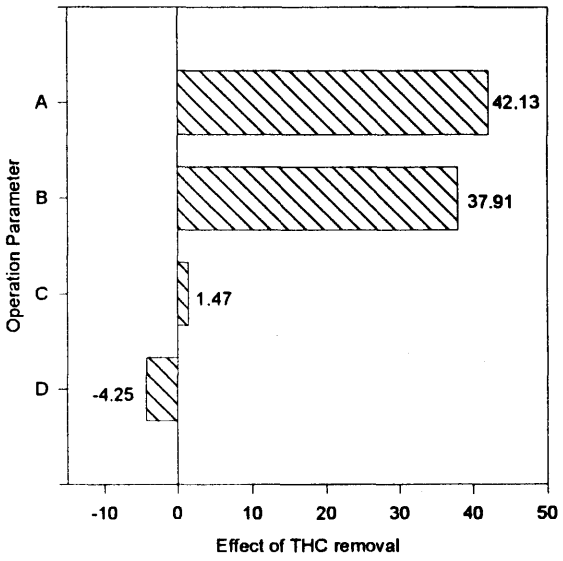

Figure 5.9 Effect of 4 operation parameters on removal of THC from field contaminated soil

(A: kiln temperature, B: solid residence time, C: purge gas flow rate, D: humidity in purge gas flow).

Three parameters including kiln rotation speed, kiln tilt angle, and solid feed rate together determine the solid residence time and can be considered as one factor in the result of Figure 5.8. Figure 5.9 shows the effect of four parameters, which are kiln temperature, solid residence time, purge gas flow, and humidity in purge gas, on THC removal. The positive effect of operation parameters are: kiln temperature > solid residence time > purge gas flow. Humidity in purge gas shows a negative effect on THC removal.

The kiln temperature and solid residence time are found to be two major factors on THC removal using statistical analysis, as shown by data in these Figures 5.8-5.9. Purge gas flow also shows positive but not significant effect compared to temperature and solid residence time. The results for evaluation of operation parameters on THC removal using statistical analysis confirmed the observation of THC desorption data which were shown in Figure 5.5 and 5.6. The statistical analysis of result data provide an efficient and convenient method for determination of operation parameter effect on THC removal in the designed experimental runs.

5.4.3 Regression Analysis of Data and Optimization of Operation Parameters

Regression analysis of thermal desorption experimental data was performed to correlate the relationship between independent variables and the dependent variable percent removal. Four operation parameters including temperature, solid residence time, purge gas flow, and humidity in purge gas were considered as independent variables, and THC removal efficiency was considered as dependant variable in this statistical analysis. Based

on data from the 20 experimental runs, an equation which correlate four independent variables to THC removal efficiency can be expressed as:

$$Y = -67.7 + 0.446\,A + 1.579\,B - 1.108\,C - 3.108 \qquad (5.1)$$

where Y = THC removal efficiency (fraction),

A = kiln temperature (°C),

B = solid residence time (min.),

C = purge gas flow rate (L/min.),

D = humidity in purge gas flow (mole fraction).

Equation 5.1 can be used as an engineering model for prediction of operation parameters required to reach a targeted THC removal. For example, assume 3 of 4 operation parameters are 36 minutes solid residence time, 20 L/min. purge gas flow rate, and 10 percent mole fraction of humidity in purge gas in an experiment run. The targeted THC removal efficiency is 99 percent. The required minimum kiln temperature can then be determined to be 166°C, using equation 5.1. An optimization of operation parameter therefore can be determined through this empirical expression form based on regression analysis method.

5.4.4 Comparison of Results on Co-Flow and Counter-Flow Runs

Results of runs 5, 9, 10, and 14 at co-flow run and counter-flow run conditions were compared. Gas temperature profiles of co-flow and counter-flow runs are shown in Figure 5.10 and 5.11. The gas temperature profiles of co-flow run is shown to increase

steadily, due to the heat contained inlet to the soil and gas as they move along the kiln axial distance in the same direction. The peaks of gas temperature in co-flow runs were near or in the exit of the kiln and were 30 to 100°C higher than the temperature at the kiln entrance.

The peaks of gas temperature in counter-flow runs were found to occur at approximately the 0.6 to 0.7 distance fraction point of kiln relative to entrance. This was due to the counter-current direction of purge gas flow at the kiln exit, where the gas absorbed the heat from the higher temperature soil at the exit end of the kiln; then lost heat to heating the cooler soil at the entrance end. Compared to the peak gas temperatures of co-flow runs, the peak gas temperatures in counter-flow runs were approximately 10 to 60°C lower.

Desorption of THC from field contaminated soils for co-flow and counter-flow runs are shown in Figure 5.12. Less THC removal occurs in counter-flow runs than co-flow runs at 2.3 and 3.3 minutes solid residence times. About 10 to 20 percent more THC remained in the soil in counter-flow run result at 200 and 250°C. The difference of THC remaining however was insignificant in the runs with 17 and 32 minute solid residence times. Less than 4 percent difference in THC remaining between co-flow and counter-flow runs were found under these two run conditions.

Overall, there is non significant difference between the results of co-flow run and counter-flow run. Slightly higher peak gas temperatures were found in co-flow runs at longer times. The result of THC removal does not show a large difference between these two different design configurations. The author suggest using the model to further explore this difference in future work.

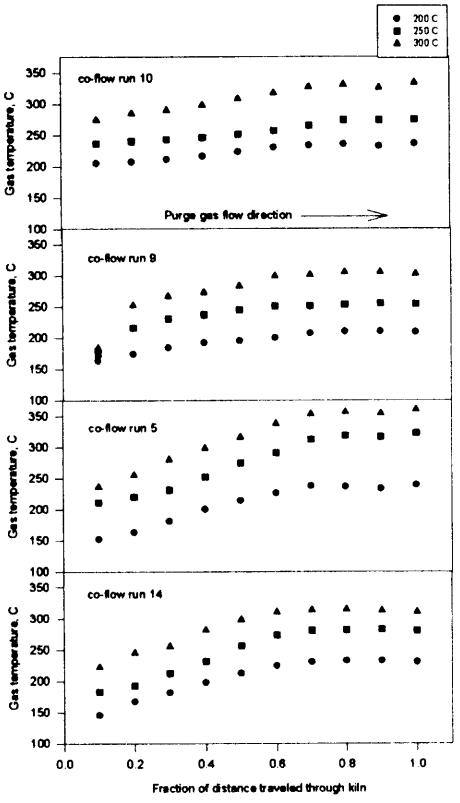

Figure 5.10 Gas temperature profiles of co-flow runs 10, 9, 5, and 14.

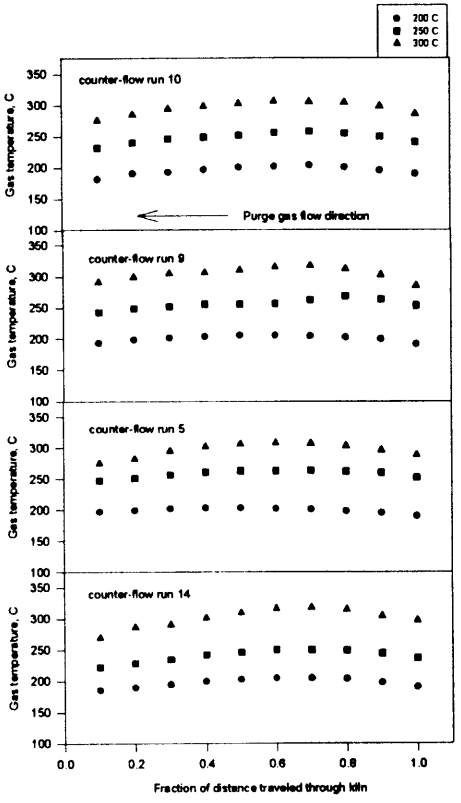

Figure 5.11 Gas temperature profiles of counter-flow runs 10, 9, 5, and 14.

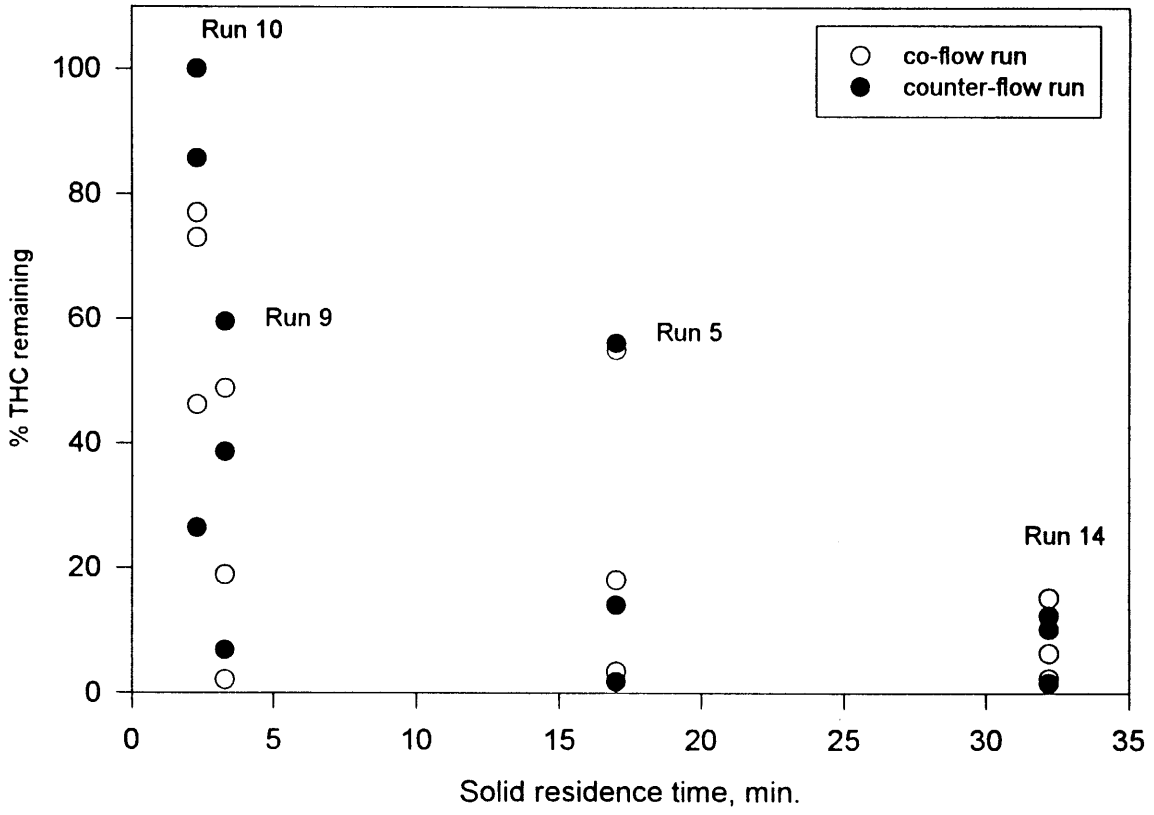

Figure 5.12 Comparison of co-flow and counter-flow runs on removal of THC from soils (Runs 5, 9, 10, and 14).

5.4.5 Results on Overall Mass Balance for Carbon

Experiments were performed at six run condition sets, each at three or more temperatures (20 runs in all) as listed in Table 5.1 to examine the mass balance for carbon. The operation conditions of these 20 runs is shown in Table 5.5. These experimental runs were selected to involve ranges of operation parameters such as direction of purge gas flow (four co-flow runs and two counter-flow runs), solid residence time (2.3 to 17

Table 5.5 Operation Condition of Six Runs to Examine Mass Balance for Carbon

Run no.	Direction of purge gas flow	Kiln tempera -ture (°C)	Solid residence time (min.)	Solid feed rate (g/min.)	Purge gas flow rate (L/min.)	Exit gas flow rate (L/min.)[a]	Humidit y in purge gas flow (mole fraction)
5	co-flow	200, 250, 300	17	120	20	33	0.03
10	co-flow	200, 250, 300	2.3	120	5	18	0.03
21	co-flow	200, 250, 300, 350	5.4	80	10	18.7	0.03
22	co-flow	200, 250, 300, 350	13.3	120	10	23	0.03
9	counter-flow	200, 250, 300	3.3	35	20	23.8	0.03
10	counter-flow	200, 250, 300	2.3	120	5	18	0.03

a: Exit gas flow rate was determined by combining the water vapor with the purge gas flow.

minutes), solid feed rate (35, 80, and 120 g/min.), and purge gas flow rate (5, 10, and 20 L/min.). Each condition set was run at three kiln temperatures (200, 250, and 300°C). Runs 21 and 22 were also at 350°C. Exit gas flow was determined by combining the moisture in soils with purge gas flow for a total gas flow, based on the assumption that the moisture in soil was entirely vaporized to water vapor.

The results on carbon flowrates (shown as moles carbon per minute) in the feed soils and effluent streams of co-flow runs 5, 10, 21, 22, and counter-flow runs 9, and 10 are shown in Figures 5.13-5.18. The determination of mole percent carbon in the feed (input) was based on the THC in feed soils; moles carbon in the output was based on the THC in treated soils, plus THC in vapor, and CO/CO_2 in vapor. The result of carbon remaining in treated soils are consistent for the different temperature runs. A range of 30 to 100 percent mole carbon was observed in the treated soils for 200°C kiln temperature run condition and much lower carbon content is observed in the higher runs.

The mole carbon in the treated soil decreased as temperature increased to 250°C. At 300 and 350°C kiln temperatures, only 3 percent or less of the carbon remains in the treated soils. The only exception is run 10, which has a 31 to 46 percent carbon remained in the treated soils at temperature 300°C, due to the operation condition was at a high soil feed rate (120 g/min.) and very short solids residence time (2.3 minutes) at 300°C.

A reasonable trend of carbon in CO/CO_2 was found in the result over the 20 runs and temperature. The mole carbon in CO/CO_2 increased as the temperature increased (except co-flow run 5). As temperature increased, not only the amount of mole carbon in CO/CO_2 increased, the fraction carbon in CO/CO_2 compared to the mole carbon in total effluent streams also increased. Only at 10 percent fraction or less of the carbon as

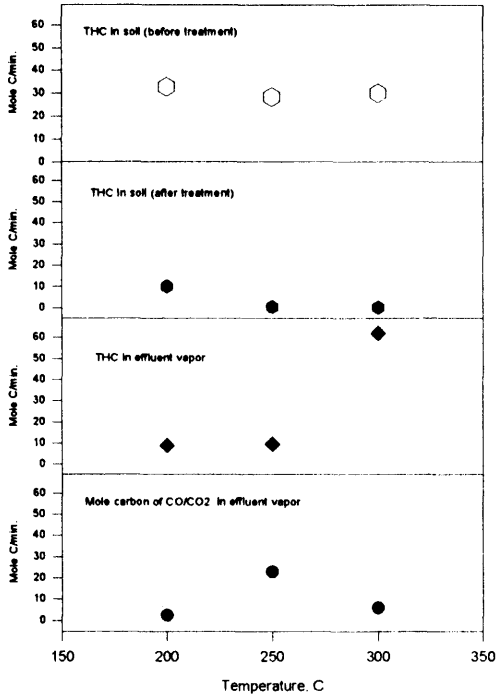

Figure 5.13 Total carbon in soil, vapor and CO/CO2 for run 5 (co-flow run).

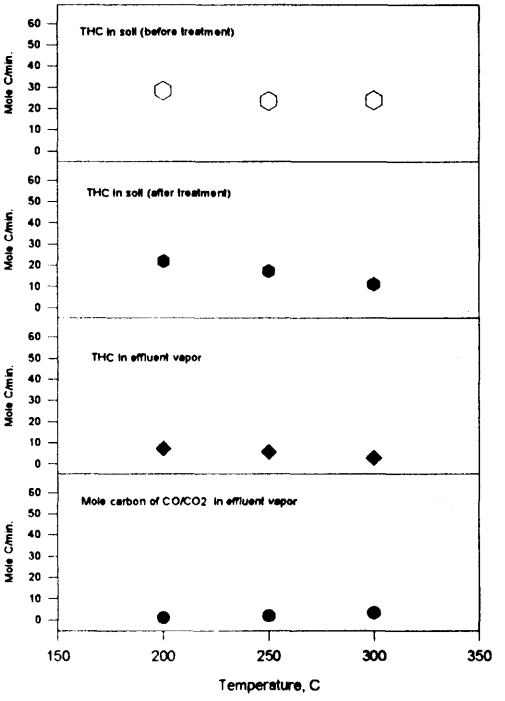

Figure 5.14 Total carbon in soil, vapor and CO/CO2 for run 10 (co-flow run).

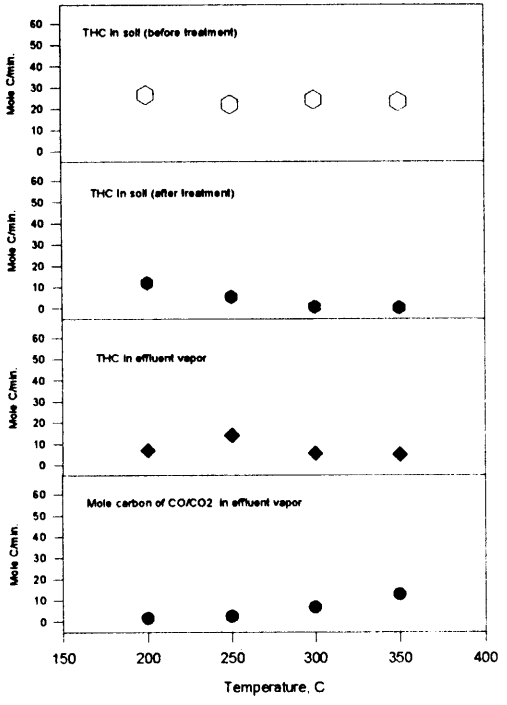

Figure 5.15 Total carbon in soil, vapor and CO/CO2 for run 21 (co-flow run).

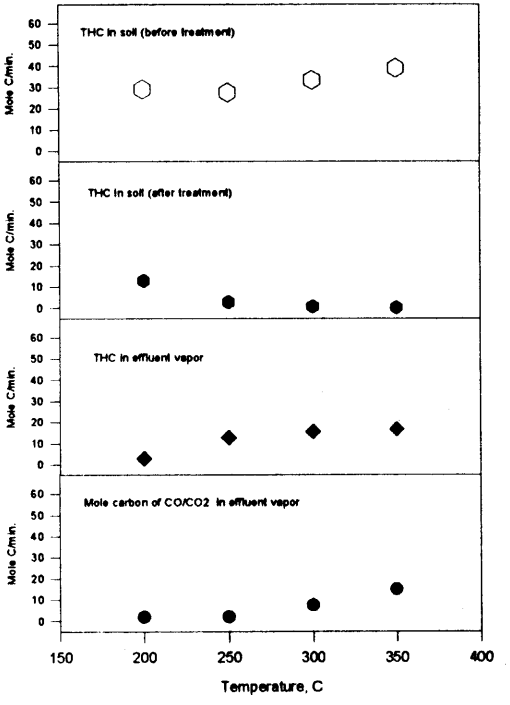

Figure 5.16 Total carbon in soil, vapor and CO/CO2 for run 22 (co-flow run).

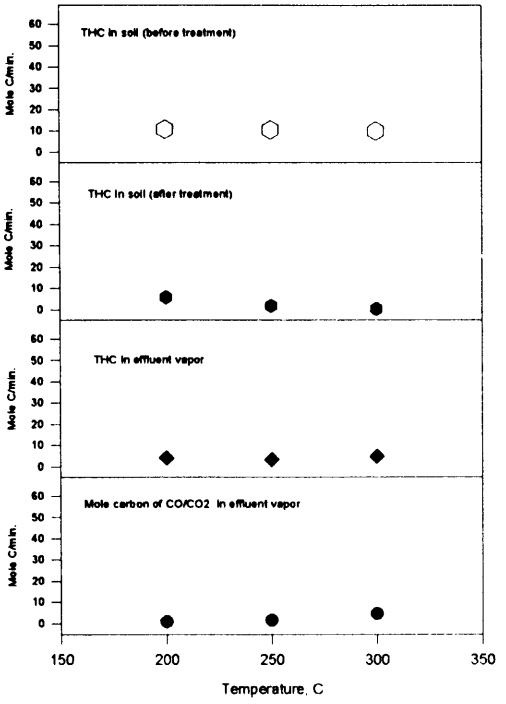

Figure 5.17 Total carbon in soil, vapor and CO/CO2 for run 9 (counter-flow run).

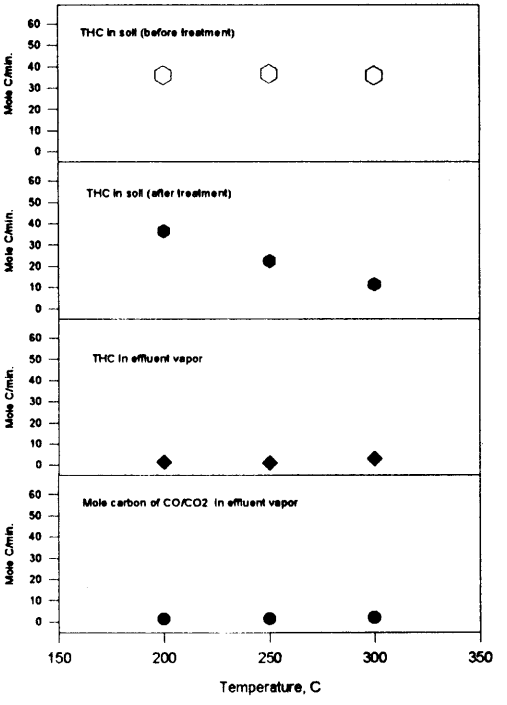

Figure 5.18 Total carbon in soil, vapor and CO/CO2 for run 10 (counter-flow run).

percent in this CO/CO_2 relative to the total mole carbon in the effluent at 200°C . This fraction increased to 47-71 percent as temperature was at above 300°C. This result indicated that the oxidation of THC took place in thermal desorption process at 200 to 350°C, and the higher temperature resulted in more conversion of hydrocarbons to CO/CO_2.

The results on mole carbon measured in the vapor (non CO/CO_2) showed more scatter. The data in co-flow run 10 showed that carbon in vapor decreased as temperature increased from 200 to 300°C. The carbon in vapor in co-flow run 22 however increased as temperature increased. A high value of carbon in vapor was found in co-flow run 5, which resulted in the carbon recovery over 200 percent. These observations indicated that the data from sampling of THC in vapor (non CO/CO_2) using impinger method was not completely consistent and more work needs to be done here to improve precision and accuracy. A higher recovery on mass balance for carbon is expected if the sampling of THC in vapor can be improved.

The results for recovery of carbon by comparing the carbon in the feed soils (input) versus effluent streams (output) is shown in Figure 5.19. High recoveries of carbon were found at 200 or 250°C, such as co-flow runs 10 and 21, and counter-flow runs 9 and 10. The carbon recovery was 97 to 108 percent in these runs. Runs with high and low carbon recovery were also observed. For example, 224 percent recovery in co-flow run 5 at 300°C and counter-flow run 10 at 300°C. This value is considered as an outlier. The results indicated that it might be more difficult to collect VOCs at the higher temperatures such as 300°C. Overall, the results for recovery of carbon in the selected 20 runs ranged from 45 to 115 percent.

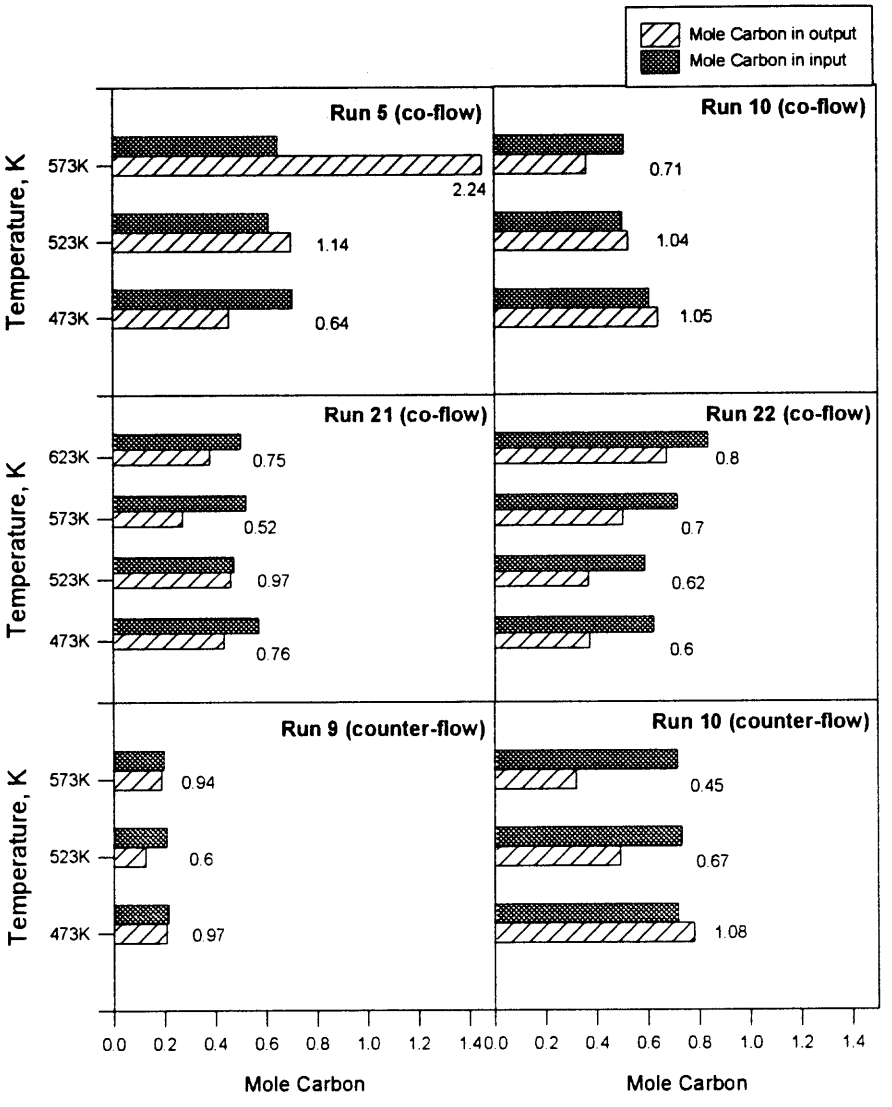

Figure 5.19 Mass balance for carbon in 20 experimental runs (numbers denote the fraction of mole carbon recovery).

5.5 Summary

Results show that the thermal desorber system is effective with desorption removal efficiencies up to 99.5 percent in removing semivolatile organics from field contaminated soils. Temperature and solid residence time are two primary parameters affecting the desorption efficiencies. Higher temperatures and longer residence times result in higher removal efficiency. Purge gas velocity is also found to be an important parameters in the desorption process. The result of mass balances for carbon illustrated that most of carbon recovery ranged from 45 to 115 percent in 20 experimental runs.

CHAPTER 6

MODELING OF HEAT AND MASS TRANSFER IN A ROTARY KILN THERMAL DESORBER

Nomenclature

As	cross sectional area of solid bed
C_{crit_lw}	critical concentration of liquid water in soil, kg/kg
C_{crit_hc}	critical concentration of liquid organics in soil, kg/kg
C_{g_hc}	gas-phase concentration of organic contaminants, kg/m^3
C_{g_vw}	gas-phase concentration of water vapor, kg/m^3
C_p	heat capacity, J/kg.K
C_{s_hc}	initial organic contaminants concentration in the soils, kg/m^3
C_{s_lw}	initial moisture concentration in the soils, kg/m^3
D	kiln diameter, m
D_m	molecular diffusivity, m^2/s
D_{sp}	soil particle size, m
F	mass flow rate, kg/s
FF	fraction of the kiln filled with the solids
F_{vg}	purge gas flow rate, m^3/s
h	heat transfer coefficient, J/s m^2.K
H_{vap}	heat of vaporization, J/kg
W_{input}	energy input, J/s

k_s	soil thermal conductivity, J/s m.K
l_s	bed chord length, m
l_{gw}	exposed wall circumference, m
l_{sw}	covered wall circumference, m
L	kiln length, m
m	soil particle mass, kg
n	number of flight per round
n_s	number of differential slice
Nu	average Nusselt number during a flight
n_r	kiln rotation rate, rev./s
P_{vap}	vapor pressure, atm
q	heat transfer rate per unit length of kiln, J/s m
R_v	evaporation rate, $kg/m^3.s$
r	radius of the kiln, m
T	Temperature, K
t_c	residence time, s
x	axial distance, m
z_0	water content (per wet soil), dimensionless

Greek letters

α	soil thermal diffusivity
β	central angle of the kiln occupied by the soil bed, rad
$\in$	emissivity

σ	Stefan-Boltzmann constant, J/ s.m^2.K^4
λg	thermal conductivity of air/water mixture, J/m.s.K

Subscripts

a	air of surrounding environment
crit	critical
g	gas
l_hc	liquid organic contaminants
lw	liquid water
rod	heater rod
s	soil
sat	saturation
sh	kiln shell
v_hc	vapor organic contaminants
vw	water vapor
w	water

6.1 Introduction

The objective of this paper is to develop a computer model of heat and mass transfer in a rotary kiln thermal desorber, where soil or solids are inlet and then heat is applied to volatilize water (moisture) and contaminants or other volatile species in soil with a purge for exhaust. The rotary kiln reactor is considered as a computation domain which is

divided into cylindrical volume segments (also called computation cell) or radial slices. These computational cells are served as increments in the model treatment. Conservation of energy and mass is formulated in each radial volume segment, where convection, conduction and radiation energy transfer is coupled with energy balance that includes volatilization of both moisture and organic contaminants. The governing equations for each computation cell (segment) are solved numerically using an iterative method and a fourth order Runge-Kutta method. The results from the mathematical model are compared with the experimental data.

6.2 Description of the Model

6.2.1 Heat and Mass Balance Equations

The kiln is of length L and is divided into thin radial slices of differential length, dx, as shown in Figure 6.1. A slice of soil bed, the kiln wall surface, and the freeboard gas with width dx is taken as the computation cell. The freeboard gas refers to the gas filled region within the kiln shell above the soil bed. The soil bed refers to a resting bed of bulk soil particles inside the kiln as the kiln rotates.

The desorption process is assumed to be one dimensional and operate under steady-state conditions. The temperature distributions of soil, gas, kiln wall and heater rods as well as the concentration distributions of moisture and organic contaminants are considered uniform in each computation cell along the kiln. The model also assumes that no chemical reaction (pyrolysis or oxidation) is involved as the process is operated at low temperatures (less than 550°C). Energy and mass balances are performed on each computation cell based on these assumptions and lead to the equations described below.

Energy Balances. The energy balance for the solid bed, freeboard gas and kiln wall within the computation cell which is shown in Figure 6.2 can be expressed as:

The energy input from heater rods into the computation cell:

$$q\text{-input}(x) = W_{input} / n_s = q(x)_{rod \rightarrow s} + q(x)_{rod \rightarrow g} + q(x)_{rod \rightarrow w} \quad (6.1)$$

Energy balance of solid bed:

$$- q(x)_{g \rightarrow s} + q(x)_{w \rightarrow s} + q(x)_{rod \rightarrow s} - R_{v\_lw} A_s (H_{vap})$$

$$= (F_s (1 - Z_0) C_{ps} + F_{lw} C_{plw}) (dT_s / dx) \quad (6.2)$$

Energy balance of freeboard gas:

$$q(x)_{g \rightarrow s} + q(x)_{w \rightarrow g} + q(x)_{rod \rightarrow g} = (F_{vg} C_{pg} + F_{vw} C_{pvw}) (dT_g / dx) \quad (6.3)$$

The axial gradients dT_s/dx and dT_g/dx in the equations (6.2) and (6.3) are calculated from the temperature distribution along the kiln using fourth order Runge-Kutta method.

Energy balance on the kiln wall:

$$q(x)_{rod \rightarrow w} = q(x)_{loss} + q(x)_{w \rightarrow s} + q(x)_{w \rightarrow g} \quad (6.4)$$

where the heat loss, $q(x)_{loss}$, which is along the kiln wall by convection and radiation to the environment, can be expressed as:

$$q(x)_{loss} = [h_{sh \rightarrow a} l_{sh} (T_{sh} - T_a)] + \frac{\sigma l_{sh} [(T_{sh})^4 - (T_a)^4]}{[(1/\epsilon_{sh}) + (l_{sh} / l_a) (1/\epsilon_a - 1)]} \quad (6.5)$$

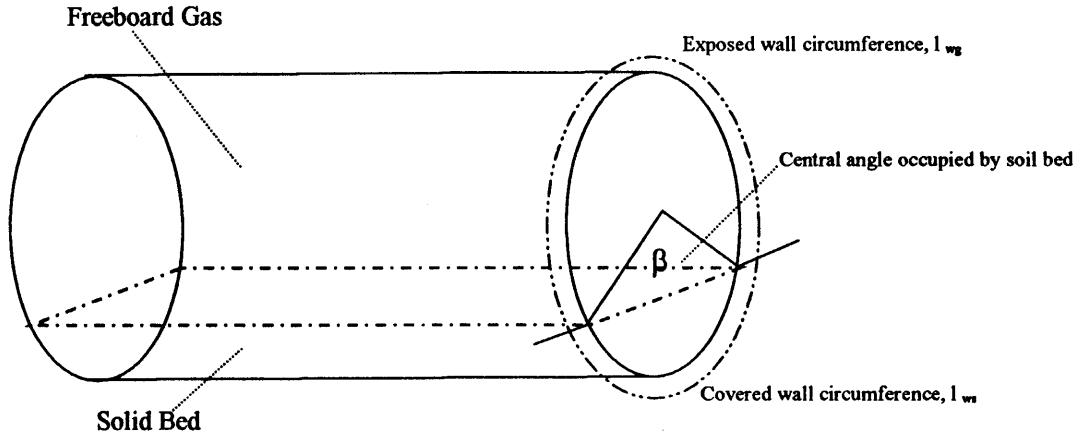

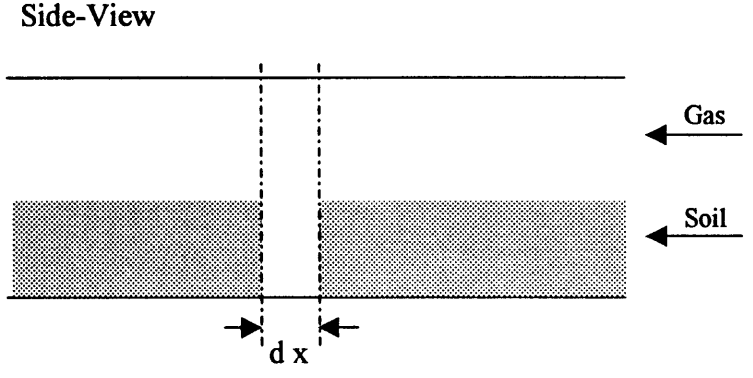

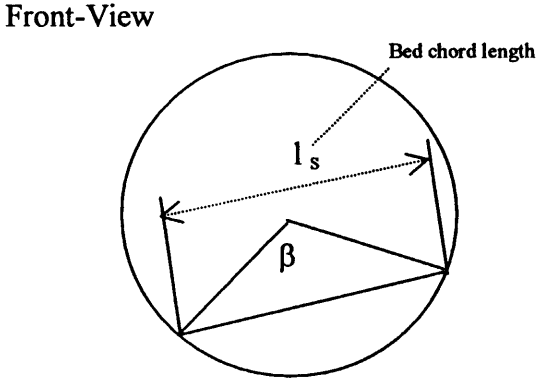

Figure 6.1 Differential slice of rotary kiln thermal desorber.

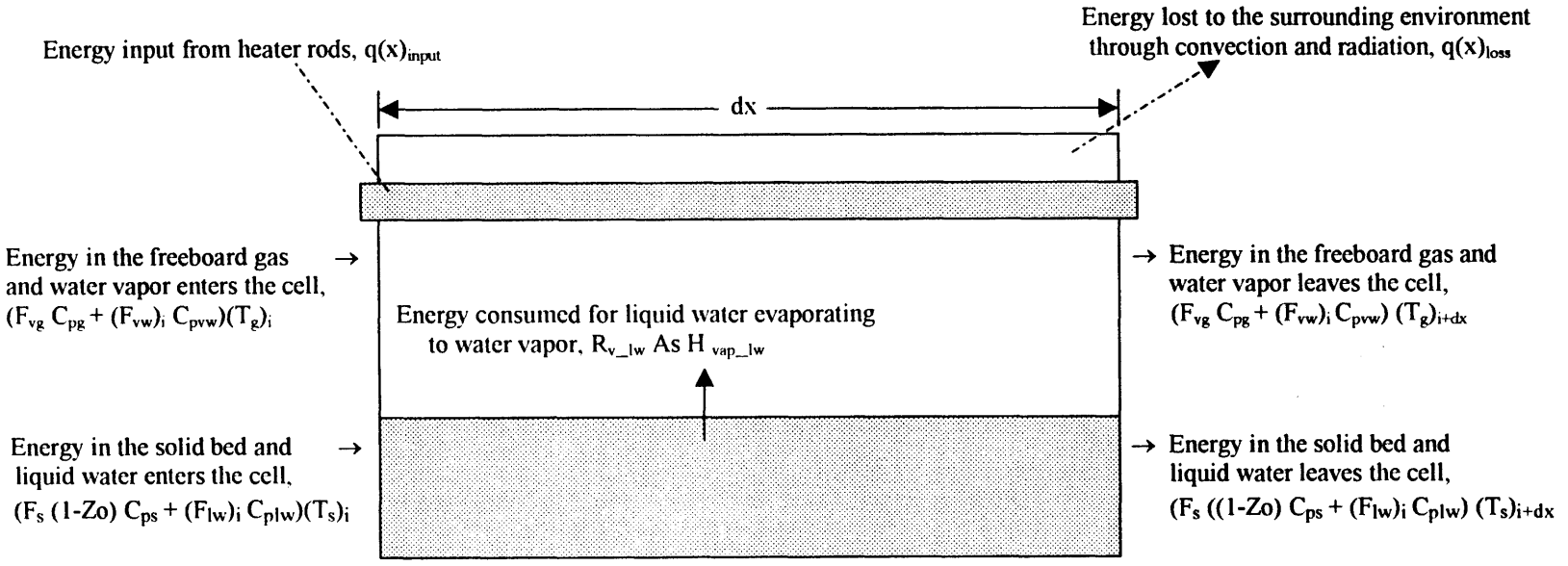

Figure 6.2 Energy balance in the $(i+dx)^{th}$ computation cell.

Combining equations (6.1), (6.2), (6.3) and (6.4) result in the following equation:

$$W_{input} / n_s = R_{v\_lw}\ As\ H_{vap} + (Fs\ (1 - Z_0)\ C_{ps} + F_{lw}\ C_{plw})\ (dT_s / dx)$$

$$+ (F_{vg}\ C_{pg} + F_{vw}\ C_{pvw})\ (dT_g / dx) + [h_{sh \rightarrow a}\ l_{sh}\ (T_{sh} - T_a)]$$

$$+ \frac{\sigma\ l_{sh}\ [(T_{sh})^4 - (T_a)^4]}{[(1/\epsilon_{sh}) + (l_{sh} / l_a)\ (1/\epsilon_a - 1)]} \qquad (6.6)$$

There are only three unknowns dT_s/dx, dT_g/dx, and T_{sh} (i.e. T_w) to be solved in eq.(6.6) considering all heat flow between solid, gas, kiln wall and T_{rod} are conserved. T_w is solved from eq. (6.6) using iteration method following by the solution of dT_s/dx and T_g/dx which is solved by Runge-Kutta method.

Details on heat flow between solid, gas, kiln wall and heater rods is described in the next section.

Mass Balances. The mass balance for the solid bed and freeboard gas within the computation cell involves the evaporation of moisture and organic contaminants from solid bed into the freeeboard gas, shown schematically in Figure 6.3.

The mass balance for the solid bed and freeboard gas is expressed as the following equations:

Mass balance of solid bed:

$$- R_{v\_lw}\ As = d\ F_{lw} / dx \qquad (6.7)$$

$$- R_{v\_hc}\ As = d\ F_{l\_hc} / dx \qquad (6.8)$$

Mass balance of freeboard gas:

$$+ R_{v\_lw}\ As = d\ F_{vw} / dx \qquad (6.9)$$

$$+ R_{v\_hc}\ As = d\ F_{v\_hc} / dx \qquad (6.10)$$

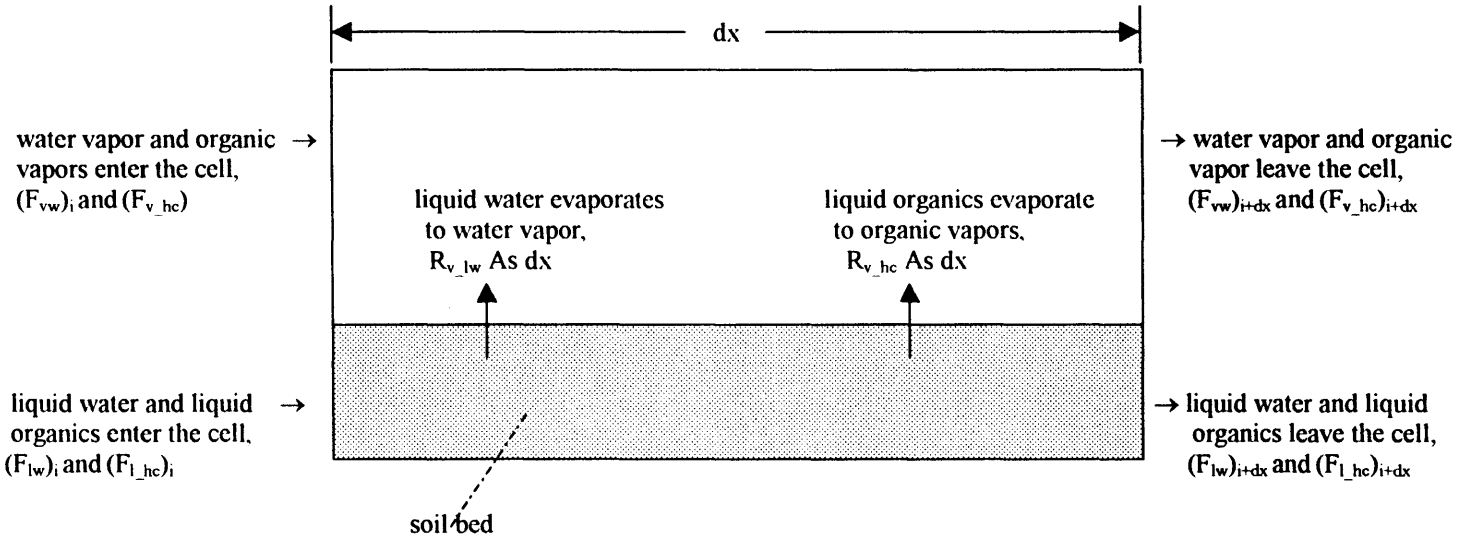

Figure 6.3 Mass balance in the $(i+dx)^{th}$ computation cell.

The evaporation rates of moisture R_{v_lw} and organic contaminants R_{v_hc} are illustrated in 6.2.4.

6.2.2 Calculation of Heat Flows Between Soils, Gases, Kiln Wall and Heater Rods

The mechanism of heat transfer involves the heat flow between soils, gases, kiln wall and heater rods. Six heat transfer steps shown in Figure 6.4 can be described as the following equations:

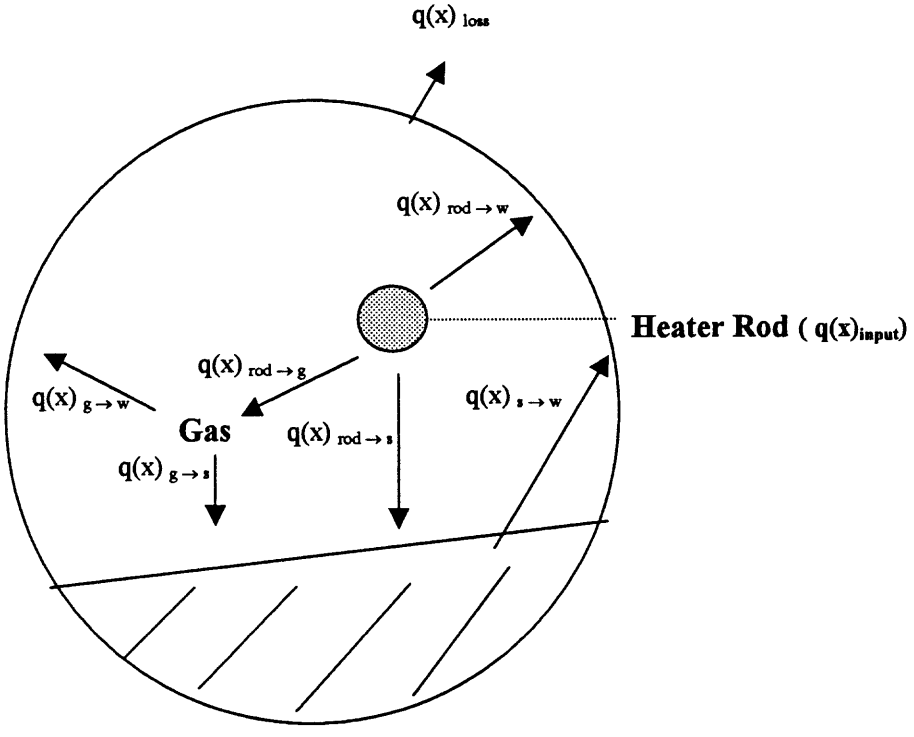

Figure 6.4 Heat flow paths in a rotary kiln: Radiation from heater rods to soil bed and kiln wall ($q(x)_{rod \rightarrow s}$ and $q(x)_{rod \rightarrow w}$) convection from heater rods to gases ($q(x)_{rod \rightarrow g}$), convection from gases to solids ($q(x)_{g \rightarrow s}$), convection from gases to kiln wall ($q(x)_{g \rightarrow w}$), and conduction from soil bed to kiln wall ($q(x)_{s \rightarrow w}$).

Radiation from heater rods to solids:

$$q(x)_{rod \rightarrow s} = \frac{\sigma l_{rod}[(T_{rod})^4 - (T_s)^4]}{[(1/\in_{rod}) + (l_{rod}/l_s)(1/\in_s - 1)]} \quad (6.11)$$

Convection from heater rods to gases:

$$q(x)_{rod \rightarrow g} = h_{rod\text{-}g}\, l_{rod}\,(T_{rod} - T_g) \quad (6.12)$$

Radiation from heater rods to kiln wall:

$$q(x)_{rod \rightarrow w} = \frac{\sigma l_{rod}[(T_{rod})^4 - (T_w)^4]}{[(1/\in_{rod}) + (l_{rod}/l_w)(1/\in_w - 1)]} \quad (6.13)$$

Convection from gases to solids:

$$q(x)_{g \rightarrow s} = h_{gs}\, l_s\,(T_g - T_s) \quad (6.14)$$

Convection from gases to kiln wall:

$$q(x)_{g \rightarrow w} = h_{gw}\, l_{gw}\,(T_g - T_w) \quad (6.15)$$

Conduction from solids to kiln wall:

$$q(x)_{w \rightarrow s} = h_{sw}\, l_{sw}\,(T_s - T_w) \quad (6.16)$$

Detail of the heat transfer coefficients is discussed in 6.2.3.

The energy balance equations (6.1)-(6.4) can be expressed in the follwoing form with the heat flow equations. Incorporating equations (6.11)-(6.16) into equations (6.1)-(6.4) yields:

The energy input from heater rods into the computation cell:

$$W_{input} / n_s = \frac{\sigma \, l_{rod} [(T_{rod})^4 - (T_s)^4]}{[(1/\epsilon_{rod}) + (l_{rod}/l_s)(1/\epsilon_s - 1)]} + h_{rod\text{-}g} \, l_{rod} (T_{rod} - T_g)$$

$$+ \frac{\sigma \, l_{rod} [(T_{rod})^4 - (T_w)^4]}{[(1/\epsilon_{rod}) + (l_{rod}/l_{gw})(1/\epsilon_w - 1)]} \qquad (6.17)$$

Energy balance of solid bed:

$$(F_s (1 - Z_0) C_{ps} + F_{lw} C_{plw}) \, d T_s / dx$$

$$= - h_{gs} \, l_s (T_g - T_s) + h_{sw} \, l_w' (T_s - T_w)$$

$$+ \frac{\sigma * l_{rod} * [(T_{rod})^4 - (T_s)^4]}{[(1/\epsilon_{rod}) + (l_{rod}/l_s)(1/\epsilon_s - 1)]} - R_{v\,lw} \, As \, H_{vap} \qquad (6.18)$$

Energy balance of freeboard gas:

$$(F_{vg} C_{pg} + F_{vw} C_{pvw}) (dT_g / dx) = h_{gs} \, l_s (T_g - T_s)$$

$$+ h_{gw} \, l_{gw} (T_g - T_w) + h_{rod\text{-}g} \, l_{rod} (T_{rod} - T_g) \qquad (6.19)$$

Energy balance on the kiln wall:

$$q(x)_{rod \rightarrow w} = [h_{sh \rightarrow a} \, l_{sh} (T_{sh} - T_a)] + \frac{\sigma \, l_{sh} [(T_{sh})^4 - (T_a)^4]}{[(1/\epsilon_{sh}) + (l_{sh}/l_a)(1/\epsilon_a - 1)]}$$

$$+ h_{sw} \, l_{sw} (T_s - T_w) + h_{gw} \, l_{gw} (T_g - T_w) \qquad (6.20)$$

There are four unknowns, which are dT_g/dx, dT_s/dx, T_w, and T_{rod} in the four energy balance equations (6.17)-(6.20). The axial temperature gradients dT_g/dx and dT_s/dx are solved by fourth order Runge-Kutta method, and the other two unknowns T_w, and T_{rod} are solved using bisection iterative method.

The complete calculation procedure solves the four mass balance equations (6.7)-(6.10) and four energy balance equations (6.17)-(6.20) simultaneously to determine final values of gas and soil temperatures as well as mass flowrates of moisture and organic contaminants in each computation cell. The detail of calculation procedure is described in 6.3.

6.2.3 Calculation of Heat Transfer Coefficients

The heat transfer coefficients of convection between heater rods and gases are determined as [81]:

$$h_{rod\text{-}g} = 2.63\ G_g^{\,0.46} / D_{rod} \qquad (6.21)$$

where G_g is gas mass flux in kiln, $kg/m^2\ s$

D_{rod} is heater rod diameter, m

The heat transfer coefficient of convection between gases and solids is determined as [82]:

$$h_{sg} = 0.46\ k\ Re^{0.535}\ Re_T^{\,0.104}\ f^{-0.341}\ D_e^{-1} \qquad (6.22)$$

where k is the gas conductivity

Re is the Renolds number of gas flow in the kiln

Re_T is the Taylor number which is the Reynolds number using the kiln angular velocity and the equivalent kiln diameter

FF is the fraction of the kiln filled with solids

D_e is the equivalent diameter of the kiln, m

The heat transfer coefficients of convection between gases and kiln wall and are determined as [82]:

$$h_{gw} = 1.54\, k\, Re^{0.575}\, Re_T^{-0.292}\, D_e^{-1} \quad (6.23)$$

The solid-wall heat transfer coefficient by conduction is estimated using a simple penetration theory model [83]:

$$h_{sw} = 2\, k_s\, (2\, n_r / \alpha\, \beta)^{0.5} \quad (6.24)$$

where k_s is soil thermal conductivity, J/s m K

n_r is kiln rotation rate, rev./s

α is the soil thermal diffusivity, m^2/s

β is central angle of the kiln occupied by the soil bed, rad

6.2.4 Evaporation of Moisture and Organic Contaminants

Thermal desorption of organic contaminants from soils involves several mass transfer steps on the moisture and organic contaminants in the soil. The primary step is evaporation of moisture and organic contaminants from soils into vapor phase. An evaporation model developed by Wendt et. al. is applied in this study to determine the evaporation rate of moisture and organic contaminants in a rotary kiln thermal desorber. The model is based on the assumption that the concentration of moisture and organic contaminants at the surface of the particle is in equilibrium with the gas phase at all points and time. The moisture and organic contaminants release from the soil particles by evaporation are followed by diffusion transport through the gas phase. The model concept is shown as Figure 6.5.

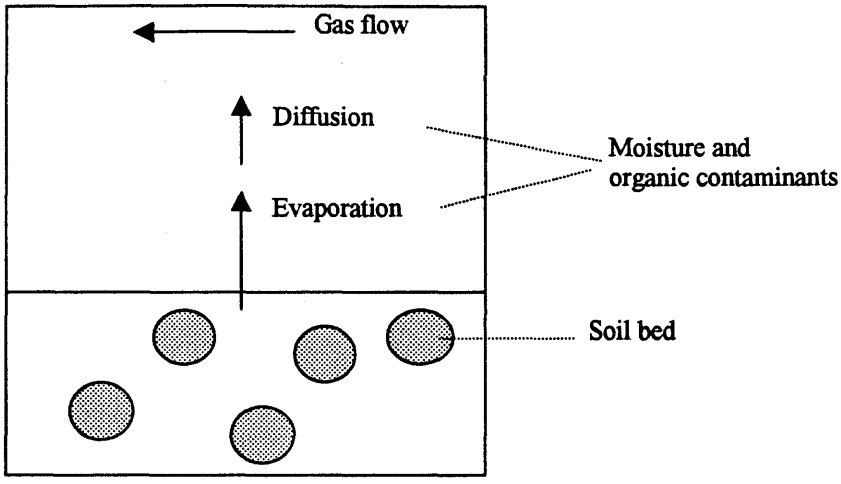

Figure 6.5 Concept of evaporation model.

Evaporation of Moisture. Evaporation of moisture in the soils based on the assumptions described, is given as [84]:

$$R_{v\_lw} = \frac{12\ D_{m\_lw}}{(D_{sp})^2}\ (C_{sat} - C_{g\_vw}) \tag{6.25}$$

Where R_{v_lw} represents evaporation rate of moisture in kg/m^3s, D_{sp} is soil particle diameter in m, and C_{g_vw} is gas-phase concentration of water vapor in kg/m^3 air. It is assumed that the Sherwood Number for an individual grain is equal to 2 and that the grains are spherical.

The molecular diffusivity of moisture in the soil bed is determined by method of Fuller et al. [85]:

$$D_{m\_lw} = \frac{(1.0 \times 10^{-7})\ T^{1.75}\ (1/M_{H2O} + 1/M_{air})^{1/2}}{P\ [(\Sigma v_{H2O})^{1/3} + [(\Sigma v_{air})^{1/3}]^2} \tag{6.26}$$

D_{m_lw} is molecular diffusivity in m^2/s, T is temperature in K, M_{H2O} is molecular weight of H_2O in kg mass/kg mol, M_{air} is molecular weight of air, and P is absolute pressure in atm. Σv_{H2O} = sum of structural volume increments of H_2O, Table 6.1.

The gas concentration at the surface of the particle, C_{sat}, is given as:

$$C_{sat} = \frac{P_{sat}}{R\,T} \tag{6.27}$$

Table 6.1 Atomic Diffusion Volumes for Use With the Fuller et al. Method

Atomic and Structural Diffusion Volume Increments, v	
C	16.5
H	1.98
O	5.48
N	5.69
Diffusion volume for simple molecules, Σv_{air}	
Air	20.1

when C_{s_lw} is higher than C_{crit_lw}, for the regimes where constant drying rate can be applied. For C_{s_lw} is less than C_{crit_lw}, i.e. for the regimes where falling drying rate can be applied, C_{sat} is given as:

$$C_{sat} = \frac{P_{sat}}{R\,T}\,\frac{C_{s\_lw}}{C_{crit\_lw}} \tag{6.28}$$

The quantity P_{sat} is the vapor pressure of moisture in equilibrium with liquid water. This vapor pressure is obtained, using the Antoine equation [84]:

$$\ln(760\,P_{vap\_lw} = \left(ANTA - \frac{ANTB}{T + ANTC}\right) \tag{6.29}$$

where P_{vap_hc} is in atm, T is in K, and ANTA, ANTB, and ANTC are Antoine vapor-pressure-equation coefficients.

C_{s_lw} represents the initial moisture concentration in the soils. The critical concentration of liquid water in the soils, C_{crit_lw},can be estimated from the experiment which is described [72]. We consider C_{crit_lw} as an adjustable parameter and assume it's value to be 15.8 (C_{s_lw}).

Incorporating eqs (6.27) and (6.28) into eq (6.25) yields:

1. For regimes where constant drying rate can be applied; i.e. for $C_{s\_lw} > C_{crit\_lw}$, the equation is:

$$R_{v\_lw} = \frac{12\, D_{m\_lw}}{(D_{sp})^2} \left(\frac{P_{vap\_lw}}{R\,T} - C_{g\_vw} \right) \tag{6.30}$$

2. For regimes where falling drying rate can be applied; i.e. for $C_{s\_lw} < C_{crit\_lw}$, the equation is:

$$R_{v\_lw} = \frac{12\, D_{m\_lw}}{(D_{sp})^2} \left(\frac{P_{vap\_lw}}{R\,T} \frac{C_{s\_lw}}{C_{crit\_lw}} - C_{g\_vw} \right) \tag{6.31}$$

The evaporation of moisture from the soils is defined in the regions where falling drying rate is applied, based on the assumed value of C_{crit_lw}. Eq. (6.31) is used in eqs (6.7) and (6.9) to determine mass flow rates of $(F_{lw})_{i+dx}$ and $(F_{v\_lw})_{i+dx}$.

Evaporation of Organic Contaminants. Evaporation of organic contaminants in the soils is given as [84]:

1. For regimes where constant drying rate can be applied; i.e. for $C_{s\_hc} > C_{crit\_hc}$:

$$R_{v\_hc} = \frac{12\, D_{m\_hc}}{(D_{sp})^2} \left(\frac{P_{vap\_hc}}{R\,T} - C_{g\_hc} \right) \tag{6.32}$$

2. For regimes where falling drying rate can be applied; i.e. for $C_{s\_hc} < C_{crit\_hc}$:

$$R_{v\_hc} = \frac{12\, D_{m\_hc}}{(D_{sp})^2} \left(\frac{P_{vap\_hc}}{R\,T} \frac{C_{s\_hc}}{C_{crit\_hc}} - C_{g\_hc} \right) \tag{6.33}$$

Where R_{v_hc} represents evaporation rate of organic contaminants in kg/m^3s, C_{s_hc} is the initial organic contaminants concentration in the soils in kg/m^3, and C_{g_vw} is gas-phase concentration of organic contaminants in kg/m^3 air. C_{crit_hc} is considered as an adjustable parameter and assumed to be 25 (C_{s_hw}).

The vapor pressure of organic contaminants, P_{vap_hc} in atm, is obtained using the Antoine equation as described in eq (6.29).

The molecular diffusivity of organic contaminants in the soil bed is determined using the method of Fuller et al. [85]:

$$D_{m\_hc} = \frac{(1.0 \times 10^{-7})\, T^{1.75} (1/M_{hc} + 1/M_{air})^{1/2}}{P\left[(\Sigma v_{hc})^{1/3} + [(\Sigma v_{air})^{1/3}]^2\right]} \tag{6.34}$$

Where D_{m_hc} is the molecular diffusivity in m^2/s, T is temperature in K, M_{hc} is molecular weight of organic contaminants in kg mass/kg mol, M_{air} is molecular weight of air, and P is absolute pressure in atm. Σv_{hc} = sum of structural volume increments of organic contaminants, Table 6.1.

The evaporation of organic contaminants from the soils is defined in the regions where falling drying rate is applied, based on the assumed value of C_{crit_hc}. Eq. (6.33) is used in eqs (6.8) and (6.10) to determine mass flow rates of $(F_{l\_hc})_{i+dx}$ and $(F_{v\_hc})_{i+dx}$.

6.3 Numerical Approach

A numerical approach is used to solve the governing mass and heat transfer equations (6.7)-(6.10) and (6.17)-(6.20) simultaneously; these are coupled with evaporation rate equations. Fourth order Runge-Kutta method is used to solve dT_s/dx and dT_g/dx, and the Bisection iteration method is applied to solve the temperature of kiln wall and heater rods in each computation cell. A PASCAL language computer program listing shown in Appendix A is used to solve the equations.

Input parameters for the computer program are listed listed in Table 6.2, which includes initial soil and gas temperatures, trial values of kiln wall and heater rod temperatures, and operation variables such as soil feed rate, purge gas flow rate, moisture content and organic contaminant concentration in the soil. Thermal properties such as heat capacity and emissivity of soil, gas and moisture are input to the program for heat balance calculation.

The flowchart of main program is shown in Figure 6.6. The computer program performs calculation incorporating two subroutines for mass balance of moisture and organic contaminants, and one subroutine for heat balance on soil, gas, kiln wall and heater rods. The evaporation rates of moisture and organic contaminants are calculated in the subroutines for mass balance, followed by the solving of mass flow rates of liquid and

Table 6.2 Representative Model Input Parameters

Parameter	Symbol	Unit	Value
Soil bed temperature	$T_s(0)$	K	298
Gas temperature	$T_g(0)$	K	473
Kiln wall temperature	$T_w(0)$	K	-1
Heater rod temperature	Trd (0)	K	-1
number of integration cell	nsi	(dimensionless)	1520
Kiln length	LL	m	0.483
Kiln diameter	DD	m	0.1
Kiln length in one integration cell	LLi	m	0.0254
Power supplied to kiln	IxV	J/s	1171
Power supplied to one integration cell of kiln	IxVi	J/s	61.6
Heater rod circumference	l_{rod}	m	0.056
Bed chord length	l_s	m	0.098
Exposed wall circumference	l_{wg}	m	0.171
Covered wall circumference	l_{ws}	m	0.140
Heat convection coefficient between heater rod and gas	h_{rod_g}	J/ s.m^2.K	20.91
Soil feed rate	F_{ss}	kg/s	0.00133
Purge gas flow rate	F_{vg}	m^3/s	0.000165
Density of gas	d_g	kg/m^3	0.674
Heat capacity of gas	$C_{pg,}$	J/ kg.K	995
Heat capacity of soil	C_{ps}	J/ kg.K	880
Heat capacity of liquid water	C_{plw}	J/ kg.K	4200
Heat capacity of water vapor	C_{pvw}	J/ kg.K	1960
Fraction of moisture in the soil	z_o		0.1
Heat convection coefficient between kiln shell and kiln wall	h_{sh_a}	J/ s.m^2.K	3
Temperature of air surrounding the kiln	T_a	K	298
Kiln shell circumference	l_{sh}	m	0.3142
Circumference of air surrounding the kiln (assumed)	l_a	m	10E+10
Density of soil particle	d_s	kg/m^3	1150
Soil particle diameter	D_{sp}	m	0.00015
Heat of vaporization	H_{vap}	J/kg	2.26E+6
Central angle occupied by the soil bed	β	rad	
Emissivity of heater rod	$\in_{rod}$	(dimensionless)	0.8
Emissivity of gas	$\in_s$	(dimensionless)	0.8
Emissivity of kiln wall	$\in_w$	(dimensionless)	0.8
Emissivity of kiln shell	$\in_{sh}$	(dimensionless)	0.8
Emissivity of air	$\in_a$	(dimensionless)	0.8

vapor phases of moisture and organic contaminants (F_{lw}, F_{l_hc}, F_{v_lw} and F_{v_hc}) using eqs. (6.7)-(6.10).

The flowchart of subroutine for heat balance calculation is shown in Figure 6.7. The calculation starts with an assumed kiln wall temperature T_w to determine the heater rod temperature T_{rod} in eq. (6.17) by iteration. With initial value of soil temperature T_s and gas temperature T_g, eqs. (6.18) and (6.19) are solved using Runge-Kutta method to determine final temperatures of T_s and T_g in each cell of the kiln. Eq. (6.6) which couples eqs. (6.1)-(6.4) then is used to determine the calculated value of T_w. The calculated T_w is compared with the guessed value of T_w. The iteration is continued until the calculated value and guessed value of T_w are sufficiently close (with relative error less than 1 K). Ten to fifteen iterations are generally required for convergence.

The step size (dx) in the numerical procedure needs to be small enough to gain a consistent integrated data result. The computation cell number however has to be as small as possible to save the program calculation time. The calculation was performed using different numbers to search an optimum computation cell number. It was found that a total of 1,520 computation cells are required to reach the convergence of the numerical procedure and consistent heat and mass balance result in all simulation runs can be obtained. It takes approximately three minutes to perform the program calculation to obtain the results of gas and soil temperature profiles as well as mass flux of moisture and organic contaminants of a simulation run using a Pentium II computer.

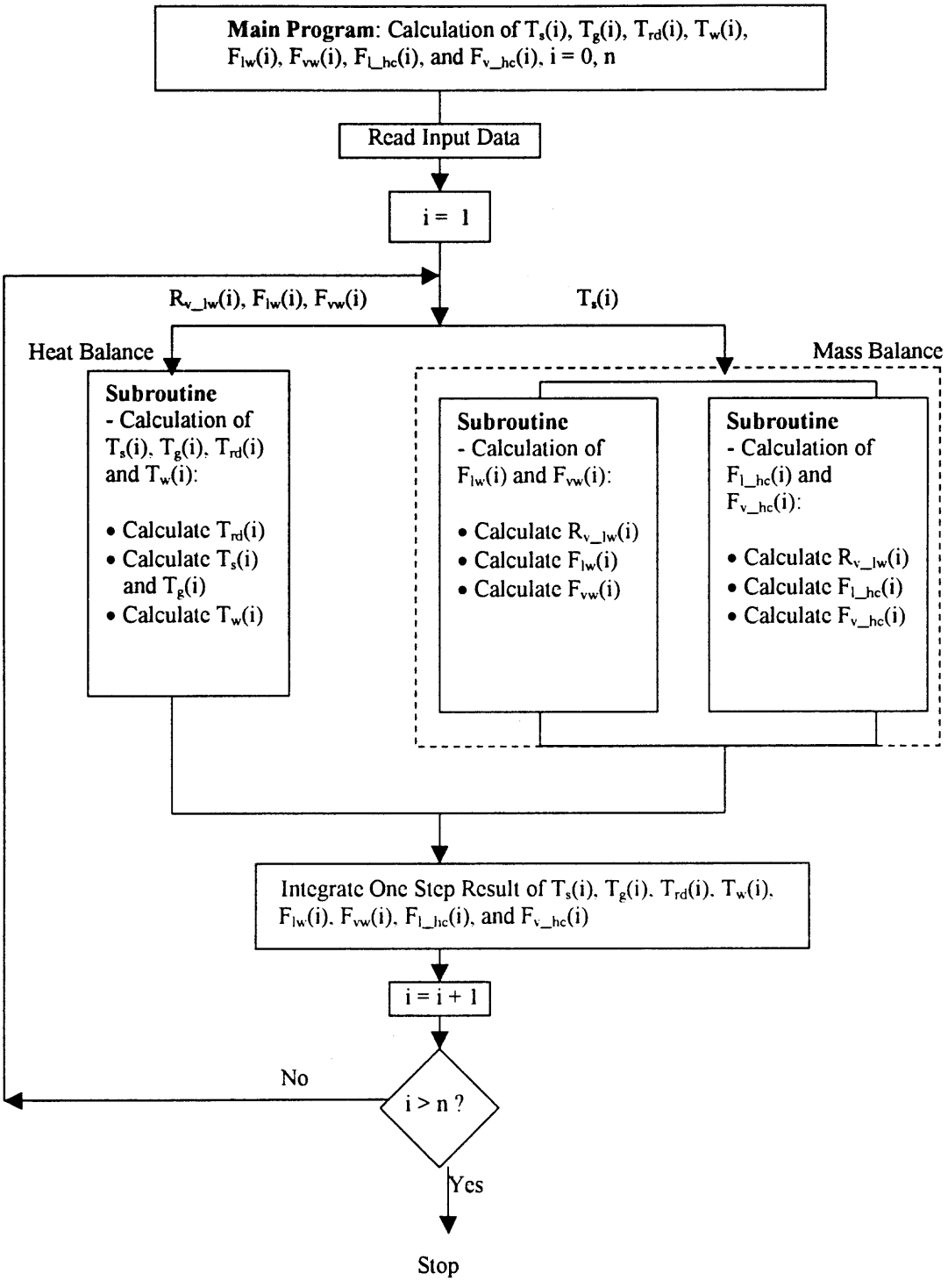

Figure 6.6 The flowchart of main program.

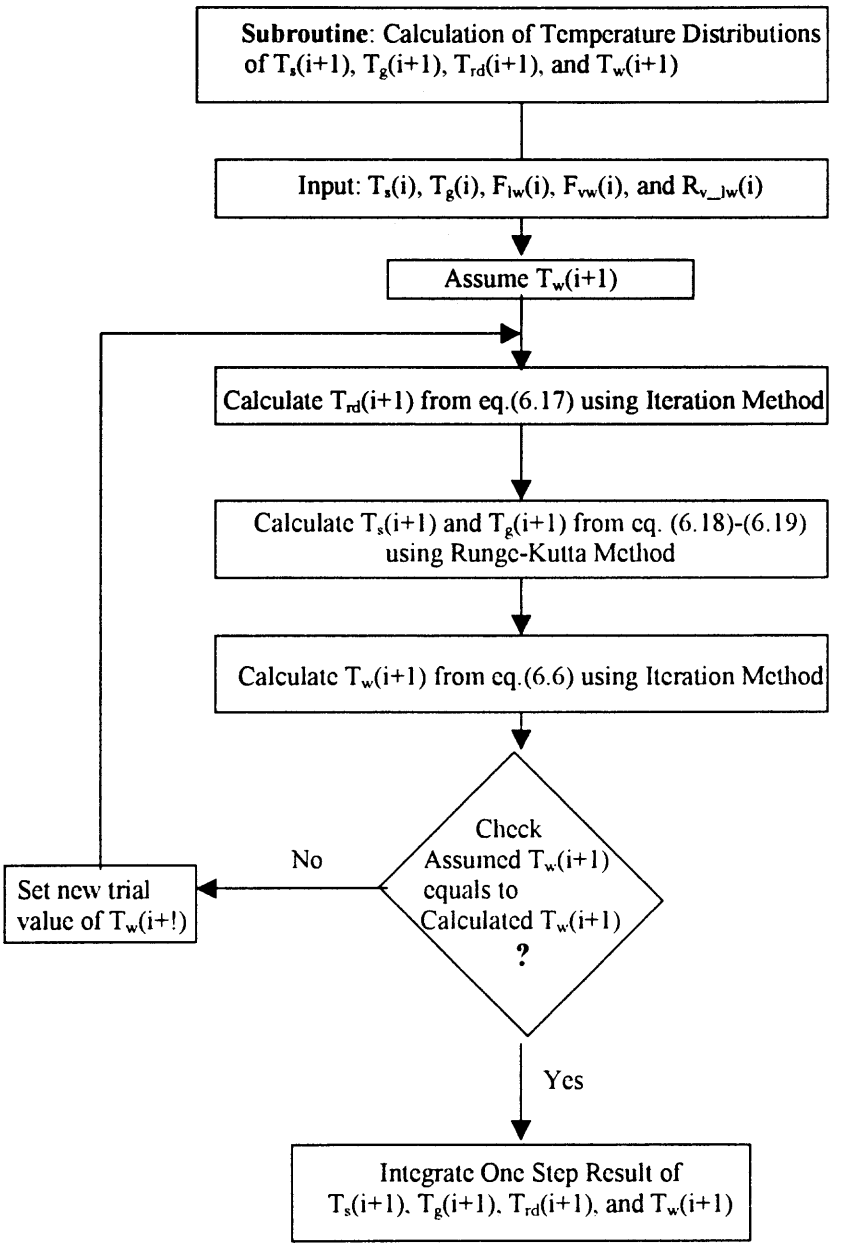

Figure 6.7 The flowchart of subroutine calculating temperature distributions of soil, gas, heater rods and kiln wall in the rotary kiln reactor.

6.4 Results and Discussion

A total of twenty two simulation runs are calculated using the computer program described in the previous section. The operation parameters in each simulation run are listed as data group A, B, and C as shown in Table 6.3. There are eight runs (run 10, 9, 6, 8, 5, 7, 14, 13) in data group A in which 3 percent humidity in purge gas is used, and other eight runs (run 3, 12, 15, 18, 17, 19, 16, 4) in data group B in which 16 percent

Table 6.3 Operation Parameters for Simulation Runs

Data Group	Run	Humidity in Gas Flow (%)	Solid Residence Time (min.)	Kiln Rotary Speed (rpm)	Soil Feed Rate (g/min)	Purge Gas Flow Rate (L/min)	Soil fill fraction in kiln
A	10	3	2.3	4.5	120	5	0.069
	9	3	3.3	4.5	35	20	0.029
	6	3	14.3	0.5	120	20	0.429
	8	3	15	0.5	35	5	0.131
	5	3	17	4.5	120	20	0.51
	7	3	20	4.5	35	5	0.175
	14	3	32	0.5	120	5	0.539
	13	3	36	0.5	35	20	0.315
B	3	16	2.3	4.5	120	20	0.069
	12	16	3.3	4.5	35	5	0.029
	15	16	14.3	0.5	120	5	0.429
	18	16	15	0.5	35	20	0.131
	17	16	17	4.5	120	5	0.51
	19	16	34	4.5	35	20	0.175
	16	16	33	0.5	120	20	0.539
	4	16	36	0.5	35	5	0.315
C	1	10	7.0	2.5	80	10	0.14
	2	10	8.2	2.5	80	10	0.164
	11	10	8.3	2.5	80	10	0.166
	20	10	9.0	2.5	80	10	0.18

- Temperatures for each run: 200°C, 250°C, 300°C.

humidity in purge gas is used. All runs in both group A and B are shown in orders of solid residence time from 2.3 to 36 minutes. Four mid-point runs (run 1, 2, 11 and 20) in group C use center value of each parameter range to check the variability of simulation results. Temperature settings of 473, 523, and 573 are used in all runs of group A, B and C.

Model predicted result includes gas and soil temperature profiles, moisture flux and organic contaminant flux distributions in the soil. Experimental data of exit organic contaminant flux in each run and exit soil temperature in four runs are compared with predicted data for validation of the presented model.

6.4.1 Data Group A - Simulation Runs With 3 Percent Mole Fraction Humidity Purge Gas (Runs 5, 6, 7, 8, 9, 10, 13, 14):

Gas Temperature Profiles. Predicted and measured gas temperature profiles of the test runs with 3 percent mole fraction humidity in purge gas at 473 K, 523 K and 573 K kiln setting temperature are shown in Figures B1.1 through B1.8 at the soil residence time from 2.3 to 36 minutes. The gas temperature profiles show a gradually increasing curve in all runs. This is due to the purge gas flow pushes the higher temperature further to the end of the kiln in co-current runs. The gas temperature at low temperature setting (473 K) increase rather smoothly than higher temperature settings along the kiln. The gas is heated in the kiln from the initial inlet temperature 473 K (preheated) to the range between 475 and 543 K in the runs with solid residence time 2.3 to 20 minutes. The gases in run 14 and 13, which are operated with solid residence time at 32.2 and 36 minutes, however are heated to above 600 K. This is due to longer solid residence time providing further heat to the soil and through heat exchange to the gas. The gas temperature

distributions increase significantly as the kiln settings are raised to 523 K and 573 K. The gas temperature increases up to 250 K at the kiln exit for 523 setting, and increase up to 300 K at the kiln exit for 573 setting compared to the initial temperature 473 K.

Besides kiln setting temperature, gas temperature distributions are also affected by purge gas flowrate. At low purge gas flowrate runs (run 10, 8, 7 and 14) the gas temperature increase after entering the kiln inlet, followed by a constant steady temperature distribution. This constant steady gas temperature portion usually starts at approximately 0.2 to 0.4 fraction of axial distance till the end of the kiln. At high purge gas flowrate runs (run 9, 6, 5 and 13) the gas temperature generally increase along kiln. Only short or even no final constant temperature portion can be found. This can be explained by the higher purge gas flow resulting in the delay of formation of a constant steady temperature distribution near the end of the kiln.

Result of experimentally measured gas temperatures is compared to the predicted temperature distributions. These experimental temperature data were measured from 10 monitoring points which were evenly distributed along the kiln. Agreement between experimental and predicted data is good in runs 10, 9, 6, 8, and 5, which are at the soil residence time from 2.3 to 17 minutes. The difference between exit predicted and experimental gas temperature are within 50 K. There is more discrepancy between predicted and experimental data at runs 7, 14, and 13, which are operated with a soil residence time over 20 minutes. This over estimation of calculated gas temperature at longer residence time runs is possible due to an under estimated heat loss through the kiln wall into the environment. There is longer time for soil to contact with kiln wall at longer soil residence time to result in more heat loss into the kiln wall. This heat loss at soil

temperature results in the decrease of gas temperature through the heat exchange between gas and soil.

The gas temperature distributions show a rather smooth curve as compared to the predicted data in all runs. The reason might be due to no mixing effect is considered in the model. The predicted gas distributions therefore do not show the curves as smooth and uniform as experimental result.

Soil Temperature Profile, and Mass Flowrate Distributions of Moisture and Organic Contaminants. Predicted soil temperature profile, plus mass flowrate distributions of moisture and organic contaminant of the simulation runs with 3 percent mole fraction humidity in purge gas at 473, 523 and 573 K are shown in Figures B2.1 through B2.8 at the soil residence time from 2.3 to 36 minutes.

Predicted soil temperature increase rapidly from 298 K when initially fed into the kiln, followed by a relatively uniform, constant temperature period till end of the kiln. This increasing section of soil temperature is approximately located in 0.1 to 0.4 fraction of the kiln distance. However, it could be the entire kiln length, such as run 6. The time required for soil particles to reach the final steady temperature depends on the center temperature setting, and soil feed rate. The higher temperature setting makes the longer distance required for soil bed in the kiln to reach a higher final temperature than the one with lower temperature setting.

The setting of soil feed rate also results in the delaying of the time required for soil temperature to reach the final steady temperature. This is due to most of water content in the soil is evaporated in the soil temperature increasing section. Only all or most of water content is evaporated and transfered into the gas phase as water vapor, the

soil temperature reaches the final steady temperature. The higher soil feed rate with higher water content in the soil bed therefore results in a delaying of soil temperature to reach the final steady temperature and also a lower final temperature.

6.4.2 Data Group B - Simulation Runs With 16 Percent Mole Fraction Humidity in Purge Gas (Runs 3, 4, 12, 15, 16, 17, 18, 19):

Gas Temperature Profiles. Predicted and measured gas temperature profiles of the simulation runs with 16 percent mole fraction humidity in purge gas at 473 K, 523 K and 573 K setting temperature are shown in Figures B3.1 through B3.8 at the soil residence time from 2.3 to 36 minutes. Overall, these eight simulation runs show a similar trend of gas temperature profiles as result of data group A. The humidity in purge gas does not show a significant effect on the gas temperature profiles.

Agreement between predicted and measure gas temperature data is good at most runs of which with 16 percent mole fraction humidity purge gas. The differences are within 110 K for seven out of eight runs. The exception is run 4 at soil residence time 36 minutes, in which the difference between predicted and measure gas temperature are near 180 K. The reason is possible due to under estimation of heat loss through kiln wall, as the discussion made in previous section.

Soil Temperature Profile, and Mass Flowrate Distributions of Moisture and Organic Contaminants. Predicted soil temperature profile, plus mass flowrate distributions of moisture and organic contaminant of the simulation runs with 16 percent mole fraction humidity in purge gas at 473, 523 and 573 K are shown in Figures B4.1 through B4.8 at the soil residence time from 2.3 to 36 minutes.

6.4.3 Data Group C - Mid-Point Runs (Run 1, 2, 11, 20):

Gas Temperature Profiles. Predicted and measured gas temperature profiles of four mid-point runs are shown in Figure B5.1 through B5.4. The mid-point runs which perform the calculation using the center value of each operation parameters, are used to check the variability of data result. A range of discrepancy exiting in these four runs is possible, due to empirical solid residence time data (7 to 9 minutes) are used in the calculation. A reasonable variability of predicted gas temperature approximately within 30 K for most runs is obtained. The discrepancy between experimental and predicted gas temperature is within 60 K for most runs.

Soil Temperature Profile, and Mass Flowrate Distributions of Moisture and Organic Contaminants. Predicted and measured soil temperature profile, plus mass flowrate distributions of moisture and organic contaminants of four mid-point simulation runs at 473, 523 and 573 K are shown in Figures B6.1 through B6.4.

6.5 Regression Analysis of Predicted Result

The predicted result of organic contaminants remaining in the soil due to different ranges of operation variables is analyzed by regression analysis, in which the positive or negative effect of operation variables as well as the relation between each operation variables can be determined. A total of six operation variables including kiln setting temperature, solid residence time, soil feed rate, purge gas flowrate, humidity in the purge gas, and soil fill fraction are investigated in the 48 runs. The regression equation based on the result of 48 runs for the effect of these six operation variables on the percent remaining of organic contaminants in the soil is:

$$Y = -0.35A - 1.3B + 0.08C - 1.06D + 17.8E + 10.9F + 138.85 \quad (6.35)$$

where Y = percent remaining of organic contaminant in the soil,

A = kiln setting temperature, °C

B = solid residence time, min.

C = soil feed rate, g/min.

D = purge gas flowrate, L/min.

E = humidity in the purge gas, mole fraction

F = soil fill fraction.

As the regression equation is developed, the value of dependent variable can be predicted with input of each operation variables. Table 6.4 shows the predicted percent remaining organic contaminants at low and high setting in the range of each operation variables using regression equation. The average values in the range of other five operation variables are used in the regression equation while one operation variable is calculated using its low and high setting value. The result shows that the positive effect of operation variable to remove the organic contaminants is: solid residence time > kiln setting temperature > purge gas flowrate; the negative effect of operation variable to remove the organic contaminants is: soil feed rate > humidity in the purge gas > soil fill fraction. The effect of operation variables on the dependent variable based on the simulation result data thus can be determined using this fast empirical method.

The effect of selected operation variables on specific runs also can be determined using regression analysis of predicted result. Table 6.5 lists the result of six runs (runs 6, 8, 5, 15, 18, and 17) in which the solid residence time falls between 14.3 to 17 minutes.

Table 6.4 Predicted Percent Remaining of Organic Contaminants in The Soil at Low and High Setting of Each Operation Variables Using Regression Analysis Result

Operation Variable	Range of setting*	Average range of setting	Percent remaining of organic contaminants	Comparison of Percent remaining of organic contaminants at low and high setting
A: kiln setting temperature, °C	200 (L) 300 (H)	250	41.6 6.6	- 35
B: soil residence time, min.	2.3 (L) 36 (H)	19.2	46.1 2.3	- 43.8
C: soil feed rate, g/min.	35 (L) 120 (H)	77.5	20.7 27.5	+ 6.8
D: purge gas flowrate, L/min.	5 (L) 20 (H)	12.5	32.1 16.2	- 15.9
E: humidity in the purge gas (mole fraction)	0.03 (L) 0.16 (H)	0.095	23.0 25.3	+ 2.3
F: soil fill fraction	0.029 (L) 0.539 (H)	0.284	21.3 26.9	+ 5.6

* Values of range in each operation variables are shown as low setting (L) and high setting (H).

The regression equation based on the result of these six runs for the effect of six operation variables on the percent remaining of organic contaminants in the soil is:

$$Y = -0.0049A + 0.00008B - 0.0007C - 0.011D + 0.218E + 0.285F + 1.62 \quad (6.36)$$

where A, B, C, D, E, and F refer to the operation variables are the same as which shown in equation 6.35. The result shows that the positive effect of operation variable to remove the organic contaminants is: kiln setting temperature > purge gas flowrate > solid feed rate; the negative effect of operation variable to remove the organic contaminants is: soil fill fraction > humidity in the purge gas. The residence time does not show a significant effect in comparison with other variables. The soil fill fraction shows as major negative effect on removal of organics from soils, when the residence times of simulation runs are close such as these six specific runs.

Table 6.5 Operation Variables and Dependent Variable of Runs 6, 8, 5, 15, 18, and 17

Run	A	B	C	D	E	F	
	kiln setting tempe -rature (°C)	solid residenc e time (min.)	soil feed rate (g/min.)	purge gas flowrate (L/min.)	humidity in purge gas (mole fraction)	soil fill fraction	percent organics remaining in soil
6	200	14.3	120	20	0.03	0.429	0.42
	250	14.3	120	20	0.03	0.429	0.19
	300	14.3	120	20	0.03	0.429	0.07
8	200	15	35	5	0.03	0.131	0.78
	250	15	35	5	0.03	0.131	0.26
	300	15	35	5	0.03	0.131	0.07
5	200	17	120	20	0.03	0.51	0.5
	250	17	120	20	0.03	0.51	0.21
	300	17	120	20	0.03	0.51	0.04
15	200	14.3	120	5	0.16	0.429	0.69
	250	14.3	120	5	0.16	0.429	0.37
	300	14.3	120	5	0.16	0.429	0.21
18	200	15	120	20	0.16	0.131	0.4
	250	15	120	20	0.16	0.131	0.09
	300	15	120	20	0.16	0.131	0.02
17	200	17	35	5	0.16	0.51	0.8
	250	17	35	5	0.16	0.51	0.46
	300	17	35	5	0.16	0.51	0.26

6.5 Summary

Heat and mass transfer modeling of thermal desorption in a rotary kiln has been developed for a rotary kiln thermal desorber. The oparation variables include temperature, purge gas flowrate, soil feed rate, kiln rotation speed and solid residence time. The heat balance and the heat flow between soil, gas and kiln wall are incorporated. Temperature profiles of gas and soil are calculated using the fourth order Runge-Kutta method. Evaporation rates of moisture and organic contaminants derived by Wendt et al. is applied for the mass balance calculation. A comparison of modeling result with experimental data for gas and soil temperature profiles as well as the mass flow rates of moisture and organic contaminants with experimental data is in reasonable agreement. Improvement in the model development is still recommended.

CHAPTER 7

CONCLUSIONS

Available thermal technologies for remediation of contaminated soils are summarized. Each treatment processes, as well as the associated treatment system components, are identified and described. Waste applicability is also included for each treatment technology. A detail list of feasible treatment processes is addressed with descriptions of site demonstration results to aid in evaluation of a selected process. Technology status is summarized to provide the current information on the technologies.

Energy components are discussed for energy cost requirement and safety considerations on thermal treatment applications. The heat loss from kiln shell to environment demands major fraction of energy requirement in bench scale thermal desorber. Only 6 percent of total energy requirement is due to heat loss to environment in full scale desorber. The major heat required in full scale desorber is used for treatment of water which consumes approximately 48 percent fraction of all energy requirement.

Results of experimental study for thermal desorption of organic contaminants from soils show that the thermal desorber system is highly effective in removing semivolatile organics from field contaminated soils. Temperature and solid residence time are two primary parameters affecting the desorption results. Higher temperatures and longer residence times result in higher removal efficiency. Purge gas velocity is also found to be an important parameter in the desorption process. The result of mass balances for carbon illustrated that most of carbon recovery ranged from 45 to 115 percent in 20 experimental runs.

Heat and mass transfer modeling of thermal desorption in a rotary kiln has been developed for a rotary kiln thermal desorber. The heat balance and the heat flow between soil, gas and kiln wall are incorporated. Temperature profiles of gas and soil are calculated using the fourth order Runge-Kutta method. Evaporation rates of moisture and organic contaminants derived by Wendt et al. is applied for the mass balance calculation. A comparison of modeling result with experimental data for gas and soil temperature profiles as well as the mass flow rates of moisture and organic contaminants with experimental data is in reasonable agreement. Improvement in the model development is still recommended.

Results from mass balance analysis on PCDD/F in municipal waste for incineration show that a range of 0.8 to 87 pg(I-TE)/g or 0.16 – 17.4 grams(I-TE) PCDD/F in 2×10^8 kg waste is present in the feed to a MSW incinerator. For 7.2 g(I-TE) PCDD/F in the feed to a MSW incinerator per year; the output in the combined gas and solid streams ranges from 0.11 to 12 g(I-TE) per year. This data indicates that input and output levels of PCDD/F in modern, efficient Municipal Solid Waste Incineration are in similar magnitude. A higher ratio of input versus output PCDD/F for MSWIs however is obtained at the evaluation based on the input fractions representative of waste in the US.

APPENDIX A

CALCULATION OF WEIGHT PERCENT OF FINE DEBRIS ATTACHED TO METAL AND GLASS IN THE MSW

The calculation of weight percent of fine debris attached to metal and lass in the MSW is shown below:

A = area

Radius of a metal bottle = R_{metal}, m

Length of a metal bottle = L_{metal}, m

Radius of a glass bottle = R_{glass}, m

Length of a glass bottle = L_{glass}, m

Assume thickness of a metal/glass bottle = 1.5 mm = 1.5E-3 m

Assume thickness of fine debris attached to a metal/glass bottle = 100 μm = 1.0E-7 m

Typical dust density = 1,800 kg/m^3[40]

Typical metal density = 8,000 kg/m^3[40]

Typical glass density = 2,600 kg/m^3[40]

Weight fraction of dust attached to the surface (bottom + two sides) of a metal bottle

$$= \frac{\text{dust weight}}{\text{metal weight}}$$

$$= \frac{(A_{\text{bottom}} + A_{\text{surface}}) \times 2_{\text{(inside \& outside)}} \times (\text{dust thickness on surface}) \times \text{dust density}}{(A_{\text{bottom}} + A_{\text{surface}}) \times (\text{metal thickness}) \times \text{metal density}}$$

$$= \frac{(\pi (R_{metal})^2 + 2\pi R_{metal} L_{metal}) \times 2 \times 1.0\text{E-}7 \text{ m} \times 1{,}800 \text{ kg/m}^3}{(\pi (R_{metal})^2 + 2\pi R_{metal} L_{metal}) \times 1.5\text{E-}3 \text{ m} \times 8{,}000 \text{ kg/m}^3} = 0.00003$$

Weight fraction of dust attached to the surface (two sides) of a glass bottle is calculated as the similar procedure:

Weight fraction of dust attached to the surface (two sides) of a glass bottle

$$= \frac{(\pi (R_{glass})^2 + 2\pi R_{glass} L_{glass}) \times 2 \times 1.0E\text{-}7 \text{ m} \times 1{,}800 \text{ kg/m}^3}{(\pi (R_{glass})^2 + 2\pi R_{glass} L_{glass}) \times 1.5E\text{-}3 \text{ m} \times 2{,}600 \text{ kg/m}^3} = 0.000092$$

Metal in MSW = 7.7 % (by weight), Glass in MSW = 5.5 % (by weight) [39]

Weight percent of fine debris attached to metal and glass

$= (0.00003 \times 7.7\ \%) + (0.000092 \times 5.5\ \%)$

$= 0.00074\ \%$

$\approx 0.001\ \%$

APPENDIX B

RESULTS OF MODEL STUDY IN CHAPTER 6

This Appendix summarizes results of model study which includes gas and soil temperature profiles as well as mass flow rates of moisture and organic contaminants in Chapter 6.

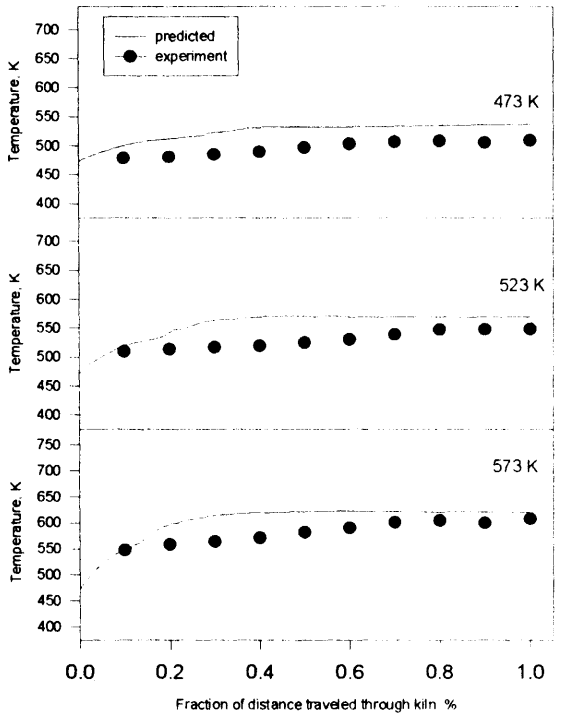

Figure B1.1 Gas temperature profiles of run 10: solid residence time = 2.3 min., purge gas flow = 5 L/min., soil feed rate = 120 g/min..

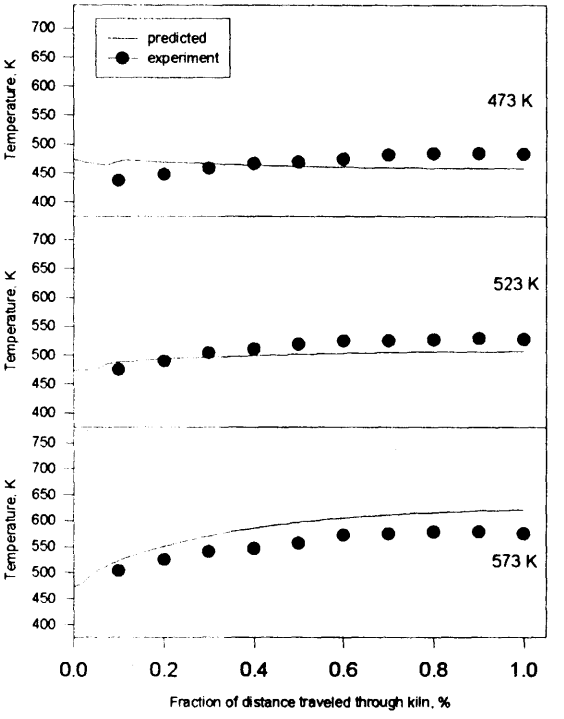

Figure B1.2 Gas temperature profiles of run 9: solid residence time = 2.3 min., purge gas flow = 20 L/min., soil feed rate = 35 g/min..

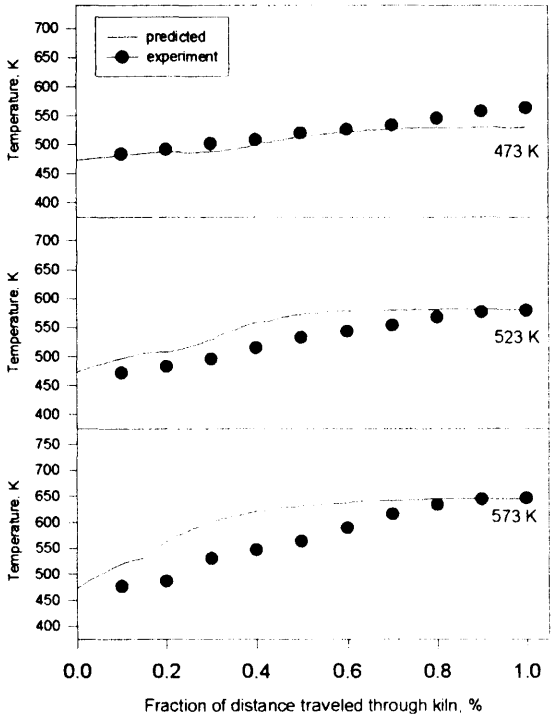

Figure B1.3 Gas temperature profiles of run 6: solid residence time = 14.3 min., purge gas flow = 20 L/min., soil feed rate = 120 g/min..

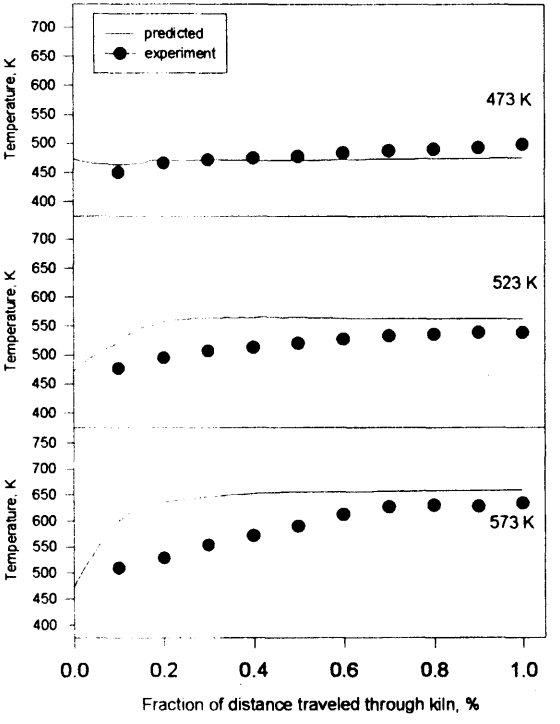

Figure B1.4 Gas temperature profiles of run 8: solid residence time = 15 min., purge gas flow = 5 L/min., soil feed rate = 35 g/min..

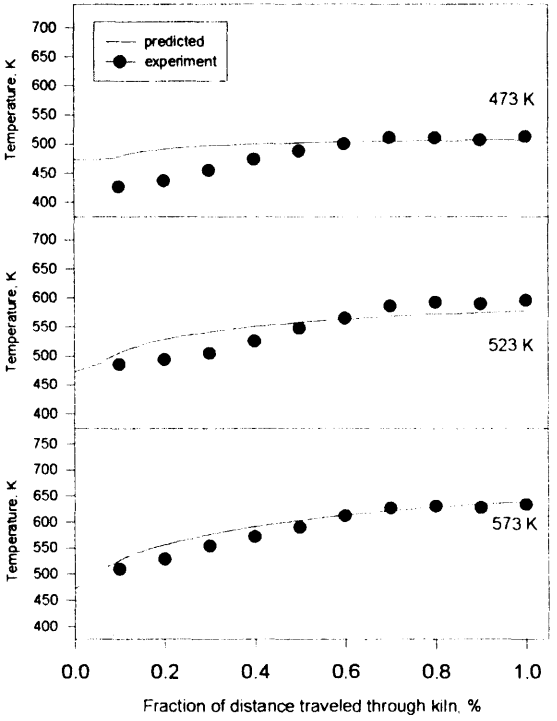

Figure B1.5 Gas temperature profiles of run 5: solid residence time = 17 min., purge gas flow = 20 L/min., soil feed rate = 120 g/min..

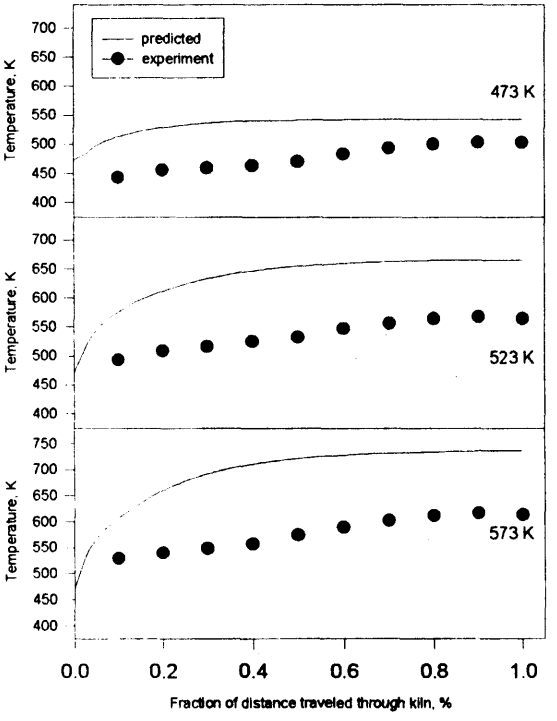

Figure B1.6 Gas temperature profiles of run 7: solid residence time = 20 min., purge gas flow = 5 L/min., soil feed rate = 35 g/min..

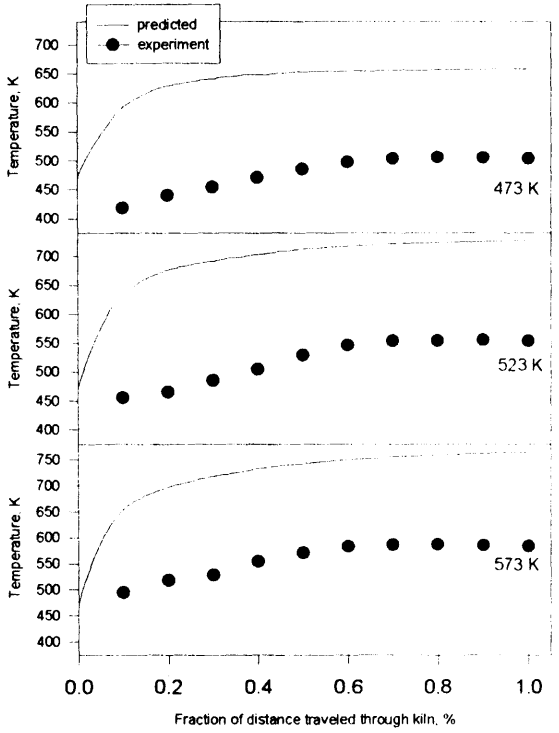

Figure B1.7 Gas temperature profiles of run 14: solid residence time = 32 min., purge gas flow = 5 L/min., soil feed rate = 67 g/min..

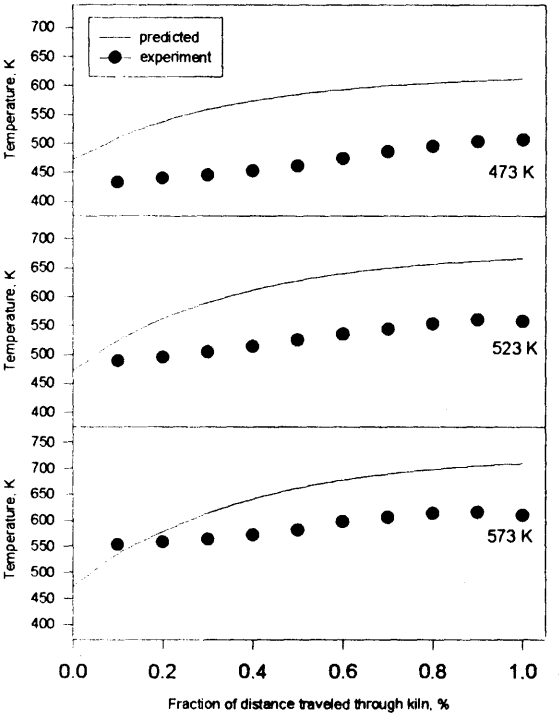

Figure B1.8 Gas temperature profiles of run 13: solid residence time = 36 min., purge gas flow = 20 L/min., soil feed rate = 35 g/min..

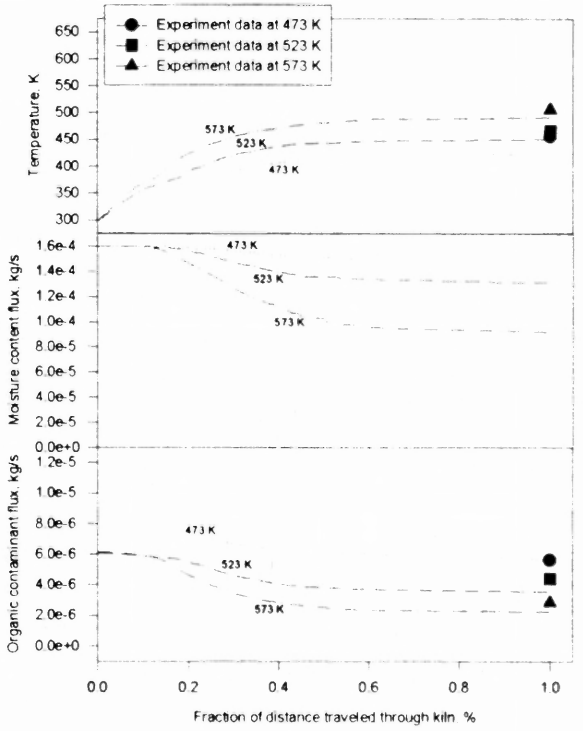

Figure B2.1 Soil temperature profiles, and mass flux distributions of moisture and organic contaminants of run 10: solid residence time = 2.3 min., purge gas flow = 5 L/min., soil feed rate = 120 g/min.

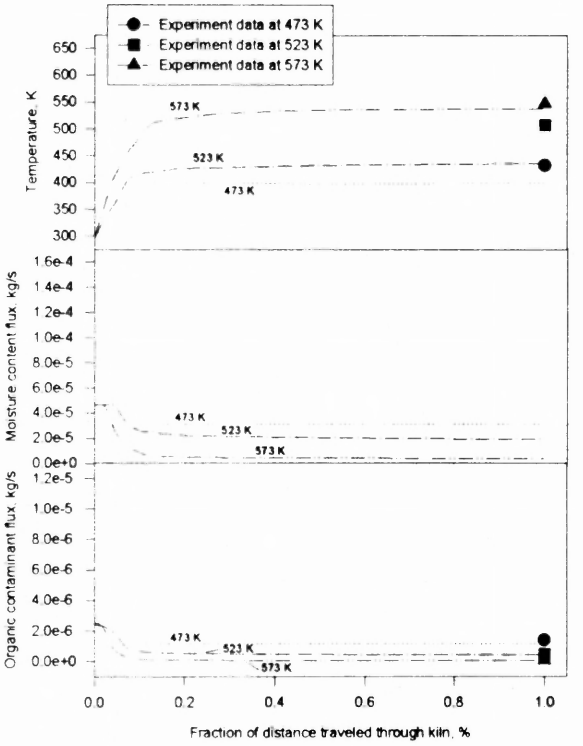

Figure B2.2 Soil temperature profiles, and mass flux distributions of moisture and organic contaminants of run 9: solid residence time = 3.3 min., purge gas flow = 20 L/min., soil feed rate = 35 g/min.

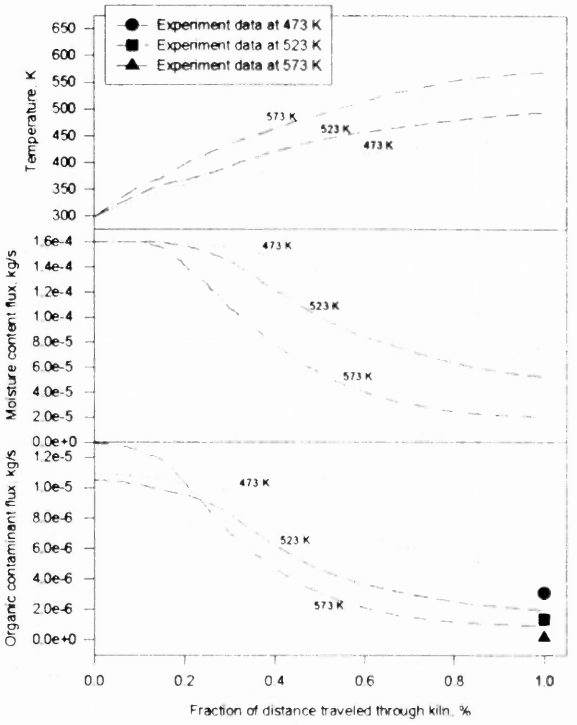

Figure B2.3 Soil temperature profiles, and mass flux distributions of moisture and organic contaminants of run 6: solid residence time = 14.3 min., purge gas flow = 20 L/min., soil feed rate = 120 g/min..

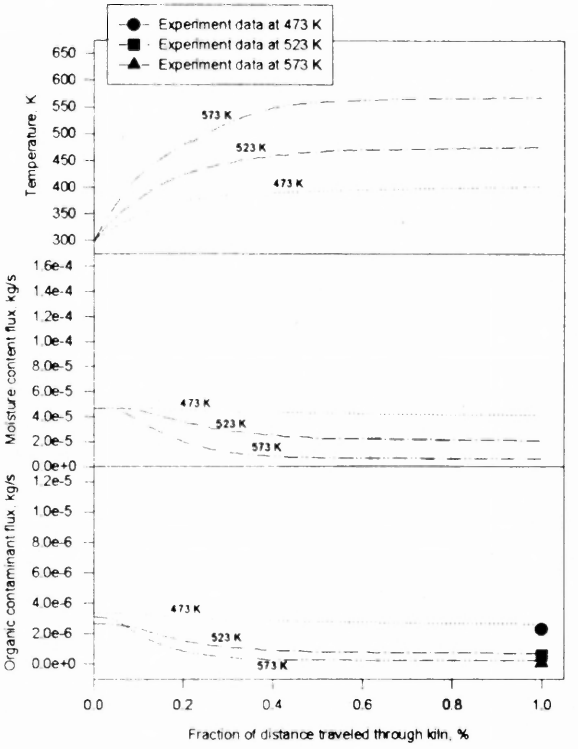

Figure B2.4 Soil temperature profiles, and mass flux distributions of moisture and organic contaminants of run 8: solid residence time = 15 min., purge gas flow = 5 L/min., soil feed rate = 35 g/min..

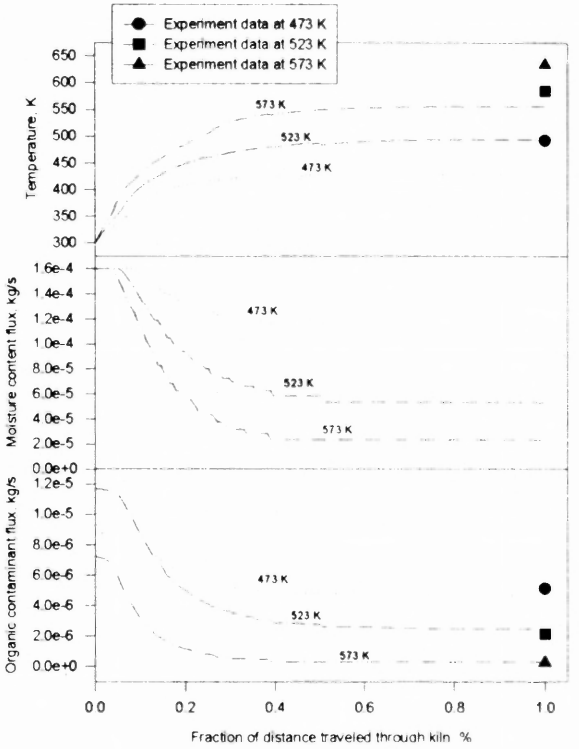

Figure B2.5 Soil temperature profiles, and mass flux distributions of moisture and organic contaminants of run 5: solid residence time = 17 min., purge gas flow = 20 L/min., soil feed rate = 120 g/min.

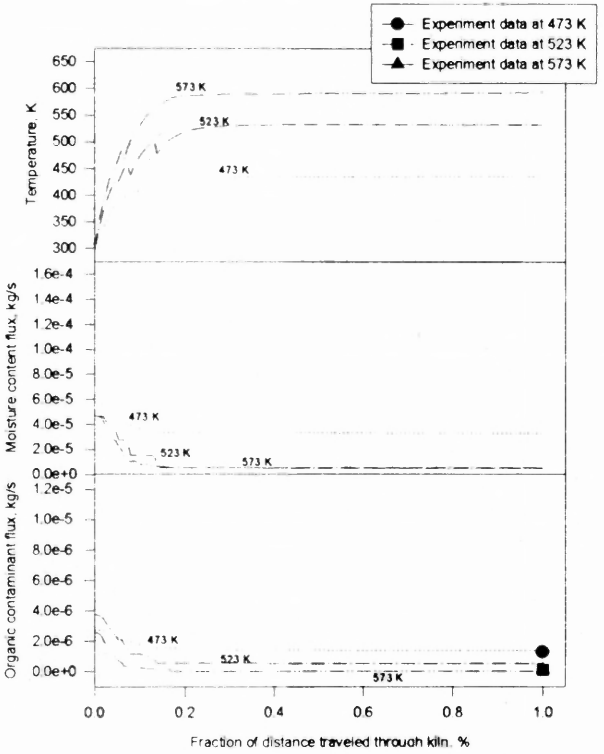

Figure B2.6 Soil temperature profiles, and mass flux distributions of moisture and organic contaminants of run 7: solid residence time = 20 min., purge gas flow = 20 L/min., soil feed rate = 35 g/min.

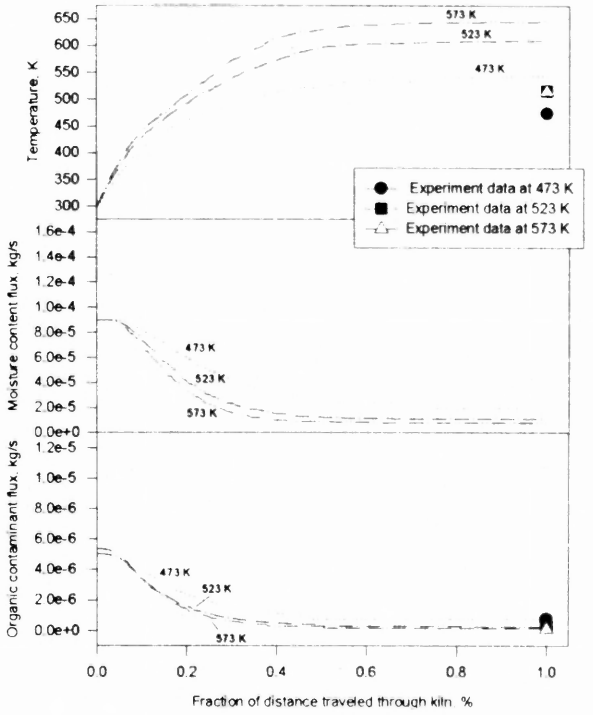

Figure B2.7 Soil temperature profiles, and mass flux distributions of moisture and organic contaminants of run 14: solid residence time = 32 min., purge gas flow = 5 L/min., soil feed rate = 67 g/min..

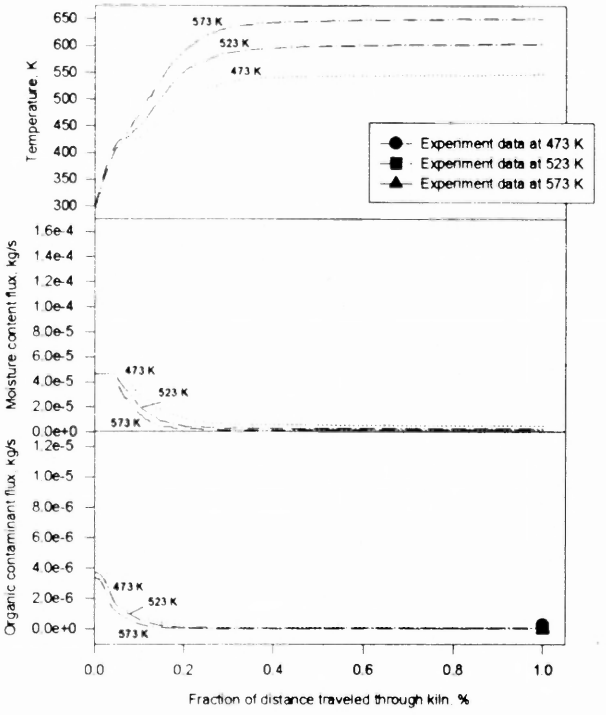

Figure B2.8 Soil temperature profiles, and mass flux distributions of moisture and organic contaminants of run 13: solid residence time = 36 min., purge gas flow = 20 L/min., soil feed rate = 35 g/min..

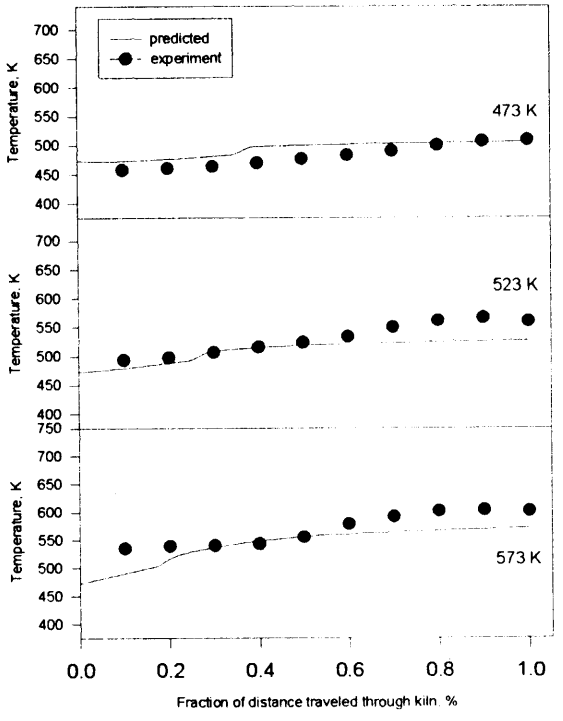

Figure B3.1 Gas temperature profiles of run 3:
solid residence time = 2.3 min.,
purge gas flow = 20 L/min.,
soil feed rate = 120 g/min..

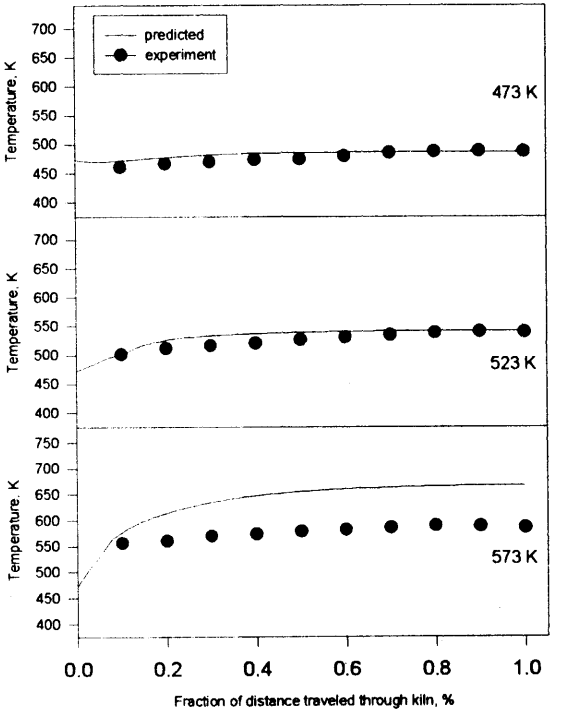

Figure B3.2 Gas temperature profiles of run 12:
solid residence time = 3.3 min.,
purge gas flow = 5 L/min.,
soil feed rate = 35 g/min..

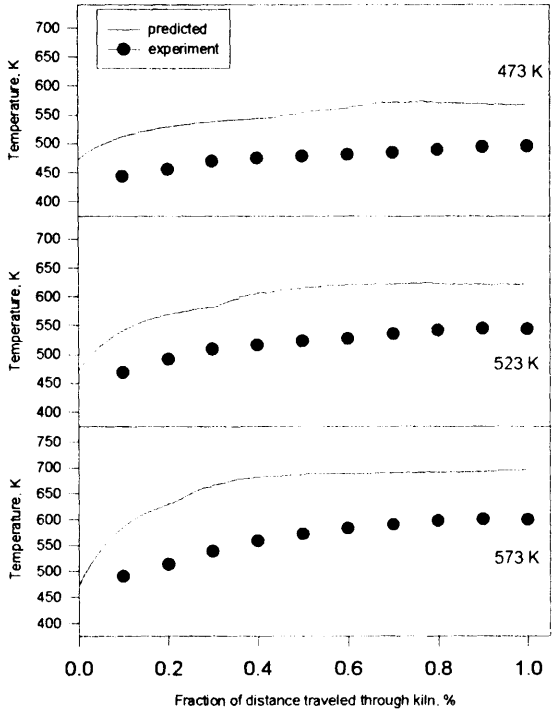

Figure B3.3 Gas temperature profiles of run 15:
solid residence time = 14.3 min.,
purge gas flow = 5 L/min.,
soil feed rate = 120 g/min..

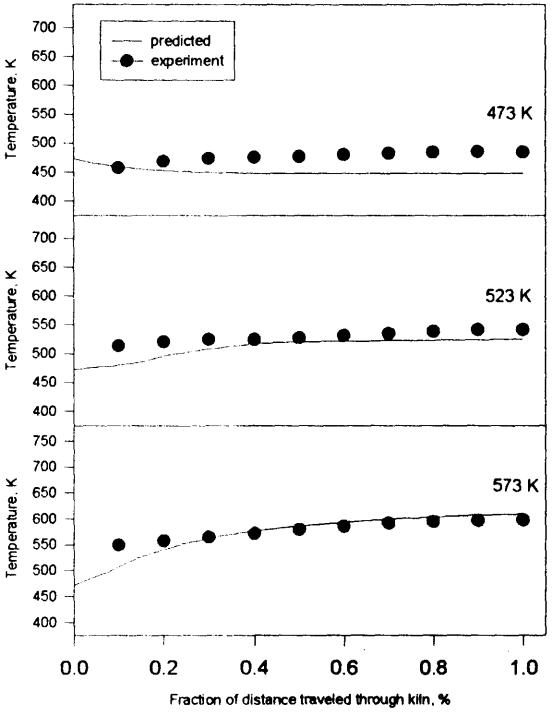

Figure B3.4 Gas temperature profiles of run 18:
solid residence time = 15 min.,
purge gas flow = 20 L/min.,
soil feed rate = 35 g/min..

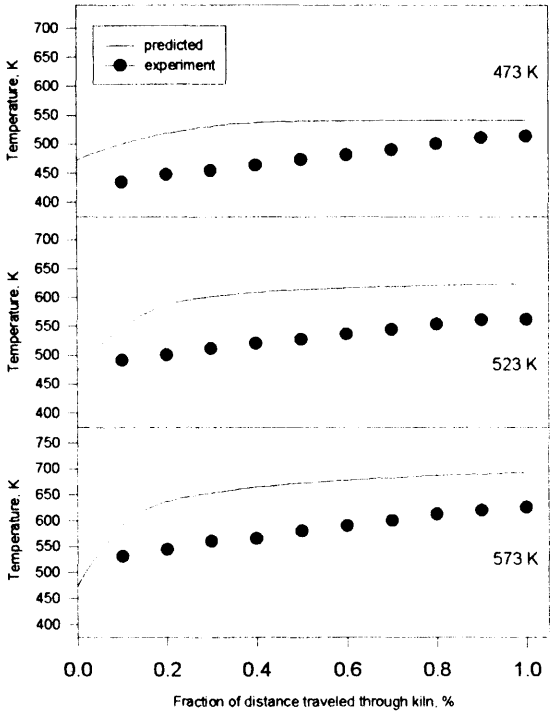

Figure B3.5 Gas temperature profiles of run 17:
solid residence time = 17 min.,
purge gas flow = 5 L/min.,
soil feed rate = 100 g/min..

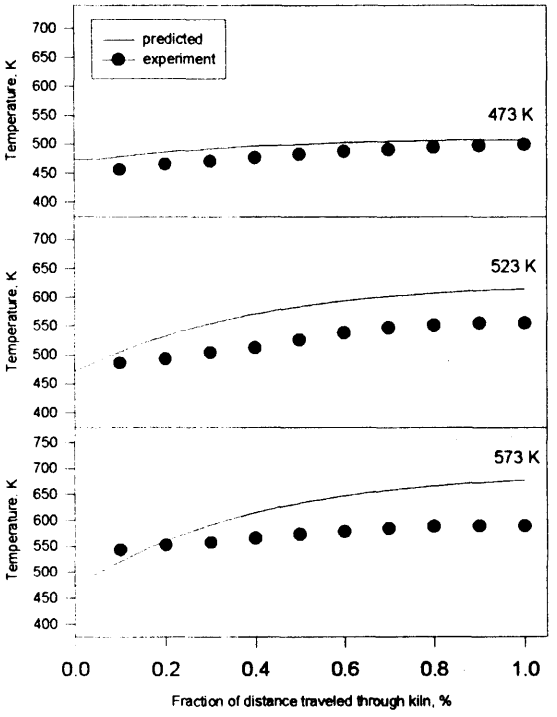

Figure B3.6 Gas temperature profiles of run 19:
solid residence time = 34 min.,
purge gas flow = 20 L/min.,
soil feed rate = 35 g/min..

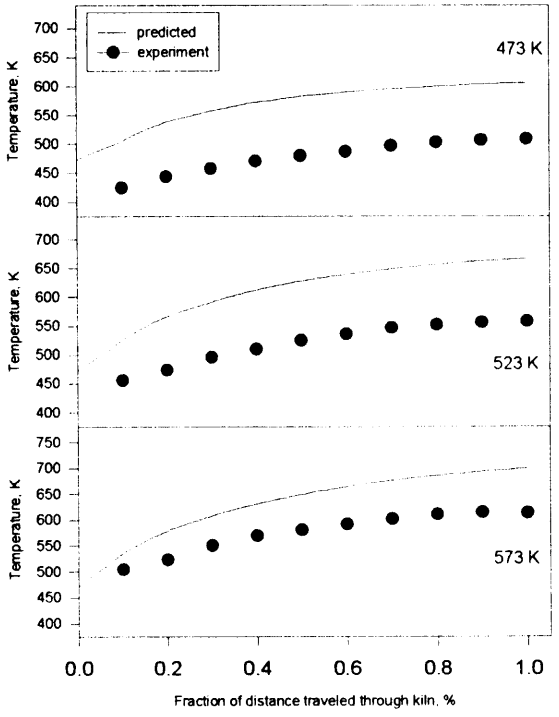

Figure B3.7 Gas temperature profiles of run 16:
solid residence time = 33 min.,
purge gas flow = 20 L/min.,
soil feed rate = 100 g/min..

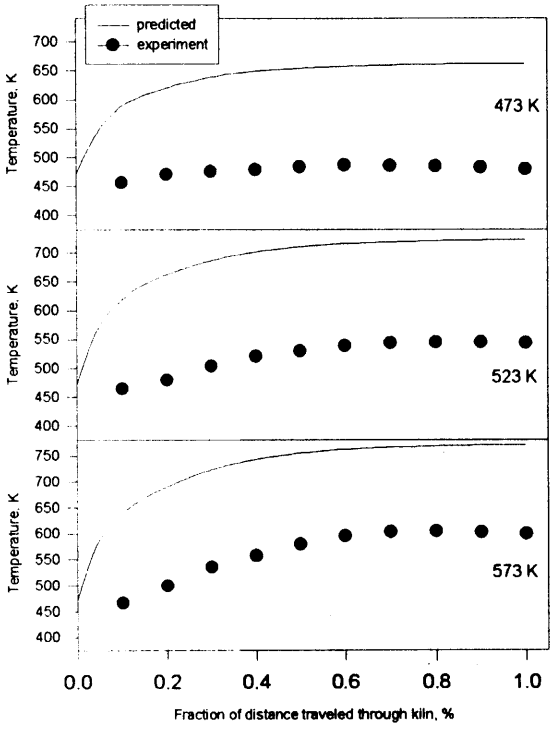

Figure B3.8 Gas temperature profiles of run 4:
solid residence time = 36 min.,
purge gas flow = 5 L/min.,
soil feed rate = 35 g/min..

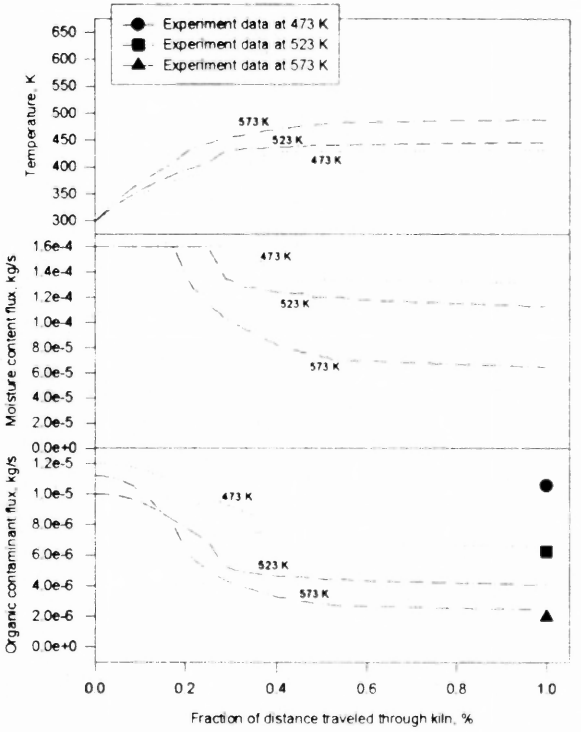

Figure B4.1 Soil temperature profiles, and mass flux distributions of moisture and organic contaminants of run 3:
solid residence time = 2.3 min.,
purge gas flow = 20 L/min.,
soil feed rate = 120 g/min..

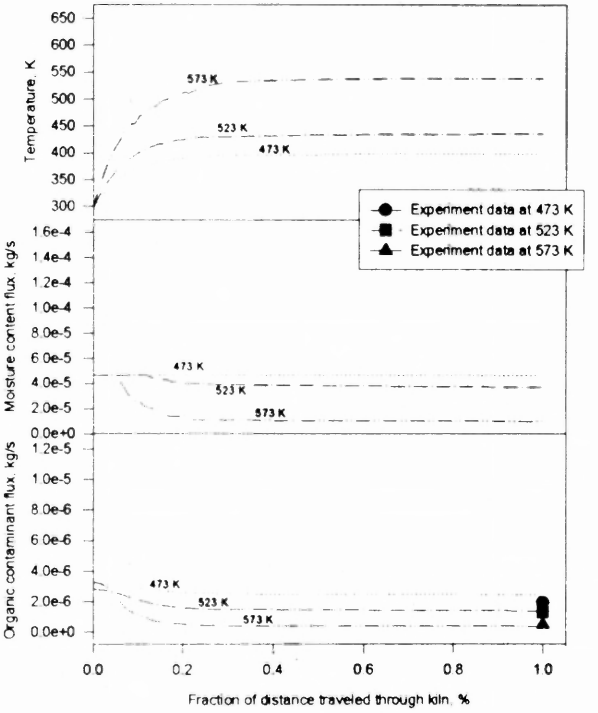

Figure B4.2 Soil temperature profiles, and mass flux distributions of moisture and organic contaminants of run 12:
solid residence time = 3.3 min.,
purge gas flow = 5 L/min.,
soil feed rate = 35 g/min.

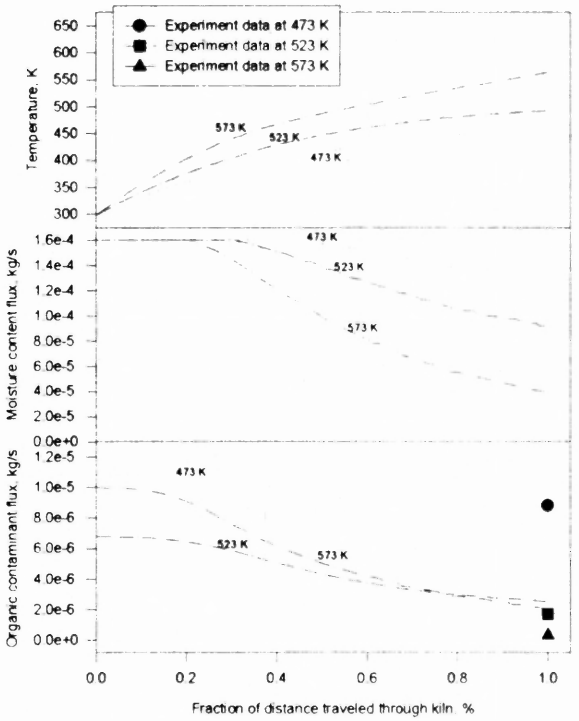

Figure B4.3 Soil temperature profiles, and mass flux distributions of moisture and organic contaminants of run 15: solid residence time = 14.3 min., purge gas flow = 5 L/min., soil feed rate = 120 g/min.

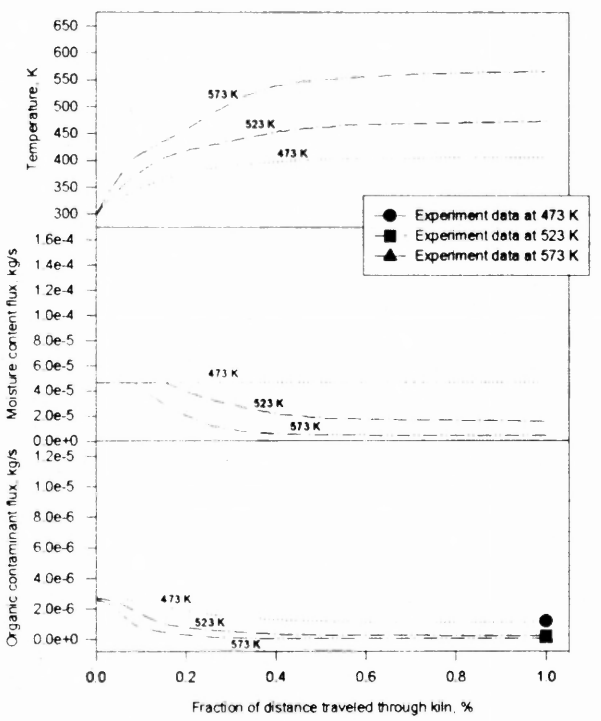

Figure B4.4 Soil temperature profiles, and mass flux distributions of moisture and organic contaminants of run 18: solid residence time = 15 min., purge gas flow = 20 L/min., soil feed rate = 35 g/min.

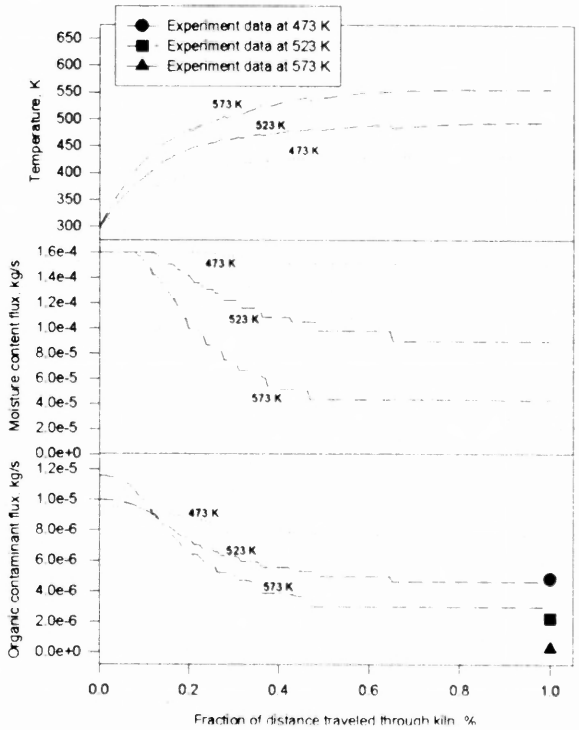

Figure B4.5 Soil temperature profiles, and mass flux distributions of moisture and organic contaminants of run 17: solid residence time = 17.7 min., purge gas flow = 5 L/min., soil feed rate = 100 g/min.

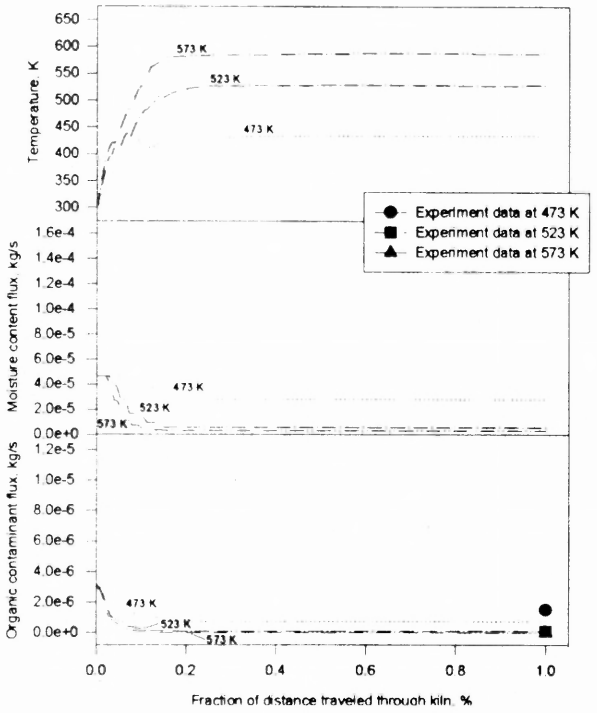

Figure B4.6 Soil temperature profiles, and mass flux distributions of moisture and organic contaminants of run 19: solid residence time = 34 min., purge gas flow = 20 L/min., soil feed rate = 35 g/min.

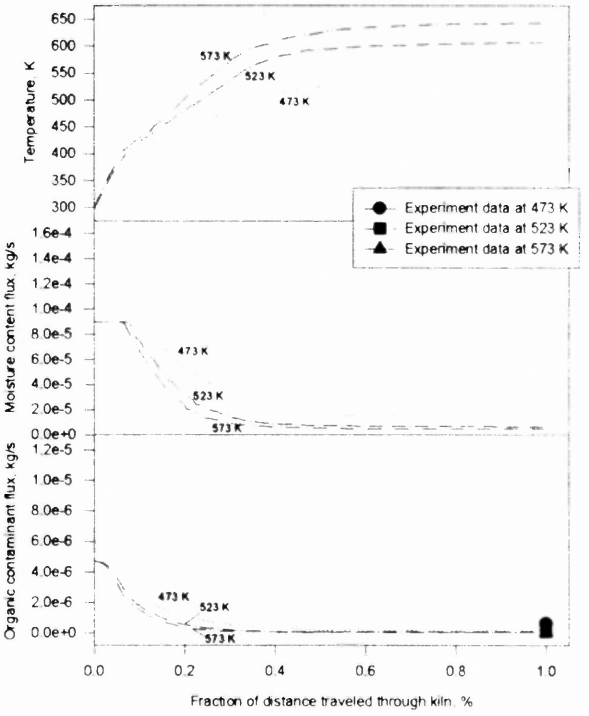

Figure B4.7 Soil temperature profiles, and mass flux distributions of moisture and organic contaminants of run 16: solid residence time = 33 min., purge gas flow = 20 L/min., soil feed rate = 100 g/min.

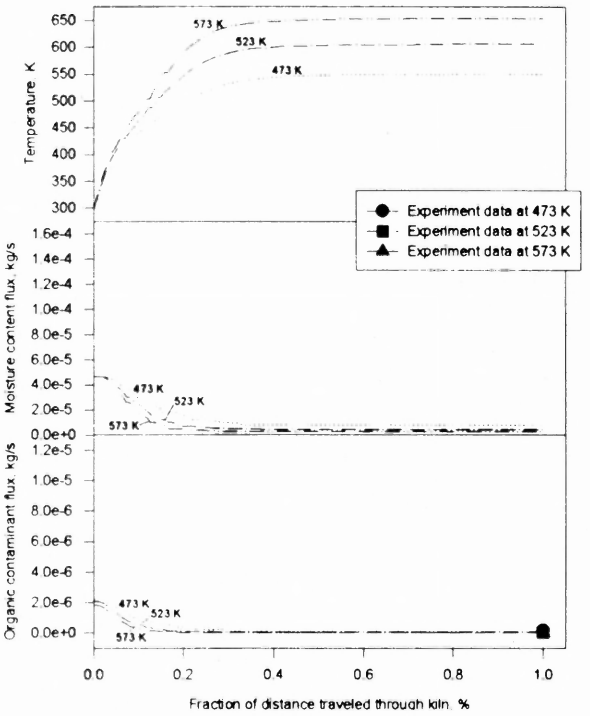

Figure B4.8 Soil temperature profiles, and mass flux distributions of moisture and organic contaminants of run 4: solid residence time = 36 min., purge gas flow = 5 L/min., soil feed rate = 35 g/min.

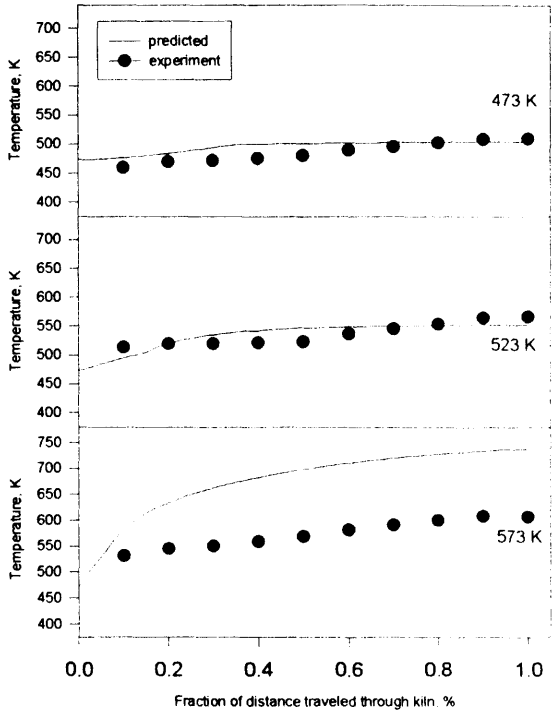

Figure B5.1 Gas temperature profiles of run 1: solid residence time = 7 min., purge gas flow = 10 L/min., soil feed rate = 80 g/min..

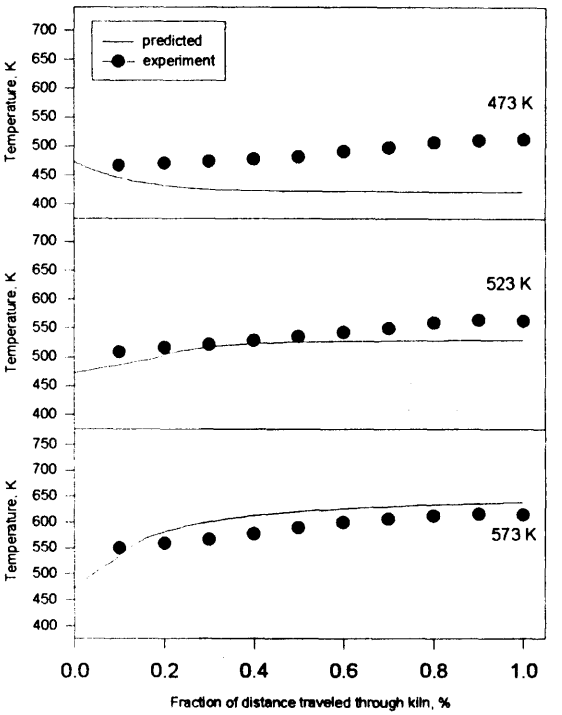

Figure B5.2 Gas temperature profiles of run 2: solid residence time = 8.2 min., purge gas flow = 10 L/min., soil feed rate = 80 g/min..

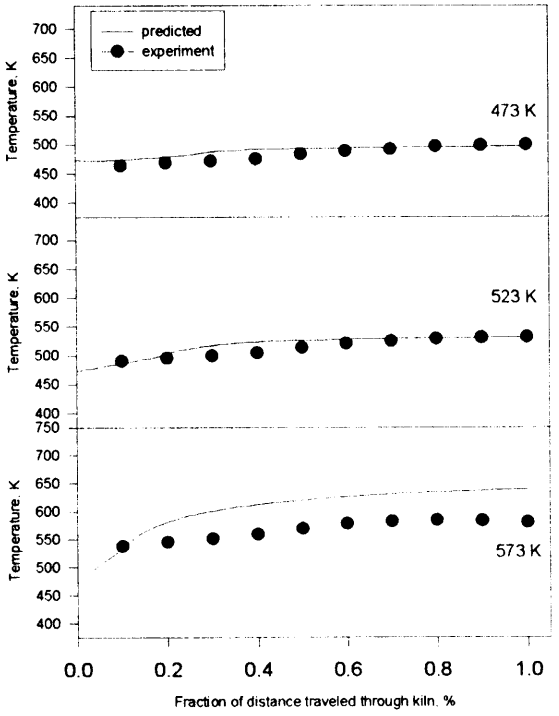

Figure B5.3 Gas temperature profiles of run 11: solid residence time = 8.3 min., purge gas flow = 10 L/min., soil feed rate = 80 g/min..

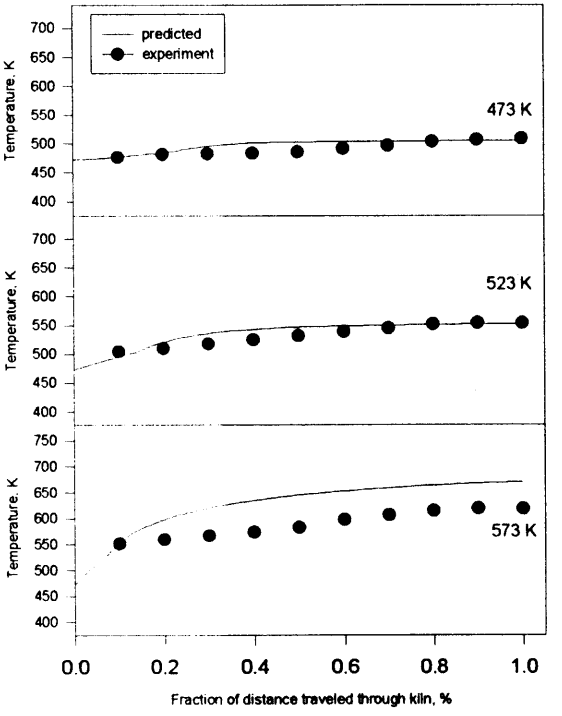

Figure B5.4 Gas temperature profiles of run 20: solid residence time = 9 min., purge gas flow = 10 L/min., soil feed rate = 80 g/min..

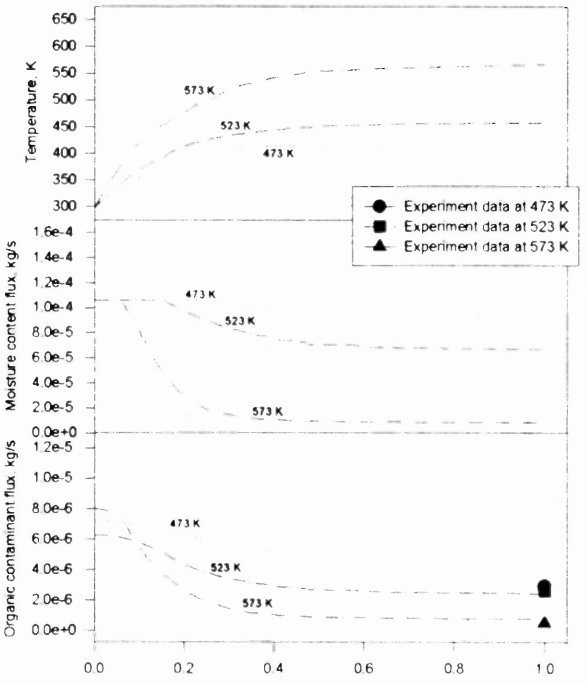

Figure B6.1 Soil temperature profiles, and mass flux distributions of moisture and organic contaminants of run 1: solid residence time = 7 min., purge gas flow = 10 L/min., soil feed rate = 80 g/min.

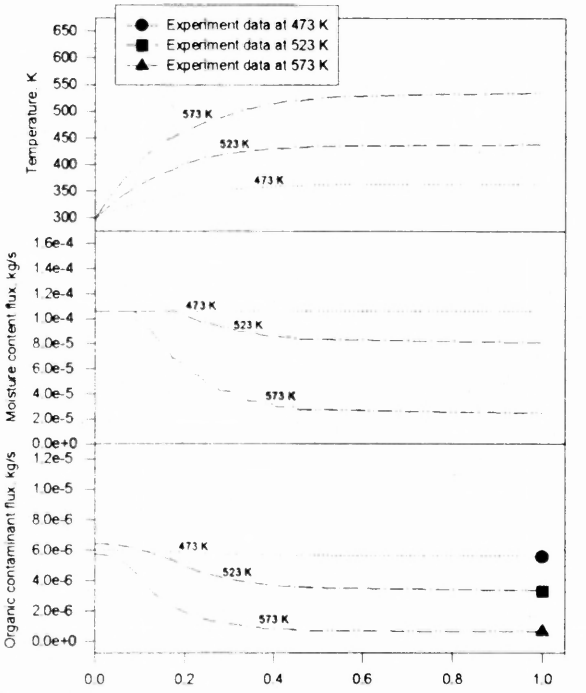

Figure B6.2 Soil temperature profiles, and mass flux distributions of moisture and organic contaminants of run 2: solid residence time = 8.2 min., purge gas flow = 10 L/min., soil feed rate = 80 g/min.

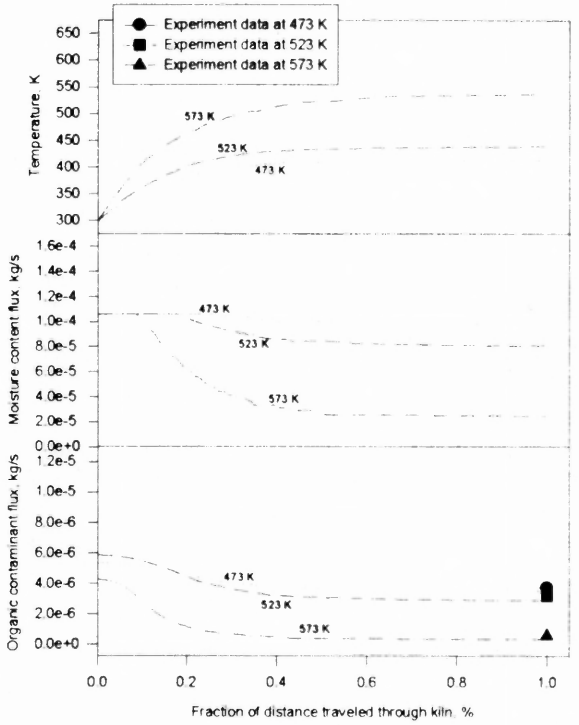

Figure B6.3 Soil temperature profiles, and mass flux distributions of moisture and organic contaminants of run 11: solid residence time = 8.3 min., purge gas flow = 10 L/min., soil feed rate = 80 g/min.

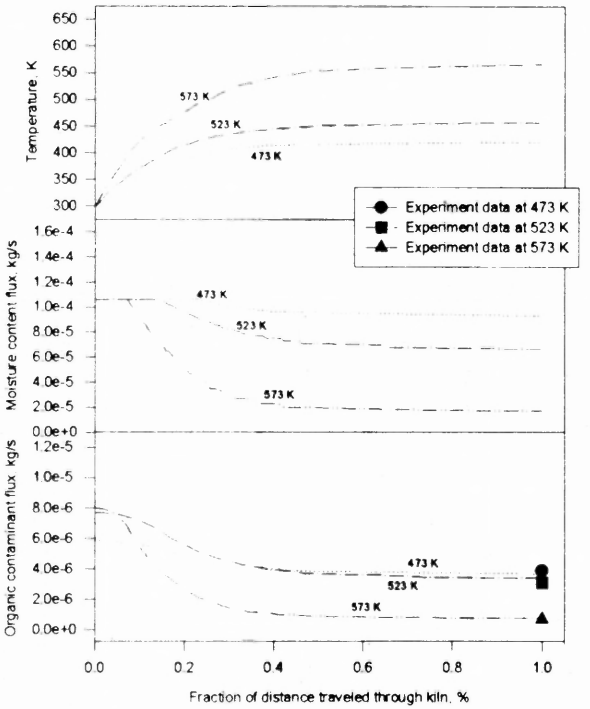

Figure B6.4 Soil temperature profiles, and mass flux distributions of moisture and organic contaminants of run 20: solid residence time = 9 min., purge gas flow = 10 L/min., soil feed rate = 80 g/min.

APPENDIX C

PROGRAM LIST OF NUMERICAL SOLUTION FOR THE HEAT AND MASS TRANSFER MODEL

The computer program listed below is developed for numerical solution of heat and mass transfer model in Chapter 6.

```
PROGRAM  Heat and mass transfer model ;
  Var
{1}   Ts,  Tg,  Tw,  Trd          : Array[0..761] of real;
      Rv_lw, Flw,  Fvw            : Array[0..761] of real;
      Rv_hc, Fl_hc, Fv_hc         : Array[0..761] of real;
      i: integer;
      Hsg, Hgw, Hsw                              : real;
      Tw1, Trd1, Ts_i, Tg_i, Fl_hc00             : real;
      Ccrit_lw, Ccrit_hc, K_Crlw, K_Crhc, Conc_THC   : real;
      pcnt_THC  : real;
      Qrd_s, Qrd_g, Qrd_w                        : real;
{5}   hoi, xo, nsi, LL, DD, LLi, IxV,  IxVi, Cso_hc, HF   : real;
{12}  lrd, ls, lwg, lws, Hrd_g, Erd, Es, Ew              : real;
{20}  Fss, Fvg, dg, Cpg, Cps, Cplw, Cpvw, zo             : real;
{27}  Hsh_a, Ta, Lsh, La, Esh, Ea                        : real;
{33}  ds, Dsp, A_tot, As, Ag, Hvap                       : real;
      LLi_index: real;   sliceindex                      : integer;
      inff, oo_HT, oo_MT, o_lw, o_hc, o_t                : text;
      Rv_limit: real;
  Const sgm  = 5.676E-8;
  { ********************************************************************** }
  PROCEDURE Readfile_R01;
   BEGIN
{lw}  { Assign(o_lw, 'd:\930\run01\o_lw.pas');   rewrite(o_lw);  }
{hc}  { Assign(o_hc, 'd:\930\run01\o_hc.pas');   rewrite(o_hc);  }
      readln(inff);{/1}     readln(inff);{/2}
{a1}   readln(inff, K_Crlw);
{a2}   readln(inff, K_Crhc);
{a3}   readln(inff, Hsg, Hgw, Hsw);
{10}   readln(inff, IxV );
{11}   readln(inff, IxVi);
{13}   read(inff, lws);{lw'} read(inff, lwg);{lw} readln(inff, ls);
{20}   readln(inff, Fss );
{21}   readln(inff, Fvg );
```

```
{11a}   readln(inff,Cso_hc);
readln(inff); readln(inff); {*****}
{1}     readln(inff,Ts[0]);
{2}     readln(inff,Tg[0]);
{3}     readln(inff,Tw[0]);
{4}     readln(inff,Trd[0]);
        readln(inff);{/3}
{5}     readln(inff,hoi);  readln(inff,xo);   readln(inff,nsi);
{8}     readln(inff,LL);   readln(inff,DD);   readln(inff,LLi);
        readln(inff);{/4}
{12}    readln(inff, lrd);
{16}    readln(inff, Hrd_g);
{17}    readln(inff, Erd); readln(inff, Es);  readln(inff, Ew);
        readln(inff);{/5}
        readln(inff, dg);
{23}    readln(inff, Cpg ); readln(inff, Cps );
{25}    readln(inff, Cplw); readln(inff, Cpvw);
{26}    readln(inff, zo  ); readln(inff);{/6}
{27}    readln(inff, Hsh_a); readln(inff, Ta);
{29}    readln(inff, Lsh); readln(inff, La);
{31}    readln(inff, Esh); readln(inff, Ea);   readln(inff);{/7}
{33}    readln(inff, ds ); readln(inff, Dsp);
        readln(inff);{/8}
{35}    A_tot:= 0.25  * pi * (DD*DD);
{36}    As   := A_tot * (lws/(lwg+lws));
{37}    Ag   := A_tot * (lwg/(lwg+lws));
{38}    readln(inff, Hvap);
   END;
 { ********************************************************************** }
 PROCEDURE  Writefile_W01_ID; {File I.D.}
   BEGIN
{ Rv_limit:= (IxVi/(LLi * As * Hvap));            }
{ writeln(o_t,'; Rv_limit = ', Rv_limit:10);      }
{lw_id} {writeln(o_lw,'      ** o_lw: " MD_136: lw "; 02/20/00.sn1 **'); }
{lw_id} {writeln(o_lw,'      ** Run 760-pt, half IxV; Cr=1.58, no coeff');}
{lw_id} {writeln(o_lw,'// OP-2; 300^C; Coeff=1.0  //');              }
{lw_id} {writeln(o_lw,'// OP-2; Fss & Fvg corrected //');            }
{lw}    {writeln(o_lw,'-------------------------------------------',   }
{lw}    {         '-------------------------');                    }
   END; {Writefile_W01}
 { ********************************************************************** }
 PROCEDURE  Writefile_W02_i00;  { both h.t. & M.T.}
   Begin
     LLi_index:= LLi ;
  { --- M.T. ------------------------------------------------------ }
{MT}  {  writeln(oo_MT);
```

```
{lw}   { write (o_lw, ' Ts[ 0]=', Ts[0]:4:0);        }
{lw}   { write (o_lw, ' ;Rv_lw[ 0]=', Rv_lw[0]:6);    }
{lw}   { write (o_lw, ' ;Flw[ 0]=',  Flw[0] :10);    }
{lw}   { writeln(o_lw, ' ;Fvw[ 0]=',  Fvw[0] :10);    }
{lw}   { writeln(o_lw);  writeln(o_lw);              }
{HC}    { writeln(o_hc, ' Ts[0]   = ', Ts[0]  :4:0);              }
{HC}    { write (o_hc, ' ;Rv_hc[ 0] =', Rv_lw[0] :10);              }
{HC}    { write (o_hc, ' ;Fl_hc[ 0] = ', Fl_hc[0] :10);             }
{HC}    { writeln(o_hc, ' ;Fv_hc[ 0] = ', Fv_hc[0] :10);            }
{HC}    { write (o_hc, ' Ts[ 0]= ', Ts[0]:4:1);                    }
{HC}    { write (o_hc, ' ;Fl_hc[ 0]= ', Fl_hc[0] :10);              }
{HC}    { writeln(o_hc, ' ;Fv_hc[ 0]= ', Fv_hc[0] :10);             }
{HC}    { writeln(o_hc, '.....');}
{t}    { writeln(o_hc, ' Ccrit_hc = ', Ccrit_hc  :10);            }
{t}    { writeln(o_hc, ' ******************************************', }
{t}    { writeln(o_hc);                                  }
   End; {Writefile_W02}
{ ********************************************************************** }
 PROCEDURE Writefile_W03_Cale06s;
   Begin
{lw}    write (o_lw, ' Ts[',i:4,']=',  Ts[i] :4:0);
{lw}    write (o_lw, ' ;Rv_lw[',i+1:4,']=', Rv_lw[i+1]:6);
{lw}    write (o_lw, ' ;Flw[',i+1:4,']=',  Flw[i+1] :10);
{lw}    writeln(o_lw, ' ;Fvw[',i+1:4,']=',  Fvw[i+1] :10);
   End; {Writefile_W03}
  { ********************************************************************** }
  PROCEDURE Writefile_W03a_Cale07s;
    var pct_THC: real;
   Begin
{hc}    write (o_hc, ' Ts[',i:4,']=',  Ts[i] :4:0);
{hc}    write (o_hc, ' ;Rv_hc[',i+1:4,']=', Rv_hc[i+1]:6);
{hc}    write (o_hc, ' ;Fl_hc[',i+1:4,']=', Fl_hc[i+1]:9);
{hc}    write (o_hc, ' ;Fv_hc[',i+1:4,']=', Fv_hc[i+1]:9);
      pct_THC:= 100 * (Fl_hc[i]/ Fl_hc00);
      writeln(o_hc, ' ;pct_THC=', pct_THC:9);
   End; {Writefile_W03a}
  { ********************************************************************** }
  PROCEDURE Writefile_W04_cale05s;
   Begin
{t1}   writeln(o_t, 'Ts[',i+1:4,'] = ',Ts[i+1]:4:0,
{t1}        ' ;Tg[',i+1:4,'] = ',Tg[i+1]:4:0, ' ;Tw[',i+1:4,'] = ',
{t1}          Tw[i+1]:4:0, ' ;Trd[',i+1:4,'] = ', Trd[i+1]:4:0) ;
     LLi_index:= LLi_index + LLi ;
{ht}{   writeln(oo_HT,' [**] LLi_index =', LLi_index:7:4); }
   End;
{ ********************************************************************** }
```

```
 PROCEDURE  Writefile_W05_End;
    Begin
{hc}    { writeln(o_hc,' ** Conc_THC = ', Conc_THC   :10, ' ppm');       }
{hc}    { writeln(o_hc,' **    %_THC = ', pcnt_THC:6:2, ' %');          }
{hc}    { writeln(o_hc,' *****            End of File       ***** ');}
        { pcnt_THC := 100 * (Fl_hc[19])/ (Fl_hc[0]) ; }
        { pcnt_THC := (Conc_THC/ 5000.0)* 100 ;}
    End; {Writefile_W05_End}
{ *** fxn_Qrad: function to cale. Q(rad) * * * * * * * * * * * * * * * * * * }
{           subp --> ff001a                                  * * * }
    FUNCTION  fxn_Qrad(T1, T2, L1, L2, e1, e2: real): real;
           var PP001, QQ001 : real;
      (*** function to cale. sq(sq(x)) ***)
      Function ff001a(xx001a, n001a :real):real;
       Begin {ff001a}
          If  n001a = 1.0        Then ff001a:= xx001a
          Else  ff001a:= xx001a * ff001a(xx001a, n001a - 1)
       End; {ff001a}
      (***)
      BEGIN {fxn_Qrad}
       PP001:= sgm * L1 * ( ff001a(T1,4) - ff001a(T2,4) )  ;
       QQ001:=  (1/e1) +  ( (L1/L2)*( (1/e2)-1) );
       fxn_Qrad:= PP001 / QQ001 ;
      END; {fxn_Qrad}
  { **  Cale_01 : Procedure to determine Trd using eq.1      ************ }
  { **          Subp: fxn_eq1(i.e. ff011); bis012                 *** }
  PROCEDURE CALE_01(Ts01, Tg01, Tw01: real; VAR Trd01: real);
     var x01a, x01b :real; index01 :integer;
   (*****)
   Function  fxn_eq1( Ts011, Tg011, Tw011, Trd011: real): real;
       var LL011, RR011, Qrd_s011, Qrd_g011, Qrd_w011, RRLL011: real;
      begin
        Qrd_s011 := fxn_Qrad(Trd011, Ts011, lrd, ls, Erd, Es) ;
        Qrd_g011 := Hrd_g * lrd * (Trd011-Tg011);
        Qrd_w011 := fxn_Qrad(Trd011, Tw011,  lrd, lwg, Erd, Ew) ;
        RR011:= Qrd_s011 + Qrd_g011 +  Qrd_w011  ;
        LL011:= (IxVi)/(LLi);
        RRLL011:= RR011 - LL011 ;
        fxn_eq1:= RR011 - LL011 ;
      end; {fxn_eq1}
   (* * * * * * * *)
   PROCEDURE BIS012(var xx012, yy012: real; Ts012, Tg012, Tw012: real);
       var zz012, AA012, CC012 : real;
      Begin {BIS012}
```

```
        zz012:= xx012 + 0.5*(yy012-xx012);
        AA012:= fxn_eq1(Ts012, Tg012, Tw012, xx012);
        CC012:= fxn_eq1(Ts012, Tg012, Tw012, zz012);
        IF (AA012) * (CC012) < (1/1.0E+10)  THEN
          begin   xx012:= xx012 ; yy012:= zz012    end
        ELSE
          begin   xx012:= zz012 ; yy012:= yy012    end
      End;
    (*****)
  BEGIN { Cale_01 }
    x01a:= 298; x01b:= 1200;
{DO1}  While        abs(x01a - x01b) >= 1.0          DO
      Begin
        BIS012(x01a, x01b,                          {VAR}
                    Ts01, Tg01, Tw01);
          index01:= index01+1;
      end;
      Trd01:= x01b;  { Idea:: Trd=const ?? Trd01:= 845.0;}
{ht}    { writeln(oo_HT, ' $ Trd01 =', Trd01:8:2);   }
END; {Cale_01}
  { **  Cale_02: Procedure to execute Runge-Kutta integration        ** }
  { **        Subp: Cale_021 (fxn_eq2; fxn_eq3);(i.e. ff023; ff024);** }
  PROCEDURE  CALE_02( var Ts02, Tg02                  : real ;
                Tw02, Trd02, Rv_lw02, Flw02, Fvw02 : real);
              { *** Only Ts02, Tg02: output; others are just input }
    var index02 :integer ;  x02: real;
    (* * * * * * * *)
    PROCEDURE  CALE_021(Var   x021, Ts021, Tg021          : real ;
                Tw021, Trd021, Rv_lw021, Flw021, Fvw021: real);
      var yt1,yt2,ka,kb,kc,kd,la,lb,lc,ld : real;
      {** fxn_eq2: soil **}
      Function fxn_eq2(xx023, Tw023, Trd023, Ts023, Tg023,
                Rv_lw023, Flw023          : real): real;
        var   Qgs023,  Qws,  Qrd_s, RR023, HH023: real;
{ A3; A1 }      { const  Hsw = 86.3;    Hsg = 55.8;  }
       Begin
        Qgs023:= - Hsg * ls  * (Ts023 - Tg023);
        Qws   :=   Hsw * lws * (Tw023 - Ts023);
        Qrd_s :=   fxn_Qrad(Trd023, Ts023, lrd, ls, Erd, Es);
        HH023 := - Rv_lw023 *  As * Hvap;
                    { *** HERE: consider "lw" volume only *** }
        RR023 :=   (Fss*(1.0 - zo) * Cps) + (Flw023 * Cplw);
                    { Unit: (kg/s * J/kg.K) +  _____  = J/s.K }
        fxn_eq2  := (Qgs023 + Qws + Qrd_s + HH023)/ (RR023) ;
       end; {fxn_eq2}
      {** fxn_eq3: gas **}
```

```
    Function fxn_eq3(xx024, Tw024, Trd024, Ts024, Tg024, Fvw024: real)
                                                    : real;
      var   Qgs024, Qwg, Qrd_g, RR024: real;
{ A2; A1 }      { const  Hgw= 3.8;   Hsg= 55.8;  }
      Begin
       Qgs024:=  Hsg  * ls  * (Ts024  - Tg024);
       Qwg   :=  Hgw   * lwg * (TW024  - TG024);
       Qrd_g :=  Hrd_g * lrd * (Trd024 - Tg024);
       RR024 :=  ((Fvg* dg)* Cpg) + (Fvw024 * Cpvw);
                  { Unit: (m3/s * kg/m3 * J/kg.K) + ___ = J/s.K }
       fxn_eq3  := (Qgs024 + Qwg + Qrd_g)/(RR024);
      End; {fxn_eq3}
   BEGIN { Cale_021: Runge-Kutta; using fxn_eq2 & fxn_eq3 }
     yt1 := Ts021;          yt2 := Tg021;
        ka:=fxn_eq2(x021,Tw021,Trd021,Ts021,Tg021,  Rv_lw021, Flw021);
        la:=fxn_eq3(x021,Tw021,Trd021,Ts021,Tg021,  Fvw021);

     x021:=x021+hoi/2;
       Ts021 := yt1+hoi*ka/2;    Tg021 := yt2+hoi*la/2;
        kb:=fxn_eq2(x021,Tw021,Trd021,Ts021,Tg021,  Rv_lw021, Flw021);
        lb:=fxn_eq3(x021,Tw021,Trd021,Ts021,Tg021,  Fvw021);
       Ts021 := yt1+hoi*kb/2;    Tg021 := yt2+hoi*lb/2;
        kc:=fxn_eq2(x021,Tw021,Trd021,Ts021,Tg021,  Rv_lw021, Flw021);
        lc:=fxn_eq3(x021,Tw021,Trd021,Ts021,Tg021,  Fvw021);
     x021:=x021+hoi/2;
       Ts021 := yt1+hoi*kc;      Tg021 := yt2+hoi*lc;
        kd:=fxn_eq2(x021,Tw021,Trd021,Ts021,Tg021,  Rv_lw021, Flw021);
        ld:=fxn_eq3(x021,Tw021,Trd021,Ts021,Tg021,  Fvw021);
     Ts021 := yt1+hoi*(ka+2*kb+2*kc+kd)/6;
     Tg021 := yt2+hoi*(la+2*lb+2*lc+ld)/6;
   END; {Cale_021}
   {************}
   BEGIN { Cale_02: eq.2-3; using Cale_021;(fxn_eq2; fxn_eq3) }
     index02:=1;  x02:= 0.0;
{DO2} While       x02 < (LLi - (hoi/1000))       DO
      Begin
{@}     CALE_021(x02, Ts02, Tg02,                        {VAR}
                  Tw02, Trd02, Rv_lw02, Flw02, Fvw02);
                    { ** real output : Ts02; Tg02 ** }
       index02 := index02 + 1;
      End;
   END; {Cale_02}
  { ** CALE_04 :: Procedure to cale. TTw4 using eq.1..4          ** }
  { **       :: subp : Bis042 (FXN_EQ1X4);(ie. ff041);         ** }
  { * HH041 corrected : at 11/12/R                          * }
  PROCEDURE CALE_04(Tsi04,  Tsf04, Tgi04, Tgf04,
```

```
{add: Trd04}        Rv_lw04, Flw04, Fvw04, Trd04: real;
                var Tw04: real);
        var x04a, x04b :real; index04 :integer;
        var QQ041, HH041, SS041, GG041,  CNV041, RAD041, Q_loss: real;
      {*****}
      Function fxn_eq1X4(Tsi041,Tsf041,  Tgi041,Tgf041, Tw041,
                  Rv_lw041, Flw041, Fvw041: real) :real;
        var  RRLL041: real;
       Begin {fxn_eq1X4}
        QQ041:= (IxVi/LLi);
        HH041:= Rv_lw041 * As * Hvap;            {11/99 corrected}
        SS041:= (Fss*(1-zo)*Cps + Flw041* Cplw) * (Tsf041 - Tsi041);
        GG041:= (Fvg* dg* Cpg   + Fvw041* Cplw) * (Tgf041 - Tgi041);
        CNV041:= Hsh_a * Lsh * (Tw041 - Ta);
        RAD041:= fxn_Qrad(Tw041, Ta, Lsh, La, Esh, Ea);
        Q_loss:= CNV041 + RAD041;
        RRLL041:= (Q_loss + SS041 + GG041) - (- HH041) - QQ041;
        fxn_eq1X4:= RRLL041 ;
       End; {Fxn_eq1x4}
      {*****}
      Procedure Bis042 (var xx042, yy042 :real; Tsi042, Tsf042,
                  Tgi042, Tgf042,  Rv_lw042, Flw042, Fvw042:real) ;
        var zz042, AA042, CC042 :real;
       Begin {Bis042}
        zz042:= xx042 + 0.5*(yy042-xx042);
        AA042:= FXN_EQ1X4(Tsi042, Tsf042, Tgi042, Tgf042, xx042,
             Rv_lw042, Flw042, Fvw042);
        CC042:= FXN_EQ1X4(Tsi042, Tsf042, Tgi042, Tgf042, zz042,
             Rv_lw042, Flw042, Fvw042);
       IF  (AA042) * (CC042) < (1/1.0E+10)  THEN
         begin    xx042:= xx042 ; yy042:= zz042    end
       ELSE
         begin    xx042:= zz042 ; yy042:= yy042    end
       End; {Bis042}
      {*****}
    BEGIN  { Cale_04: eq.4 }
      index04:= 1;
{ht-valve2}
      x04a:= 298;    x04b:= Trd04 {1200: wrong!!};
{Do3}   WHILE        abs(x04a - x04b) >= 1.0          DO
       Begin
{@}        BIS042(x04a,   x04b,  Tsi04,   Tsf04, Tgi04, Tgf04,
             Rv_lw04, Flw04, Fvw04);
         index04:= index04 + 1;
{ht}     { writeln(oo_HT,' *** Index04 = ',index04:3,' >>  i =',i:4); }
       End;
```

```
      Tw04:= x04b ;
    END; {Cale_04}
  { ** MAINCALE_101 // subp: Cale_01; Cale_02; Cale_04          ** }
  { ** Input : Tsi, Tgi, Tw_x, --                              ** }
  PROCEDURE MAINCALE_101(var  Ts101,  Tg101,  Tw101,  Trd101: real;
                    Rv_lw101, Flw101,  Fvw101      : real);
     var Ts_ii, Ts_ff,  Tg_ii, Tg_ff: real;
    BEGIN { MAINCALE_101 }
      Ts_ii:= Ts101;  Tg_ii:= Tg101;
{@}   CALE_01(Ts101, Tg101, Tw101,
                      Trd101);                  {VAR}
                    { *** Output : Trdi (from Twi ; i.e. Tw_x) }
{@}   CALE_02( Ts101, Tg101,                              {VAR}
                    Tw101, Trd101, Rv_lw101, Flw101, Fvw101);
      Ts_ff:=Ts101;  Tg_ff:=Tg101;
                    { *** Output : Tsf; Tgf          ** }
{@}   CALE_04(Ts_ii,Ts_ff,Tg_ii,Tg_ff, Rv_lw101, Flw101, Fvw101, Trd101,
        Tw101); {VAR}
                    { *** Output : TTw1; i.e. Tw_xx      ** }
    END; {Maincale_101}
  { ** 440:: CALE_05 :: Heat Balance -- eq.1..4                ** }
  { **          & Procedure to Check TTw3(+) and TTw4(++)      ** }
  { **          Subp : Bis052 -> Cale051 (.. Maincale_101)     ** }
  { **  Imp't: (Rv_lw/Flw/Fvw) :: at Cale_02/ Cle_05 -- input only   ** }
  { **  Change: ff001 -> fff051 -> "Twx_xx";                   ** }
  PROCEDURE CALE_05(var  Ts05,  Tg05,  Tw05,  Trd05: real ;
                Rv_lw05, Flw05, Fvw05     : real);
     var x05a, x05b, Ts05i, Tg05i, Trd05i :real;  index05 : integer;
     {*****}
     Procedure Cale051(VAR Ts051, Tg051,  Tw051, Trd051, Twx_xx051: real;
                  Rv_lw051, Flw051, Fvw051          : real);
       var  Tw_x, Tw_xx :real;
       Begin {Cale051}
        Tw_x := Tw051;
{@}       Maincale_101(Ts051,Tg051,Tw051,Trd051,              {VAR}
                              Rv_lw051, Flw051, Fvw051);
        Tw_xx := Tw051 ;     Twx_xx051:= Tw_xx - Tw_x ;
       End; {Cale051}
     (*****)
     Procedure Bis052(var xx052, yy052,  Ts052, Tg052, Trd052: real;
                Rv_lw052, Flw052, Fvw052          : real) ;
       var zz052, AA052, CC052, Twx_xx, xx052i, yy052i, zz052i : real;
         Ts052i, Tg052i, Trd052i   : real ;
       Begin {Bis052}
        zz052 := xx052 + 0.5*(yy052-xx052);
        Twx_xx:= 0.0;
```

```
        Ts052i:= Ts052;  Tg052i:= Tg052;  Trd052i:= Trd052;
        xx052i:= xx052;  yy052i:= yy052;  zz052i := zz052;
{@A}      Cale051(Ts052i,   Tg052i, xx052, Trd052i, Twx_xx,        {VAR}
           Rv_lw052, Flw052, Fvw052);
        AA052:= Twx_xx ;
                  { // Twx_xx : i.e. (Tw(**) - Tw(*)) // }
        { ------------------------------------------------------- }
        Ts052i:= Ts052;  Tg052i:= Tg052;  Trd052i:= Trd052;
{@B}      Cale051(Ts052i,   Tg052i, zz052, Trd052i, Twx_xx,        {VAR}
           Rv_lw052, Flw052, Fvw052);
        CC052:= Twx_xx ;
        IF (AA052) * (CC052) < (1/1.0E+10) THEN
          begin   xx052:= xx052i ; yy052:= zz052i    end
        ELSE
          begin   xx052:= zz052i ; yy052:= yy052i    end ;
        Ts052:=Ts052i;  Tg052:=Tg052i;  Trd052:=Trd052i;
      End; {Bis052}
      (*****)
   BEGIN { Cale_05 :: Check Tw(*) vs Tw(**) }
      index05:= 1;
      Ts05i:= Ts05;  Tg05i:= Tg05;  Trd05i:= Trd05;
      x05a := 298;   x05b := 1200;
{DO4} While         abs(x05a - x05b) >= 1.0          DO
     Begin
      Ts05:= Ts05i;  Tg05:= Tg05i;  Trd05:= Trd05i;
{@}      BIS052(x05a, x05b, Ts05, Tg05, Trd05,                {VAR}
                              Rv_lw05, Flw05, Fvw05);
{ht} {   writeln(oo_HT);  writeln(oo_HT);  writeln(oo_HT);  writeln(oo_HT);
{ht} {   writeln(oo_HT,
{ht} {   '        ****  Next Trial for Cale_05   ****', ' >> i =',i:4);}
      index05:= index05+1;
{ht} {   writeln(oo_HT,' /// Index05 = ',index05:3);        }
     end;
     Tw05:= x05b ;
   END; {Cale_05}
 { ********************************************************************** }
 { ** 610:: CALE_06 :: Mass Balance -- eq.5..6 (subp: fxn_061Rv_lw)   ** }
 { **          --> (9)^24 = exp(24* ln(9))                    ** }
 { **  "Ts" --> input only;                                  ** }
 { ** For organics, should make an INPUT file for all para. values **}
 PROCEDURE  CALE_06(Ts06: real;  VAR Rv_lw06, Flw06, Fvw06: real);
     var  Cs_lw, Cg_vw, Dm, Pvap                  : real;
     Function  fxn_061Rv_lw(Ts061, Cs_lw061, Cg_vw061,
           C_crit061: real): real;
       const  { H2O: bp = 373 K }
           anta06 = 18.3036;   antb06 = 3816.44;   antc06 = -46.13;
```

```
          mw    = 18.0  ; {kg/kg-mol}
          R     = 0.082 ; {atm.m3/ kg-mol.K}
        var Dm, Pvap, xx, AA, BB, CC                : real;
      BEGIN { fxn_061Rv_lw; Antoine eq. }
        Dm := 1.28E-9 * ( exp(1.75* ln(Ts061)) ) ;
        Pvap := ( exp(anta06 - (antb06/ (Ts061+ antc06))) )/ 760 ; {atm}
        AA:=  (( Pvap* mw * Cs_lw061)/( R* Ts061* Ccrit_lw));
        BB:=  ( AA - Cg_vw061);
{/ coef:1}  CC:=  (12.0 * Dm)/(Dsp * Dsp);
                        { C10: Coeff= 3.0E-6; Cr=0.5:: for OP-2 }
        Fxn_061Rv_lw :=  BB * CC ;
      END; {fxn_061Rv_lw}
    { ** ---------------------------------------- ** }
  Begin {Cale_06}
    Cs_lw:= Flw06/ (( Fss*(1-zo)+ Flw06 )/ ds) ;
                        { Unit : (kg/s)*(kg/m3)/(kg/s) = kg/m3 }
    Cg_vw:= Fvw06/ ( Fvg + (Fvw06/ dg) ) ;
                        { Unit : (kg/s) /(m3/s) = kg/m3    ... }
{@@}    Rv_lw06:=  fxn_061Rv_lw( Ts06, Cs_lw, Cg_vw, Ccrit_lw);
  IF Rv_lw06 < 0.0 THEN  begin
    Rv_lw06:= 0.0;
    Flw06:=  Flw06 - ( Rv_lw06 * ( As * LLi )) ;
    Fvw06:=  Fvw06 + ( Rv_lw06 * ( As * LLi )) ;
                end
  ELSE
                begin
    {   IF (Rv_lw06 - Rv_limit) > 0.0 THEN  begin  }
    {      Rv_lw06:= Rv_limit;          end    }
    {   ELSE                        begin  }
    {      Rv_lw06:= Rv_lw06;           end;   }
    Flw06:=  Flw06 - ( Rv_lw06 * ( As * LLi )) ;
    Fvw06:=  Fvw06 + ( Rv_lw06 * ( As * LLi )) ;
                end;
  End; {Cale_06}
 { *** Cale_07: HCx (C10H8)          ********************************** }
 PROCEDURE  CALE_07(Ts07: real;  VAR Rv_hc07, Fl_hc07, Fv_hc07: real);
    var  Cs_l_hc, Cg_v_hc, Dm07, Pvap07 : real;

    Function  fxn_071Rv(Ts071, Cs_l_hc071, Cg_v_hc071: real): real;
      const  { C10H8:: Naphthalene: bp = 491 K }
          anta07 = 16.1426;   antb07 = 3992.01;   antc07 = -71.29;
          mw07   = 128 ;   {kg/kgmol}
          R      = 0.082 ; {atm.m3/ kgmole.K}
        var  Dm071, Pvap071, AA071, BB071, CC071       : real;
      BEGIN { fxn_071Rv; Antoine eq. }
```

```
        Dm071 := 2.933E-10 * ( exp(1.75* ln(Ts071)) ) ;
        Pvap071 := ( exp(anta07 - (antb07/ (Ts071+ antc07))) )/ 760 ;    {atm}
        AA071:= (( Pvap071* mw07 * Cs_l_hc071)/( R* Ts071* Ccrit_hc));
        BB071:= ( AA071 - Cg_v_hc071);
{/ coef:2}  CC071:= (12.0 * Dm071)/(Dsp * Dsp);
                    { C10: Coeff= 3.0E-6; Cr=0.5:: for OP-2 }
        Fxn_071Rv := BB071 * CC071 ;
      END; {fxn_071Rv}
    { ** ---------------------------------------- ** }
  Begin {Cale_07}
  {REM:} Cs_l_hc:= Fl_hc07/ (Fss/ ds) ;
                    { Unit : (kg/s)*(kg/m3)/(kg/s) = kg/m3 }
      Cg_v_hc:= Fv_hc07/ Fvg ;
                    { Unit : (kg/s) /(m3/s) = kg/m3    ... }
{@@}      Rv_hc07 := fxn_071Rv( Ts07, Cs_l_hc, Cg_v_hc);
      IF (Rv_hc07 < 0.0)    THEN        begin
        Rv_hc07:= 0.0;
        Fl_hc07:= Fl_hc07;  Fv_hc07:= Fv_hc07;
                                end
      ELSE                        begin
        Fl_hc07:= Fl_hc07 - (Rv_hc07 *( As * LLi)) ;
        Fv_hc07:= Fv_hc07 + (Rv_hc07 *( As * LLi)) ;
                                end;
  End; {Cale_07}
 { *** Cale_0701              ********************************** }
 PROCEDURE CALE_0701;
  Begin
     CALE_07(Ts[i],
             Rv_hc[i], Fl_hc[i], Fv_hc[i]);          {VAR}
     IF ( Fl_hc[i] < 0.0)    THEN            begin
       Rv_hc[i+1]:= Rv_hc[i];
       Fl_hc[i+1]:= 0.0;  Fv_hc[i+1]:= Fss * Cso_hc ;
       Writefile_W03a_cale07s;
                                end
     ELSE                           begin
       Rv_hc[i+1]:= Rv_hc[i];
       Fl_hc[i+1]:= Fl_hc[i];   Fv_hc[i+1]:= Fv_hc[i];
       Writefile_W03a_cale07s;
                                end;

  End; {Cale_0701}
 { *** Cale_08: Main Routine      ********************************** }
 PROCEDURE CALE_08;
  Begin
{DO5}
   For    i:= 0    to    759     Do
```

```
      BEGIN
{@}     CALE_06(Ts[i],
                Rv_lw[i], Flw[i],  Fvw[i]);          {VAR}
        CALE_0701;
        IF    (Flw[i] < 0)    THEN          Begin  {w/o H2O}
          While    i  <  759   Do
           begin
            Rv_lw[i+1]:= 0.0;
            Flw[i+1]  := 0.0;
            Fvw[i+1]  := Flw[0] + Fvw[0];
{@}           CALE_05( Ts[i],  Tg[i],  Tw[i],  Trd[i],   {VAR}
                Rv_lw[i+1], Flw[i],  Fvw[i]);
            Ts[i+1]:= Ts[i];        Tg[i+1] := Tg[i];
            Tw[i+1]:= Tw[i];        Trd[i+1]:= Trd[i];
            Writefile_W04_cale05s;          { i:= i+1;}
           end;
                                    End
      ELSE                             Begin

         IF  (Rv_lw[i] < 0)  THEN
           begin
            Rv_lw[i+1]:= 0.0;
            Flw[i+1]  := Flw[i];  Fvw[i+1]  := Fvw[i];
            Writefile_W03_cale06s; {lw}
{@}           CALE_05( Ts[i],  Tg[i],  Tw[i],  Trd[i],   {VAR}
                  Rv_lw[i+1], Flw[i],  Fvw[i]);
            Ts[i+1]:= Ts[i];        Tg[i+1] := Tg[i];
            Tw[i+1]:= Tw[i];        Trd[i+1]:= Trd[i];
            Writefile_W04_cale05s; {Temp}     { i:= i+1;}
           end
         ELSE
           begin
            Rv_lw[i+1]:= Rv_lw[i];
            Flw[i+1]:= Flw[i];      Fvw[i+1]:= Fvw[i];
            Writefile_W03_cale06s; {lw}
{@}           CALE_05( Ts[i],  Tg[i],  Tw[i],  Trd[i],  {VAR}
                  Rv_lw[i+1], Flw[i],  Fvw[i]);
            Ts[i+1]:= Ts[i];        Tg[i+1]:=  Tg[i];
            Tw[i+1]:= Tw[i];        Trd[i+1]:= Trd[i];
            Writefile_W04_cale05s;{Temp}      { i:= i+1; }
           end;
                                    End
    END;
   End; {Cale_08}
{*********************************************************************** }
  PROCEDURE  CALE_09;
```

```
  Begin
    Readfile_R01;       Writefile_W01_ID;
{H2O}  Rv_lw[0]:= 0.0;
    Flw[0]  := Fss * zo ; {kg/s}
    Fvw[0]  := (Fvg * 1000.0 * HF * 0.018) / 24.436 ; {kg/s}
{/ Cr:1} Ccrit_lw := (K_Crlw) * ( (Fss * zo)/ (Fss/ ds) );
{HCx}  Rv_hc[0]:= 0.0;
    Fl_hc[0]:= Fss * Cso_hc;  {(kg/s)* (kg/kg)}
    Fl_hc00 := Fss * Cso_hc;  {= const: for calculation of %hc}
    Fv_hc[0]:= 0.0;         {kg/s}
{/ Cr:2} Ccrit_hc:= (K_Crhc) * ( (Fss* Cso_hc)/ (Fss/ ds) );
    Writefile_W02_i00;      LLi_index:= LLi ;
     Cale_08;
    { ****************************************** }
    Ts[0]:= Ts[760];
    Tg[0]:= Tg[760];
    Rv_lw[0]:= 0.0;
    Flw[0]  := Flw[760]; {kg/s}
    Fvw[0]  := Fvw[760];
{HCx}  Rv_hc[0]:= 0.0;
    Fl_hc[0]:= Fl_hc[760];{(kg/s)* (kg/kg)}
    Fv_hc[0]:= Fv_hc[760];       {kg/s}
    { ****************************************************** }
    Writefile_W05_End;
     Writeln(o_hc,'==========>>                          ==>',
        '       #22: 300^C; IxVi=0.8928  75% setting');
  End; {Cale_09}
{*************************************************************************}
 Procedure Run03a_xx;                                  begin
   Assign(inff,  'c:\951\run03a\inff.pas');   reset (inff);
{vv} Assign(o_t,  'c:\951\run03a\o_t.pas');    rewrite(o_t);
   Assign(o_lw,  'c:\951\run03a\o_lw.pas');   rewrite(o_lw);
   Assign(o_hc,  'c:\951\run03a\o_hc.pas');   rewrite(o_hc);
   Cale_09;
   Close(inff);  Close(o_t);  Close(o_lw);  Close(o_hc);   end;
{ ************************************************************** }
 Procedure Run03b_xx;                                  begin
   Assign(inff,  'c:\951\run03b\inff.pas');   reset (inff);
{vv}Assign(o_t,  'c:\951\run03b\o_t.pas');    rewrite(o_t);
   Assign(o_lw,  'c:\951\run03b\o_lw.pas');   rewrite(o_lw);
   Assign(o_hc,  'c:\951\run03b\o_hc.pas');   rewrite(o_hc);
   Cale_09;
   Close(inff);  Close(o_t);  Close(o_lw);  Close(o_hc);   end;
{ ************************************************************** }
 Procedure Run03c_xx;                                  begin
   Assign(inff,  'c:\951\run03c\inff.pas');   reset (inff);
```

```
{vv}Assign(o_t,  'c:\951\run03c\o_t.pas');     rewrite(o_t);
    Assign(o_lw, 'c:\951\run03c\o_lw.pas');    rewrite(o_lw);
    Assign(o_hc, 'c:\951\run03c\o_hc.pas');    rewrite(o_hc);
    Cale_09;
    Close(inff); Close(o_t); Close(o_lw); Close(o_hc);    end;
{ ************************************************************** }
 BEGIN
    Run03a_xx;
    Run03b_xx;
    Run03c_xx;
 END. {Main Program: End}
```

REFERENCES

1. US EPA. 1999. The Superfund Innovative Technology Evaluation (SITE) Program: Demonstration Program, Office of Research and Development. Cincinnati, Ohio.

2. US EPA. 1990. Engineering Bulletin - Mobile/Transportable Incineration Treatment, EPA/540/2-90/014, Office of Emergency and Remedial Response, Washington, D.C.

3. US EPA. 1993. Engineering Bulletin - Thermal Desorption Treatment, EPA/540/0-00/000, Office of Emergency and Remedial Response, Washington, D.C.

4. US EPA. 1994. Remediation Technologies Screening Matrix and Reference Guide, 2nd Edition, EPA/542/B94/013, Office of Solid Waste and Emergency Response, Washington, D.C.

5. J. A. Soesilo and, S. R. Wilson, 1997, Hazardous Waste Site Remediation, Lewis Publishers, New York.

6. J. Lighty, M. Choroszy-Marshall, M. Cosmos, V. Cundy, and P.D. Percin, 1993, Innovative Site Remediation Technology: Thermal Desorption, edited by Anderson W.C., published by the American Academy of Environmental Engineers, Annapolis, MD.

7. W. L. Troxler, J.J. Cudahy, P.P. Zink, S.I. Rosenthal, and J.J. Yezzi., 1993. Treatment of Nonhazardous Petroleum-Contaminated Soils by Thermal Desorption Technologies, *Journal of the Air and Waste Management Association*, Vol. 43, pp. 1512-1525.

8. D.W. Major and J. Fitchko, 1990. Emerging On-Site and In Situ Hazardous Waste Treatment Technologies, Cahners Publishing Company, Des Plaines, IL.

9. R.D. Fox, E.S. Alperin, and H.H. Huls. 1991. Thermal Treatment for The Removal of PCBs and Other Organics from Soil, *Environmental Progress*, Vol. 10, No. 1, pp. 40-44.

10. US EPA. 1992. Applications Analysis Report, Low Temperature Thermal Treatment (LT^3) Technology, Roy F. Weston, Inc. EPA/540/AR-92/019. Office of Research and Development. Washington, D.C.

11. S.E. Manahan, 1990. Hazardous Waste Chemistry, Toxicology and Treatment, Lewis Publishers, Chelsea, Michigan.

12. US EPA. 1989. Applications Analysis Report, Shirco Infrared Incineration System, EPA/540/A5-89/010. Risk Reduction Engineering Laboratory, Office of Research and Development. Washington, D.C.

13. US EPA. 1992. Demonstration Bulletin - SoilTech Anaerobic Thermal Processor: Outboard Marine Corporation Site, EPA/540/MR-92/078, Washington, D.C.

14. A.J. Pisanelli and N.A. Maxymillian, 1996. Development of An Indirectly Heated Thermal Desorption System for PCB Contaminated Soil, Maxymillian Technologies Inc.

15. R.K. Nielson and M.G. Cosmos, 1989. Low Temperature Thermal Treatment (LT^3) of Volatile Organic Compounds from Soil: A Technology Demonstrated, Environmental Progress, Vol. 8, No. 2, pp. 139-142.

16. Ayen R., Matz P. and Meyers, G., 1994. Thermal Desorption of PCB-Contaminated Soil at the Re-Solve Superfund Site, *Proceedings of the Superfund Conference XV Conference*, Washington, D.C., 653-659.

17. US EPA, 1995. Innovative Treatment Technologies: Annual Status Report, 8th Edition, EPA/542/R96/010, Office of Emergency and Remedial Response, Washington, D.C.

18. Hoppe T. and Grob B., 1990. Heat Flow Calorimetry for Preventing Runaway Reactions, *Chem. Eng. Prog.*, Jan. 1990, pp. 13-17.

19. Gygax R. W., 1990. Scaleup Principles for Assessing Thermal Runaway Risks, *Chem. Eng. Prog.*, pp. 53-60.

20. R. Gygax, 1988. Chemical Reaction Engineering for Safety, *Chem. Eng. Sci.*, Vol. 43, No. 8, pp. 1759-1771.

21. D.W. Smith, 1984. Assessing the Hazards of Runaway Reactions, *Chem. Eng.*, pp. 54-60.

22. D.W. Smith, 1982. Runaway Reactions and Thermal Explosion, *Chem. Eng.*, pp. 79-84.

23. E.R. Ritter and J.W. Bozzelli, 1991. THERM: Thermodynamic Property Estimation for Gas Phase Radicals and Molecules, Itnl J. of Chem. Kinetics, Vol. 23, pp. 767-778.

24. C.T. Chiou, T.D. Shoup, 1985. Soil Sorption of Organic Vapors and effects of Humidity on Sorptive Mechanism and Capacity, *Environ. Sci. Technol.*, Vol. 19, No. 12, pp. 1196-1201.

25. Lester T.W., Cundy V. A., Sterling A. M., and Leger C. B., 1991. Rotary Kiln Incineration. Comparison and Scaling of Field-Scale and Pilot-Scale Contaminant Evolution Rates from Sorbent Beds, *Environ. Sci. Technol.*, Vol. 25, No. 6, pp. 1142-1152.

26. Olie, K., Vermeulen, P., Hutzinger, 1977. O. *Chemosphere* 6, 455.

27. Fiedler, H., 1993. *Organohalogen Compd., 11*, 221.

28. Alcock, R., Jones, K., 1996. *Environ. Sci. Technol.* 30, 3133-3143.

29. U. S. EPA., 1998. *The Inventory of Sources of Dioxin in the United States*. External Review Draft; EPA/600/P-98/002Aa; The Office of Research and Development, National Center for Environmental Assessment: Washington, DC, 1998.

30. MSNBC News, May 17, 2000.

31. U.S. EPA Report, *Guidance on Collection of Emissions Data to Support Site-Specific Risk Assessments at Hazardous Waste Combustion Facilities*. EPA530-D-98-002, 1998.

32. Iino, F., Imagawa, T., Takeuchi, M., and Sadakata, M., 1999. *Environ. Sci. Technol.* 33, 1038-1043.

33. Tejima, H., Nakagawa, I., and Shinoda, T., 1996. *Chemosphere* 32: 169-175.

34. Kato, T., Osada, S., Sakai, S., and Hiraoka M., 1996. *Chemosphere* 32: 145-150.

35. Akimoto Y., Nito S., and Inouye, Y, 1997. *Chemosphere* 34: 791-799.

36. Fujii, T., Murakawa T., and Maeda N, 1994. *Chemosphere* 29: 2067-2070.

37. Commoner, B., McNamara, M., Shapiro, K., and Webster T, 1984. *Environmental and Economic Analysis of Alternative Municipal Solid Waste Disposal Technologies, part II: The Origins of Chlorinated Dioxins and Dibenzofurans Emitted by Incinerators That Burn Unseparated Municipal Solid Waste, and an Assessment of Methods of Controlling Them*. Center for the Biology of Natural Systems, Queens College, CUNY, Flushing, New York.

38. Commoner, B., Webster T., K. Shapiro K., and McNamara M., 1985. *The Origins and Methods of Controlling Polychlorinated Dibenzo-p-dioxin and Dibenzofuran Emissions from MSW incinerators*. Presented at: 78th Annual Meeting of the Air Pollution Control Assoc.; Detroit, MI.

39. Commoner, B.; Shapiro K.; Webster T., 1987. *Waste Management and Research* 5: 327-346.

40. Clement, R., Tosine, H., Osborne, J., Ozvacic, V., Wong, G., 1988. *Biomedical and Environmental Mass Spectrometry*, 17: 81-96.

41. Hay, D.J., Finkelstein, A., and Klicius, R., 1986. *The National Incineration Testing and Evaluation Program: An Assessment of Two-Stage Incineration and Pilot Scale Emission control.* Paper Presented to U.S. EPA Science Advisory Board, Washington, DC. Environment Canada, Ottawa, Ontario, Canada..

42. Environment Canada. *The National Incineration Testing and Evaluation Program: Two-Stage Combustion (Prince Edward Island). Environment Canada,* Ottawa, Ontario, Canada. Report EPS 3/UP/1. September 1985.

43. Tosine, H., Clement, R, Ozvacic, V., and Wong, G., 1985. *Chemosphere* ,14: 821-827.

44. Velhow J., Karlsruhe F., 2000. *Proceedings of International Conference on Combustion, Incineration/Pyrolysis and Emission Control*, Seoul, Korea.

45. Fabrellas B., Sanza P., Abadb E., and Rivera J., 2001. The Spanish dioxin inventory Part I: incineration as municipal waste management system. *Chemosphere* 43: 683-688.

46. Abad E., Adrados M., Caixach J., Fabrellas1 B, and Rivera J., 2000. Dioxin mass balance in a municipal waste incinerator. *Chemosphere* 40: 1143-1147.

47. Abad E., Adrados M., Caixach J., Rivera J., 2002. Dioxin Abatement Strategies and Mass Balance at a Municipal Waste Management Plant. *Environ. Sci. Technol.* 2002, 36, 92-99.

48. Wilken, M. and Cornelson, B., 1992. *Chemosphere* 25: 1517-1523.

49. Lahl, U.; Jager, J., *Chemosphere* 1991, 23: 1481.

50. International Ash Working Group: Chandler, A.; Eighmy, T.; Sloot, H.; Velhow, L. *Municipal Solid Waste Incinerator Residues*, Elsevier, Amsterdam, 1997.

51. BGA. Sachstand Dioxine, Bericht des Umweltbundesamtes 5/85: 264, 1985.

52. Shin, D.; Choi, J.; Choi, S. *Proceedings of International Conference on Combustion, Incineration/Pyrolysis and Emission Control*, Seoul, Korea, June, 2000.

53. NATO CCMS. *International Toxicity Equivalency Factors (I/TEF) Method of Risk Assessment for Complex Mixtures of Dioxins and Related Compounds*, Report 178, 1998.

54. Hiraoka, M. *Chemosphere* 1989, 19: 361.

55. Vogg, H, and Velhow, J., 1991. VDI Berichte 895, 193.

56. Johnke, B., Stelzner, E., 1992. Results of the German Dioxin Measurement Programme at MSW Incinerators. *Chemosphere* 10:345-355.

57. ITU - Forschung measurements (Kolonnenstr. 26, D - 1000, Berlin 62, FRG).

58. Hagenmaier, H. unpublished (Institute of Organic Chemistry, University of Tubingen, D-7400 Tubingen, Federal Republic of Germany).

59. Konig, J., Theisen J., and Buchen M., 1993. *Chemosphere* 26: 851-861.

60. Lohmann, R., Green, N., and Jones, K., 1999. *Environ. Sci. Technol.* 33: 4440-4447.

61. Takuma, M., Kira, M.,Gohlke, O., Busch, M. 2000. *Proceedings of International Conference on Combustion, Incineration/Pyrolysis and Emission Control*, Seoul, Korea.

62. Joschek, H., Dorn, I., Kolb, T., 1995. *Mitt. VGB* 75: 338 -347.

63. Sakai, S., 2000. *Proceedings of International Conference on Combustion, Incineration/Pyrolysis and Emission Control*, Seoul, Korea, June, 2000.

64. U. S. EPA. 1999. *Characterization of Municipal Solid Waste in the United States.* March. 2001 <http://www.epa.gov>.

65. Perry R., Green D., 1997. *Perry's Chemical Engineers' Handbook.* Seventh Edition, McGraw-Hill, Inc., New York.

66. US EPA, 1997. Evaluation of Rotary Kiln Incinerator Operation at Low-to-Moderate Temperature Conditions. EPA/600/SR-96/105, National Risk Management Research Laboratory, Cincinnati, OH.

67. Cudahy, J. M. and Troxler, W. L., 1992. Thermal Remediation Industry Survey, *J. Air Waste Management Assoc.* 42, 844-849.

68. Chern H. T. and J. W. Bozzelli, 2002. Comment on Formation of Dioxins during the Combustion of Newspapers in the Presence of Sodium Chloride and Poly(vinyl chloride), *Environ. Sci. Technol.*, Vol. 36, No. 9.

69. Ayen R. J. and Swanstorm C., 1991. Development of a Transportable Thermal Separation Process, *Environmental Progress*, 10, No. 3, 175-181.

70. Cundy V. A., Stering A. M., Lester T. W., and Conway R. B., 1991. Incineration of Xylene/Sorbent Packs. A Study of Conditions at the Exit of a Full-Scale Industrial Incinerator, *Environ. Sci. Technol.*, Vol. 25, No. 2, 223-232.

71. Lemieux P. M., Pinak W. P., Wendt J. O.L., and Dunn J. E., 1994. Operating Parameters to Minimize Emissions During Rotary Kiln Emergency Safety Vent Openings, *Hazardous Waste and Hazardous Mateirials*, Vol. 11, No. 1.

72. Lighty J. S., and Pershing D. W., 1990. Fundamentals for the thermal remediation of contaminated soils. Particle and bed desorption models, *Environ. Sci. Technol.*, 24, 750-757.

73. Silcox G. D. and Pershing D. W., 1990. The Effects of Rotary Kiln Operating Conditions and Design on Burden Heating Rates as Determined by a Mathematical Model of Rotary Kiln Heat Transfer, *J. Air Waste Manage. Assoc.*, 40: 337-344.

74. Owens W. D., Silcox G. D., Lighty J. S., and Pershing D. W., 1991. Thermal Analysis of Rotary Kiln Incineration: Comparison of Theory and Experiment, *Combustion and Flame* 86: 101-114.

75. Cundy V. A., Larsen F. L. and Lighty J. S., 1996. A Comprehensive Heat Transfer Model for Rotary Desorbers, *The Canadian Journal of Chemical Engineering*, Vol. 74, 63-76.

76. Gilot P., Howard J. B. and Peters W. A., 1997. Evaporation Phenomina during Thermal Decontamination of Soils, Environ. Sci. Technol. Vol. 31, No. 2, 461-466.

77. Smith M. T., Berruti F. and Mehrotra A. K., 2001. Thermal Desorption Treatment of Contaminated Soils in a Noval Batch Thermal Reactor, *Ind. Eng. Chem. Res.*, 40, 5421-5430.

78. Statgraphics software, 1993. Statistical Graphics Corporation of Princeton, NJ.

79. EPA Method 418.1, 1979. Petroleum Hydrocarbons, Total Recoverable. In Methods for Chemical Analysis of Water and Wastes; U.S. EPA: Washington, DC, 1979; EPA 600/4-79/020.

80. Skoog, D. A., and Leary, J. J., 1992. Principles of Instrumental Analysis, fourth edition, Saunders College Publishing, Orlando, Florida.

81. Perry R, Green, D., Perry's Chemical Engineers' Handbook, 1997. 7th Ed., McGraw-Hill, N.Y..

82. Tscheng, S.H., and Watkinson, A.P., 1979. Convective Heat Transfer in a Rotary Kiln, *Canadian J. Chem. Engr.*, 57, 433.

83. Leger, C.B., and Cundy, V.A., 1993. Bed Mixing and Heat Transfer in a Batch Loaded Rotary Kiln, *Envirinmental Progress*, 12, 101.

84. Wendt J. O. and Linak W. P., 1988. Mechanisms Governing Transients from the Batch Incineration of Liquid in Rotary Kilns, *Combust. Sci. and Tech.*, 61, pp. 169-185.

85. Reid R. C., 1977. The Properties of Gases and Liquids, Third Ed., McGraw-Hill Book Company.